“SYNTHESIS OF METAL AND METAL OXIDE NANOPARTICLES CONJUGATED WITH FUNCTIONAL GLYCANS (GLYCO NANOPARTICLES) AND THEIR BIOLOGICAL APPLICATIONS”

THESIS SUBMITTED TO THE UNIVERSITY OF PUNE

FOR THE DEGREE OF

DOCTOR OF PHILOSOPHY
IN
CHEMISTRY

BY
VILAS RAMTENKI

UNDER THE GUIDANCE OF

DR. B. L. V. PRASAD

AND CO-GUIDANCE OF

DR. C. V. RAMANA

PHYSICAL AND MATERIALS CHEMISTRY DIVISION
NATIONAL CHEMICAL LABORATORY
PUNE – 411008, INDIA

SEPTEMBER 2013

“SYNTHESIS OF METAL AND METAL OXIDE NANOPARTICLES CONJUGATED WITH FUNCTIONAL GLYCANS (GLYCO NANOPARTICLES) AND THEIR BIOLOGICAL APPLICATIONS”

THESIS SUBMITTED TO THE UNIVERSITY OF PUNE

FOR THE DEGREE OF

DOCTOR OF PHILOSOPHY
IN
CHEMISTRY

BY
VILAS RAMTENKI

UNDER THE GUIDANCE OF

DR. B. L. V. PRASAD

AND CO-GUIDANCE OF

DR. C. V. RAMANA

PHYSICAL AND MATERIALS CHEMISTRY DIVISION
NATIONAL CHEMICAL LABORATORY
PUNE – 411008, INDIA

SEPTEMBER 2013

CERTIFICATE

This is to certify that the work incorporated in the thesis entitled **"Synthesis of Metal and Metal oxide Nanoparticles Conjugated with Functional Glycans (Glyco Nanoparticles) and their Biological Applications"** by **Vilas Ramtenki**, submitted to the University of Pune for the degree ***Doctor of Philosophy in Chemistry*** was carried out under my supervision at the Physical and Materials Chemistry Division of National Chemical Laboratory, Pune. Such material as has been obtained by other sources has been duly acknowledged in this thesis. To the best of my knowledge, the present work or any part thereof has not been submitted to any other University for the award of any other degree or diploma.

Date:
Place: Pune

Dr. B. L. V. Prasad
(Research Guide)

CERTIFICATE

This is to certify that the work incorporated in the thesis entitled **"Synthesis of Metal and Metal oxide Nanoparticles Conjugated with Functional Glycans (Glyco Nanoparticles) and their Biological Applications"** by **Vilas Ramtenki**, submitted to the University of Pune for the degree ***Doctor of Philosophy in Chemistry*** was carried out under my joint supervision at the Organic Chemistry Division of National Chemical Laboratory, Pune. Such material as has been obtained by other sources has been duly acknowledged in this thesis. To the best of my knowledge, the present work or any part thereof has not been submitted to any other University for the award of any other degree or diploma.

Date:
Place: Pune

Dr. C. V. Ramana
(Research Co-Guide)

DECLARATION

I hereby declare that the thesis entitled **"Synthesis of Metal and Metal oxide Nanoparticles Conjugated with Functional Glycans (Glyco Nanoparticles) and their Biological Applications"** submitted for the degree Doctor of Philosophy in Chemistry to the University of Pune, has been carried out by me at the Physical and Materials Chemistry Division and Organic Chemistry Division of National Chemical Laboratory, Pune, under the joint supervision of Dr. B. L. V. Prasad and Dr. C. V. Ramana. Such material as has been obtained by other sources has been duly acknowledged in this thesis. The work is original and has not been submitted in part or full by me for any other degree or diploma to other University.

Date: Vilas Ramtenki

Place: Pune (Research Student)

Acknowledgements

I like to thank my guides Dr. B. L. V. Prasad and Dr. C. V. Ramna, for their invaluable guidance. Their tireless enthusiasm and extraordinary ability to interact and collaborate with scientists from diverse backgrounds have been a source of inspiration and are beneficial for working in a new and interdisciplinary field. I also thank them for facilitating and encouraging me to visit UK to carryout joint research work.

I like to thank our Ex-director, Dr. S. Sivaram and present director, Dr. Sourav Pal, for giving me an opportunity to work in NCL. CSIR's financial support is gratefully acknowledged. I thank Dr. Anil Kumar, head of the Physical and Materials Chemistry Division, for always being supportive. I thank all scientists of the Physical and Materials Chemistry Division for being very supportive.

During my research work, I was fortunate to interact with many senior scientists. I am grateful to Dr. P. A. Joy, Dr. Avinash A Kumbhar and Dr. P. Poddar for useful discussions, advice and elderly support.

I wish to thank Dr. M. V. Badiger and his student Mr. Anumon for the collaborative work on polyurethane gels. I thank Prof. M Brust from University of Liverpool, UK, for his help and support during my research collaborative visit, and I extend my sincere thanks to UKIERI grant for giving financial support to visit UK for Six months during my research period.

I would also like to thank NCL Library staff and technical staff especially at CMC for their assistance. I would like to thank TEM engineers Mr. Naren, Mr. Anuj, Mr. pandy raj, Mr. Pankaj and Ms. Sravani for doing my TEM samples. Administrative staff of NCL is duly acknowledged. I really appreciate the support extended by Mr. Dipak Jori regarding the official formalities.

I would like to thank my senior labmates Dr. Pratap, Dr. Sanjay, Dr. Deepti, Dr. Manasi, Dr. Priyanka, Dr. Sheetal, Dr. Vijaykumar, and Dr. Maggie for their help while getting familiarized with research environment and their constant support and encouragement. I enjoyed the company of my colleagues Anal kumar, Ravi, Bala, Pushpanjali, Jhumur, Prabhu, Poulomi, Arun, Pravin, Kabir, Nikunj, Prakash, Ajay, Sameer and all my Ramana Sir`s lab mates especially Dr. Rahul, Dr. Pitamber, Dr. Sunil,

Dr. Kulbhushan, Dr. Sharad, Goriya, Paresh, Atul, Ravindra, Mangesh, Jitendra, Narendra and Dinesh, during the journey of thesis. Thank you all for your help and support regarding experimental work and the lab chores. I also thank all the project students and guest workers.

I would especially like to thank Dr. Santosh and Yadagiri for their continuous support and help. I would like to thank NCL telugu samiti friends and seniors, Dr. Raman, Dr. Rajendar, Dr. Sridhar, Dr. Swaroop, Dr. Satyanarayana, Dr. Raghupathi, Dr. Srinivas, Dr. Ramesh, Dr. Kiran, Chandrababu, Suneel, Chaitanya Kiran, Manoj, Venu, Rambabu, MIrchi tammudu (Shantivardhan), Bogesh, Narasimha, Laxmi, Innaiah, Dr. Raju (Bio), Ramireddy, Chaitanya and all others helped create a relaxing atmosphere.

Finally, I'd like to thank my family especially my parents, sister and my wife Sunitha for their physical and moral support which kept me going even through the most difficult times. Without their help, unconditional love and encouragement, this thesis would not have been possible...

Vilas R

Table of Contents

Chapter 1

Introduction

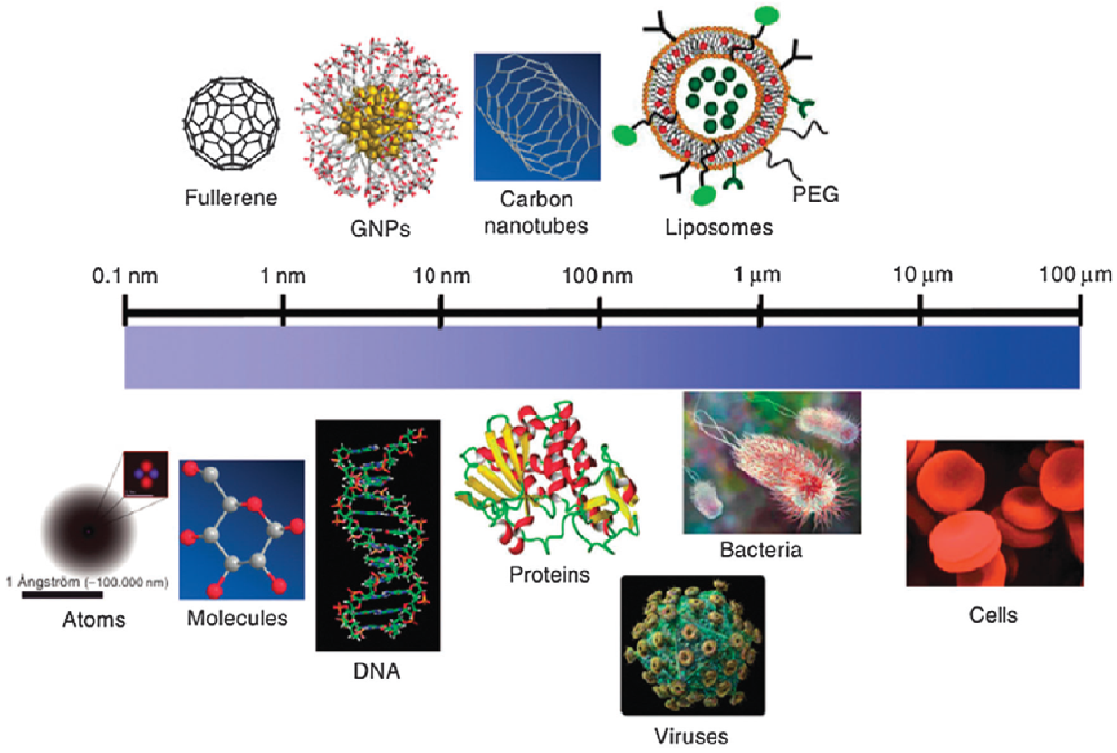

1.1 Introduction

Nanoscience can be defined as a branch of science that involves the investigation of materials consisting of tens of atoms to thousands of atoms. These objects are referred to as nanoparticles (NPs).[1] This means that dimension of the NPs are in between small molecules and bulk materials. However, their physical, electronic, and chemical properties do not resemble neither those of bulk nor those of molecular compounds, but rather strongly depend on the particle size, interparticle distance, nature of the protecting organic shell, and shape of the nanoparticles.[2, 3] The so-called 'size effect' influences the electronic structure and can result in, for example, a unique structural/electronic modification.[4] A decrease in size is also accompanied by a dramatic change in the surface to volume ratio.[1] Due to ease in the surface functionalization and control on the size of NPs, they offer the possibility to create a variety of products with novel characteristics, functions and applications. The dimension of NPs allows them to get incorporated into cells for *in vitro* and *in vivo* imaging, drug-delivery, and targeting tumor cells.[5-7] The term 'nanobiotechnology' was created to describe this group of applications.[8]

NPs can be composed of variety of materials like insulating materials (organic/inorganic), semiconducting materials (organic/inorganic), or metals, either in their neutral valence state or in other forms such as their oxides, sulfides, phosphines, nitrides, etc.[1]

The nanomaterials field is immensely diverse and evolving rapidly. A great variety of nanomaterials have been synthesized for biomedical applications. A large number of polymeric nanomaterials were synthesized by applying the techniques like nanofabrication[9-11] or via molecular self-assembly.[12-16] These polymers, containig multiple or multifunctional ligands/molecules through covalent linkages or physical encapsulation, have been used in biomedical imaging, as carriers for drug delivery and also as scaffolds in tissue engineering.[16-23] The functionalities on these polymeric nanomaterials are in general built into the material synthesis rather than by surface functionalization.

1.2 Nanomaterials in biomedical applications

Noble metal NPs (Au and Ag NPs) are excellent materials providing a powerful platform in biomedical applications such as biomolecular recognition, sensing, drug delivery and imaging.[24, 25] Au NPs are among the most used and studied

nanomaterials because of their easy preparation procedures, stability, well-established surface functionalization protocols, their unique optoelectronic properties bio-compatibility and non-toxicity. The surface plasmon resonance (SPR), generally observed in noble metal NPs is produced by the collective oscillation of conducting electrons of the metal upon interacting with the incident light. The SPR is dependent on size and shape of the NP, the dielectric property of the media and the distance between particles.[26] This provides a unique and convenient platform for monitoring the molecular recognition events occurring close to the surface of the NPs. Colorimetric bioassays have thus been established based on the SPR shift when molecular interactions take place at the surface of the NPs, and have been employed to study fundamental biorecognition processes including cell-cell communication, enzymatic activity, protein-protein interaction and DNA hybridization. When the NPs aggregate because of ligand receptor interaction, there will be large SPR shifts producing intense color changes visible to the naked eyes.[27] An additional advantage of NPs is the multivalent presentation on the NP surface that could drastically enhance affinities of specific monovalent interactions via the multivalent binding between NPs and the biological target.[28] Binding affinity of mannose decorated Au NPs with Concanavalin A (Con A) was found to be several orders of magnitude higher in comparison with that of single mannose units with Con A in solution.[29] Similarly, SDC-1721, which is a structural fragment of the HIV inhibitor TAK-77 and displays no inhibition activity in solution, became a potent inhibitor when coupled to 2 nm Au NPs.[30] The authors attributed the enhanced activity to the multivalency effect, where multiple ligands are present on the nanoparticle surface.

NPs of semiconducting materials (e.g. ZnS, CdSe) that display quantum confinement effect are called quantum dots (QDs).[31] In these systems, the semi-conducting band gap increases with decreasing particle size, and therefore smaller QDs emit light at higher energy, i.e., lower wavelength and blue-shift, whereas larger QDs absorb and fluoresce at longer wavelengths and red shift. QDs have broad excitation spectra, but narrow and tunable emissions, and have thus been widely used as optical labels in a wide range of biomedical applications including immunoassays for proteins, nucleic acids, bacteria and toxin analysis.[32, 33] The advantages of these systems over conventional dye molecules, organic fluorophores, or radioactive labels are tunable fluorescence signatures, narrow emission spectra, brighter emission, long

fluorescence lifetime and high photostability.[34, 35] Thus they enable multiplex imaging with a single excitation source and preventing overheating of cells or tissue during multicolor imaging.[31, 36] Apart from their biological applications, semiconductor nanoparticles serve as converters of sunlight into electricity in solar cells.[1, 37-42]

Magnetic nanoparticles show remarkable new phenomena such as superparamagnetism. Magnetic nanoparticles of iron oxides have been investigated the most and have shown remarkable potentials in biomedical research. A unique feature of magnetic particles is their ability to move easily under the influence of an external magnetic field. Magnetic nanoparticles with the appropriate surface chemistry have thus generated increasing interests and have been widely used in the life sciences[43-48] including magnetic resonance imaging (MRI) contrast enhancement,[49-51] drug delivery,[52-55] hyperthermia,[56-58] cell separation[59-62] and tissue repair.[63]

1.3 Glyconanoparticles

NPs with carbohydrates as functional ligands are called glyconanoparticles (GNPs). The surface of mammalian cells is covered by a dense coating of carbohydrates named glycocalyx.[64] With a dense packing of carbohydrate group bearing ligands on their surface, GNPs provide a glycocalyx like surface that mimics the presentation of carbohydrate epitopes of cell surface glycoconjugates.[65] Therefore, they have been the subject of many investigations involving the study and evaluation of carbohydrate interactions. Furthermore, they can also be utilized as biolabels, biosensors, to intervene in carbohydrate mediated processes in biomedicine, or as building blocks in material science.[66]

1.3.1 Synthesis and functionalization of nanoparticles with glycoconjugats

Functionalization of nanoparticle surface with gycans is a very important step in developing assays that can assess inherently weak carbohydrate–protein and carbohydrate–carbohydrate interactions. Numerous conjugation strategies of different glycans and NPs have been employed with great success. Here, we discuss three of the most common and versatile routes that have been developed for building chemically diverse libraries of substrates for surface functionalization. These are i) direct immobilization on a metal surface (i.e., thiol chemistry), ii) [3+2] cycloaddition (click) chemistry using the copper catalysed azide–alkyne cyclo-addition (CuAAC) and iii) amide bond formation. We restrict our examples to carbohydrates bearing

molecules and their decoration on nanoparticle surfaces as these are the main focus of the present work. Such surface modification strategies lead to surfaces of nanostructures decorated by the glycans with control over their numbers, density and orientation (Fig. 1.1).[67-73]

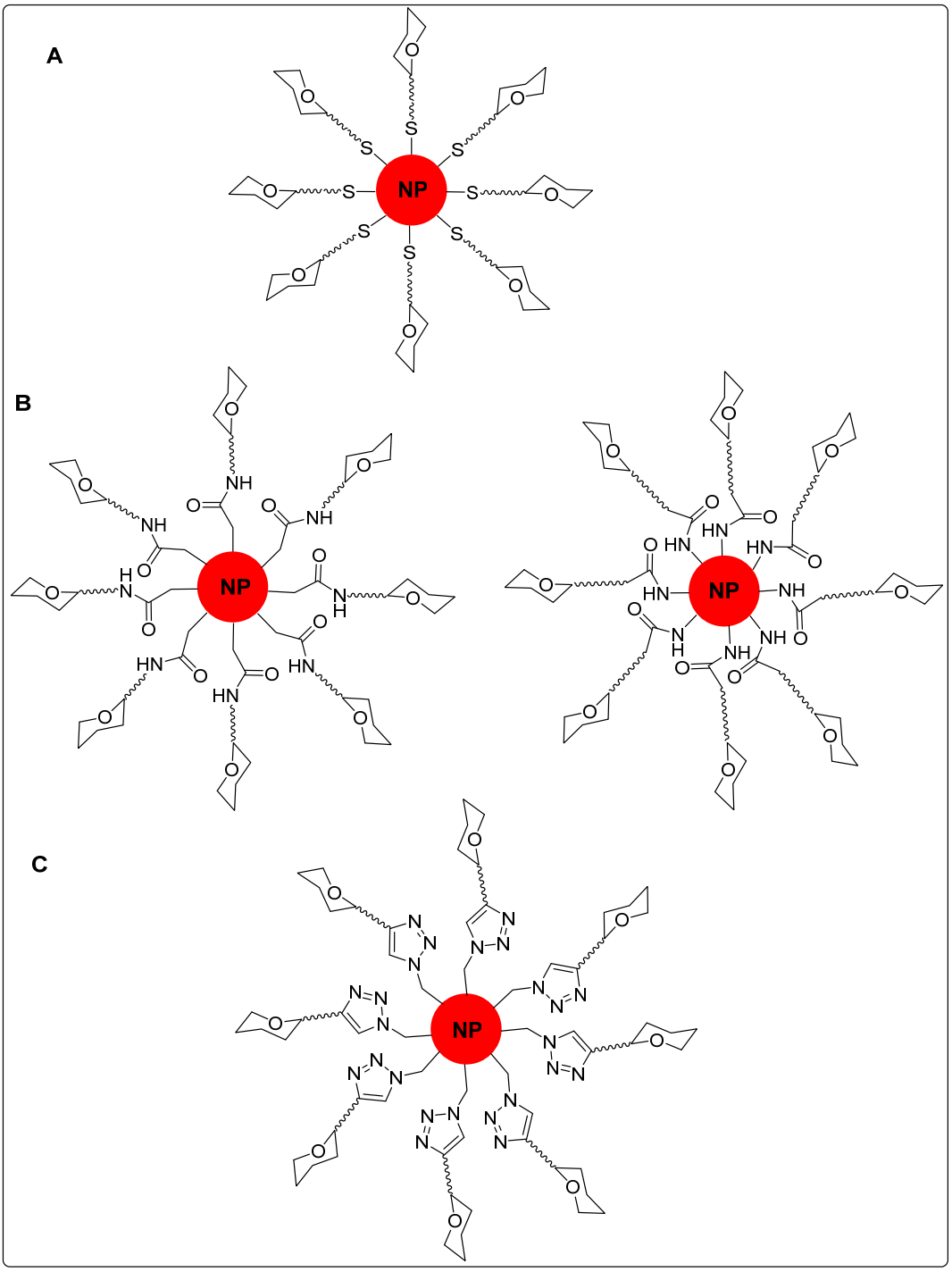

Figure 1.1. *schematic representation of nanoparticle surface functionalisation by direct functionalisation with (A) thiolate, (B) amide bond formation of an amine and carboxylic acid, and (C) triazole formation from a CuAAC reaction.*

Direct immobilization of thiolates on gold and silver surfaces is a popular method for functionalizing these materials. Ligating thiols on the surface of gold and silver nanostructures has been established as a standard method for preparing these materials. Gold glyconanoparticles were first described by Penades *et al.* in 2001 as an example for the multivalent presentation of carbohydrates on nanoparticle surfaces.[74, 75] The carbohydrate- containing molecules are attached to the gold surface using well known Au-thiol covalent bonds. They are typically prepared by a reduction reaction, in which glycol-linked thiols are mixed with tetrachloroauric acid. To this mixture a reducing agent was added to get the carbohydrate capped NPs (Fig. 1.2). The resulting highly water-dispersible particles can be characterized by several conventional techniques such as ^{1}H NMR and transmission electron microscopy (TEM) to reveal the particle size. Carbohydrate structures that have been attached to gold nanoparticles using this strategy include glucose, lactose, maltose, the Lewis X trisaccharide and the Lewis Y tetrasaccharide.[76]

Azide and alkynes are known to undergo Huisigen`s (3+2) cyclo addition in presence of catalysts like Cu(I) salts. This reaction is one of the popularly known click chemistry reaction (CuAAC). The ease with which azides and alkynes are introduced into organic compounds, their bioorthogonal properties and tolerance to a wide range of solvents (including water) make this click reaction an ideal technique for bioconjugation purposes.[77-80]

In addition, the CuAAC profits from the *in vivo* incorporation of unnatural amino acids containing azides or alkynes during translation and expression of proteins. As a result, numerous biomolecules including DNA, peptides, proteins, oligosaccharides and glycoconjugates (Fig. 1.3) as well as pseudo-biomolecules (such as peptoids, and peptidomimetic oligomers) have been anchored on NPs with various appendages by means of the CuAAC.[81, 82]

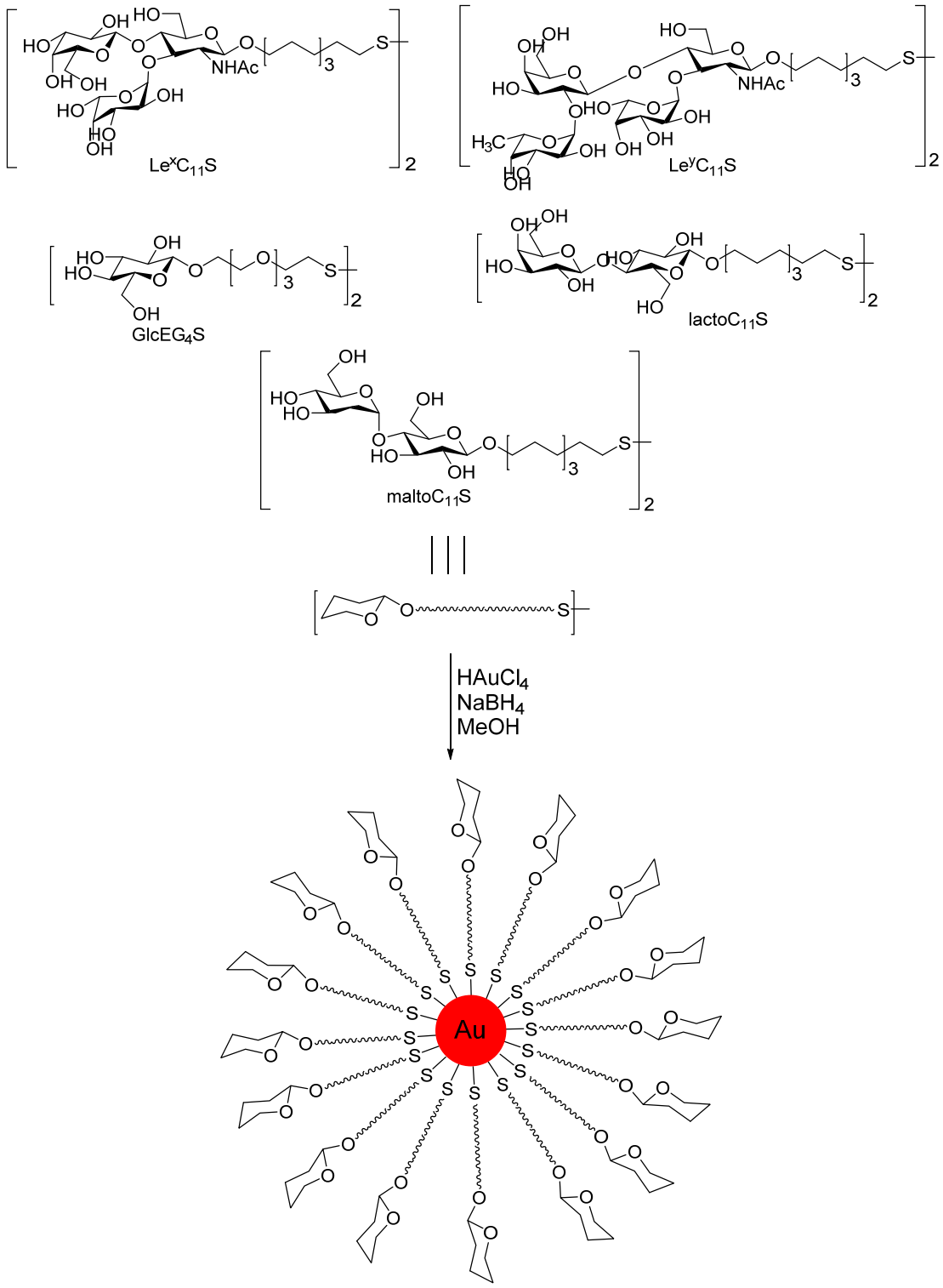

***Figure 1.2**. Synthesis of Le^x, Le^y, glucose, lactose and maltose gold glyconanoparticles by Penades' methodology (Ref. 66).*

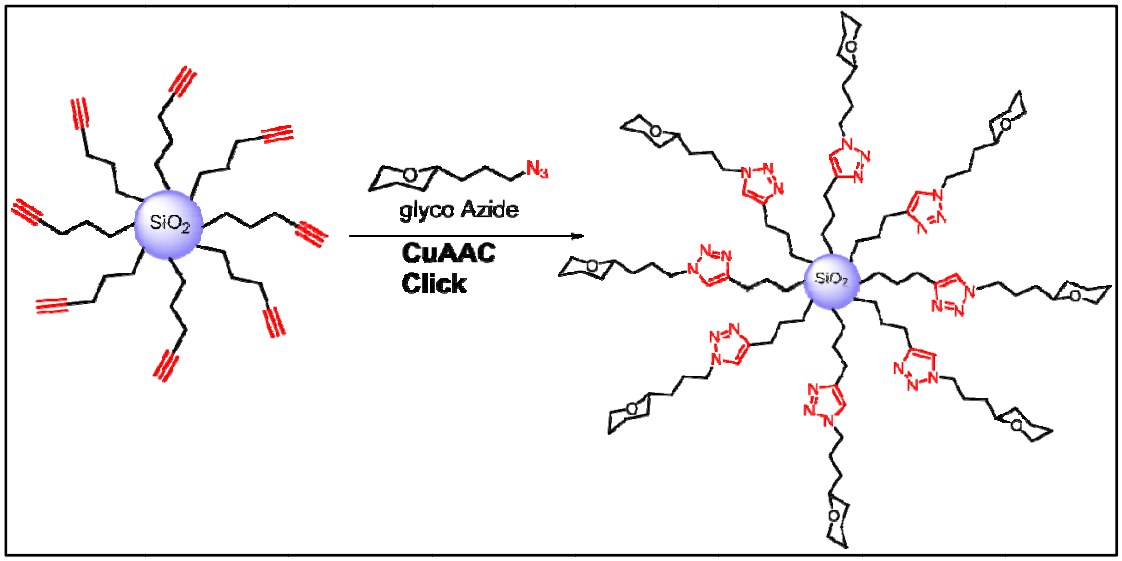

Figure 1.3. *Schematic representation of Silica-based clicked hybrid glyco nanoparticles.*

The orthogonality of the CuAAC reaction renders it attractive to chemists and biochemists. However, some drawbacks do exist. Upon characterization of the final functionalized surfaces, copper can often be detected as a contaminant. The catalyst can become trapped at the surface or bind to the triazoles formed from the coupling process. Terminal alkynes themselves can also bind to gold and silver surfaces resulting in nonspecific interactions.[83] Nevertheless, the CuAAC reaction is adaptable to most materials and can be used to achieve specific binding to make complex structures in the presence of common biological functional groups.

Amide bond formation has been employed to functionalize silica-coated surfaces as well as other amine and carboxylate-functionalized surfaces. Amide bonds can be created without the need of a catalyst. This technique is commonly applied to functionalize particles, surfaces and other materials, and can be used in conjunction with the CuAAC to design more complex materials in a stepwise manner.[84, 85]

Synthesis of water dispersible magnetic nanoparticles with size control and suitably coated with polymers or other coating material is of interest for cell labeling and separation and for magnetic resonance imaging.[86-88] Most commonly, iron oxide nanoparticles are prepared by co-precipitation of ferrous and ferric salts solution and stabilized by using biocompatible molecules as dextran or oleic acid. In a second step, the biomolecules are attached by covalent or electrostatic coupling to the protected nanoparticle. Penades et al. had reported the synthesis of magnetic GNPs

functionalized with glucose, maltose and lactose in aqueous solution. Using such protocols, the exceptionally small gold particles coated iron oxide magnetic GNPs of stable colloidal solutions were prepared in water. These were accessed by adding a solution of the sugar disulfide ligand in methanol to a aqueous solution of $FeCl_3$ to which aqueous solution of $HAuCl_4$ was subsequently added. The mixture was left 5 min at 60 °C, and then an aqueous solution of $NaBH_4$ was added in small portions with rapid stirring. The brown suspension formed was stirred for an additional 2 h and the formed GNPs were purified by centrifugation. As these particles consist both Fe_3O_4 and Au NPs they possess the magnetic properties and the presence of Au entails easy and convenient surface modification. These magnetic GNPs have been used in biological applications like contrast agents in MRI and specific cell labeling.[89-91] Huang et al. had synthesized silica coated iron oxide GNPs with six different glycosyl moieties by employing CuAAC click reaction and amide coupling. Briefly, in the first step silica coated iron oxide NPs fuctionalized with azide or amine and glycosyl moieties were linked to terminal alkynes or carboxyli acid. These two were then subjected to CuAAC click reaction or amide coupling[92, 93] to get glycosyl functionalized silica coated iron oxide GNPs (Fig. 1.4).

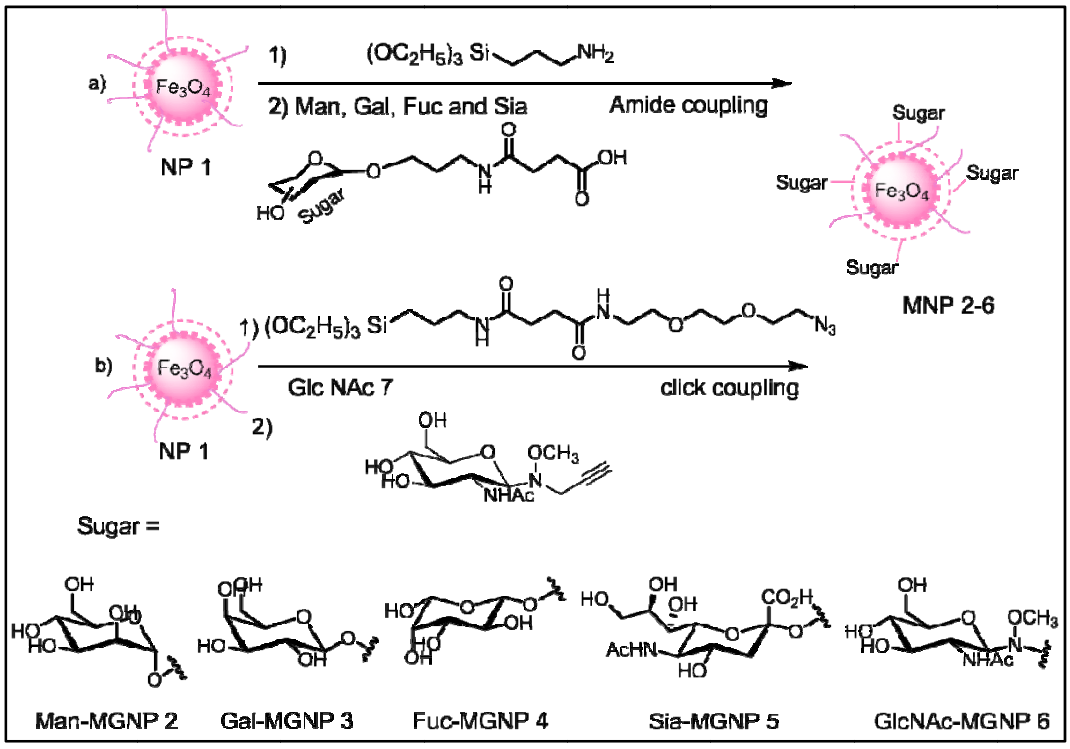

Figure 1.4. *Synthesis of MGNPs. Figure taken from Ref. 42.*

Nanocrystals of semiconducting materials (QDs), have fascinated physicists, chemists, and electronic engineers for past four decades. The most exciting feature of these materials is their chemical and physical properties which differ markedly from those of the bulk solid.[94] Since their quantum size effects were understood, fundamental and applied research on these systems has become increasingly popular. Most commonly, QDs are first prepared at high temperature in the presence of protective agents like ligands to prevent crystal aggregation and to regulate the growing rate. Alternatively, the protection process can be performed in solution using thiols with hydrophilic end groups to confer stability and water solubility to the QDs. In a second step, the biomolecules are attached to the protected nanocrystals for cell labeling. QDs bio-conjugated to peptides and proteins,[95-102] antibodies,[96, 103, 104] DNA,[105-108] and other molecules[109-111] have been prepared mainly by coupling the biomolecules to the thiol protected QDs and tested as biological markers.

The synthesis of polysaccharide protected QDs was reported first by Rosenzweig et al.[112] This group prepared CdSe-ZnS quantum dots passivated with carboxymethyldextran and polylysine, and they proved the high affinity of the QDs toward the glucose binding protein-Con A. Chaikof et al. reported the coupling of commercially available QDs-streptavidin with a biotin end-terminated lactose glycopolymer[113] and have used Confocal microscopy to confirm fluorescent staining of *Ricinus communis agglutinin* (RCA_{120}) immobilized agarose beads due to the glycopolymer–lectin interaction. Penades et al. have reported the preparation of water soluble nanoclusters of cadmium sulphide and zinc sulphide covalently bound to biologically significant neoglycoconjugates by a single step solution procedure (Fig. 1.5).[114] The synthesis of Le^x and maltose protected CdS and Zns nanocrystals were carried out. The procedure was also used for the synthesis of tiopronin and tiopronin-Tat functionalized QDs which were able to label the nucleus of human fibroblasts.[97] CdSe/ZnS quantum dots (QDs) have also been functionalized using direct thiol ligation.[115-117]

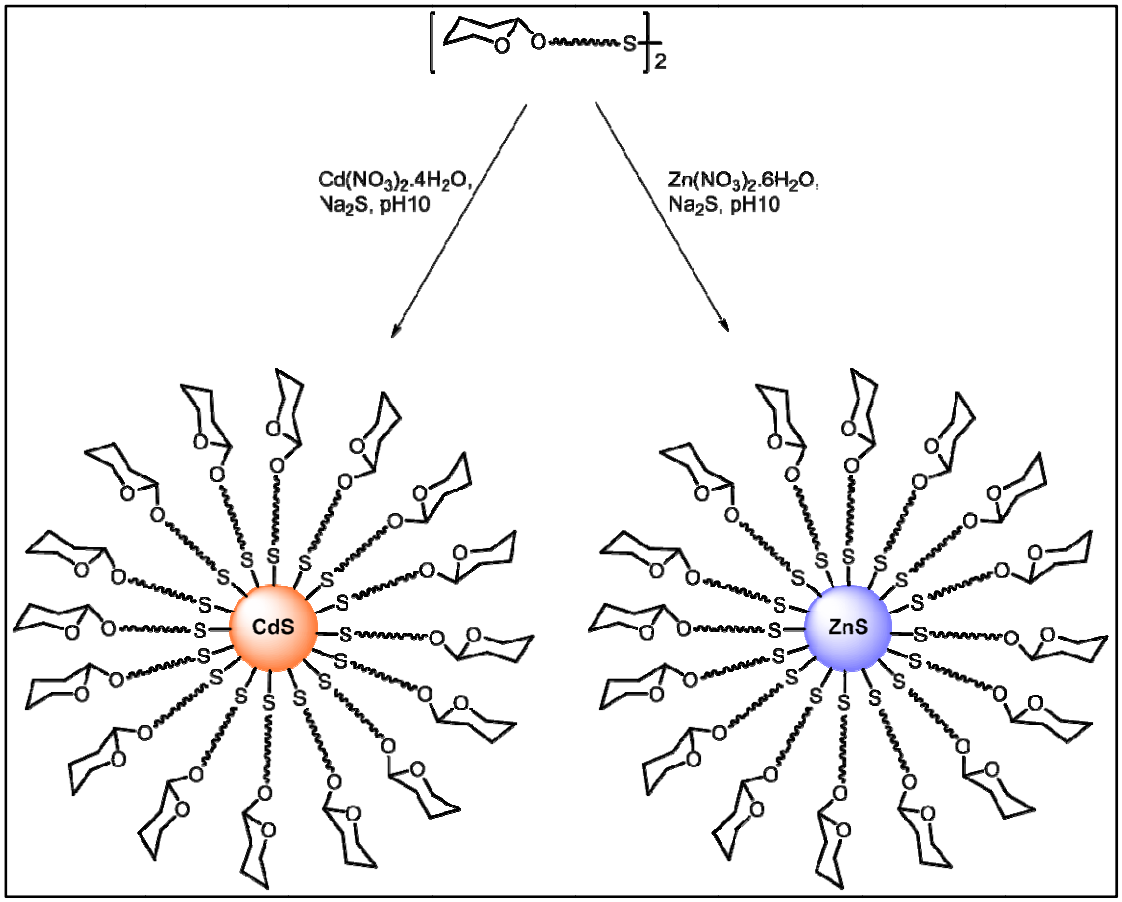

Figure 1.5. *schematic representation of glyco-QDs synthesis (Ref. 66).*

1.4 Applications of glyconanoparticles

1.4.1 Metal glyconanoparticle

Glyconanoparticles (GNPs) have direct applications related to biomedical sciences. The synthesis and characterisation of such materials has been recently reviewed.[118, 119] The specific properties of different core materials have led to the development of unique composites that can target and report specific biomolecular events. Glycosylated gold NPs, magnetic iron oxide NPs and CdSe/ZnS QDs, have been synthesized and effectively applied to overcome challenges in medicine and molecular biology. The simplicity with which gold NPs can be functionalised using thiolate chemistry to readily form water soluble sugar-functionalised nanoscaffolds has made these particles a primary target for many researchers aiming to apply nanotechnology to problems in glycobiology. Gold NPs have been used to study carbohydrate–carbohydrate interactions, specifically the calcium mediated self-aggregation of Lewis X (Le^x).[120] Gold NPs functionalised with Le^x were shown to

aggregate upon addition of calcium ions to a solution of suspended particles as determined by transmission electron microscopy (TEM) compared to lactose-functionalised particles that exhibited little aggregation under the same conditions. Lin et al. have used SPR technique to quantitatively analyze the interaction between mannose gold glyconanoparticles and the Con A lectin.[121] They have found that the binding has a strong multivalent effect and that the affinity of mannose GNPs for Con A could be adjusted by altering the nanoparticle size or the sugar moiety (Fig. 1.6).

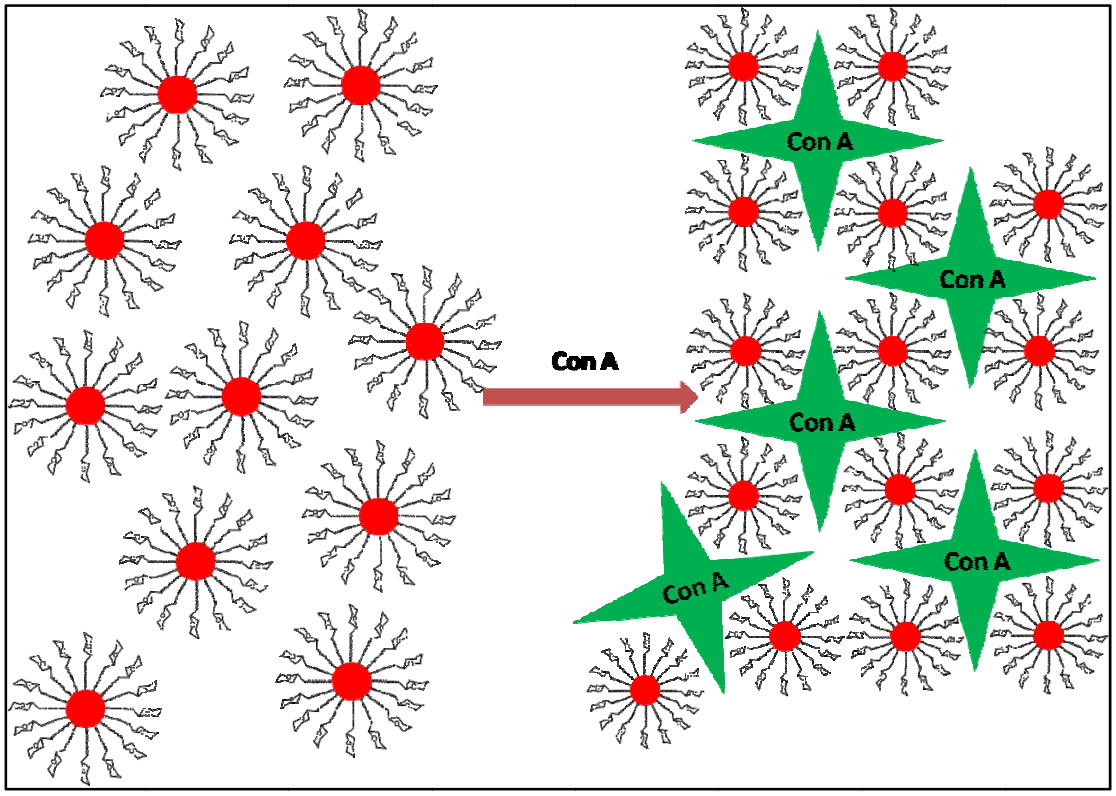

Figure 1.6*. Schematic illustration of the interactions of glyconanoparticles and ConA.*

Penades el al. have shown that lactose functionalized gold GNPs could be used for anti-adhesive therapy.[65] Adhesion of tumour cells to the vascular endothelium cells is the critical step in metastasis. After this adhesion step, tumour cells transmigrate and create new tumour foci in the body. Interactions between tumour-associated antigens and epithelial cell selectins promote tumour cell metastasis. In addition to this mechanism, carbohydrate–carbohydrate interactions between glycosphingolipids expressed on the tumour and endothelial cell surfaces also seem to be involved in the critical adhesion step.[122] A carbohydrate–carbohydrate interaction between GM3 expressed in a murine melanoma cell line (B16) and Gg3 or

lactosylceramide of endothelium cells has been proposed to be involved in the first adhesion step of tumour cells to endothelium before transmigration.[123]

Therefore, inhibition of adhesion step by GNPs that present carbohydrate antigens expressed either in the tumour or the endothelium cells might provide effective anti-adhesion therapy (Fig. 1.7). Based on the involvement in cell adhesion of the antigen lactosylceramide, lactose capped glyconanoparticles were tested as a potential inhibitor of the binding of melanoma cells to endothelium. *Ex vivo* experiments were carried out to evaluate the anti-metastasis potential of the GNPs. Mice were injected with melanoma cells pre-incubated with lactose functionalised gold GNPs, and after 3 weeks, the animals were sacrificed and both lungs evaluated under the microscope for analysis of tumour foci. A 70% of tumour inhibition was reported as compared with the group inoculated only with melanoma cells.[65]

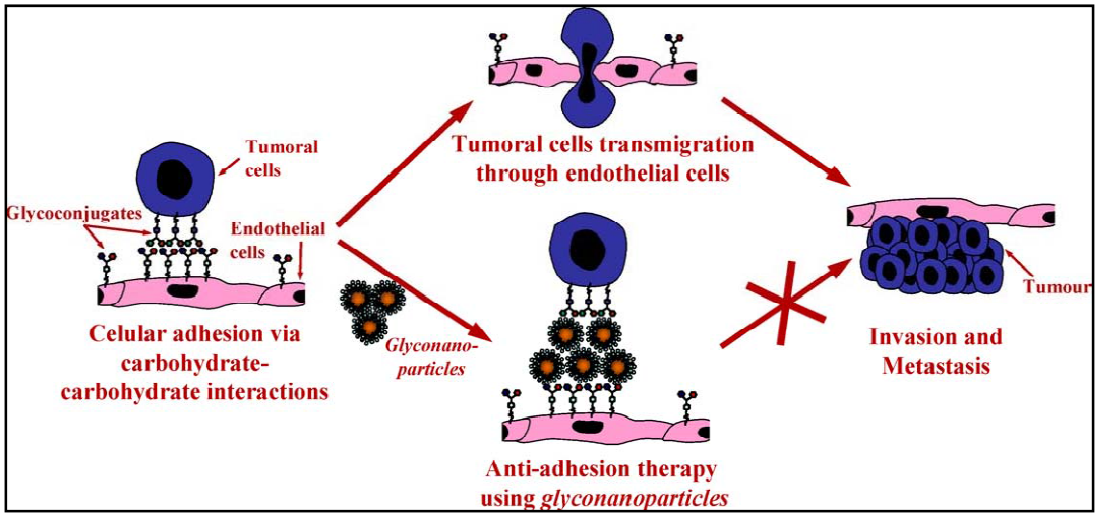

Figure 1.7. *Possible action mechanism of lacto-Au in anti-adhesive therapy. This figure has been taken from Ref. 12.*

1.4.2 Magnetic glyconanoparticles

Magnetic glyconanoparticles have also found use in bacterial adhesion studies. Magnetic GNPs has been used to capture and removal of bacteria by using concept of carbohydrate–lectin binding interactions. This method shows potential for the identification and removal of pathogens with carbohydrate coated magnetic particles (Fig. 1.8).[61] Capture of both bacteria and viruses may be possible in a specific and targeted manner with tailored materials that present unique sugar surfaces to specifically target pathogens of choice.

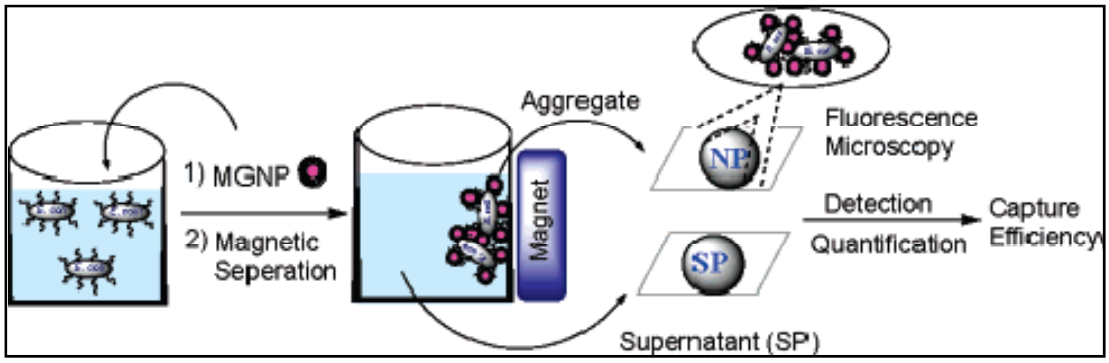

Figure 1.8. *Schematic demonstration of pathogen detection by MGNPs. This figure has been taken from Ref. 42.*

Submicrometric magnetic GNPs composed of multiple-single magnetite crystallites (~10 nm in diameter) and functionalized with the Le^X antigen have been used to detect and isolate dendritic cells by magnetic capture.[124] Previously, sub-micrometric and micrometric galabiose-functionalized magnetic particles were used to separate the Gram-positive pathogen *Streptococcus suis*[125] following a strategy similar to that previously reported for *E. coli* detection with smaller GNPs.[61] The highly sulphated natural glycosaminoglycan heparin, clinically important as an anticoagulant, has been employed to prepare heparin-coated superparamagnetic iron oxide nanoparticles for labelling human mesenchymal stem cells (hMSCs) by MRI.[126] Heparin provides high biocompatibility, but also can strongly bind to vascular endothelial growth factor (VEGF) and epidermal growth factor (EGF) through the interaction with sulphate groups.

Galactose-functionalised magnetic NPs have been used to target HepG2 cancer cells.[127] Glucose and galactose-coated iron oxide NPs have been recently prepared and the influence of the sugar versus poly(ethylene glycol)-coating on the cellular uptake of GNPs by several cell lines have been studied.[128] The density of the coating molecule was crucial to prevent nonspecific uptake of NPs by Vero cells. Moreover, it was shown that NPs with a high number of glucose molecules are endocytosed by caveolae and end up in the lysosomes. Lin et al. prepared, in a three-step synthesis, fluorescent silica-coated magnetic nanoparticles modified with a mono- and triantennary dendritic galactoside ligand (Fig. 1.9) to investigate the effect of ligand-spatial orientation on the cellular targeting of the asialoglycoprotein receptor (ASGP-R).[127] The result showed that the avidity of a triantennary galactoside for the

asialoglycoprotein receptor is dramatically enhanced by proper spacing of the three terminal galactose groups.

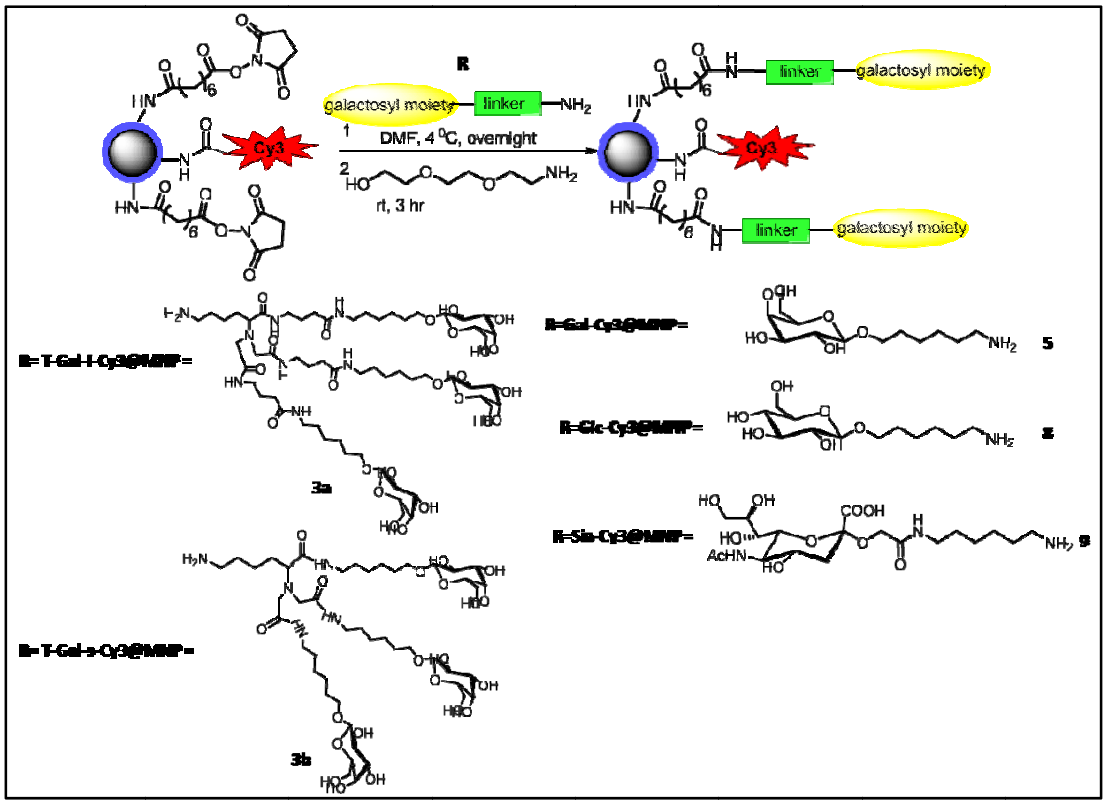

Figure 1.9. *Synthesis of dual fluorescent-magnetic galactosyl-glyconanoparticles for cell labelling. This figure has been taken from Ref. 66.*

1.4.3 Quantum dot glyconanoparticles

Glycosylated QDs have been used to study the targeting of these materials to the liver both *in vitro* and *in vivo*. *In vitro* assays show preferential binding and uptake of galactose-coated QDs by HepG2 cells that express asiaglycoprotein (ASGPR) compared to QDs capped with polyethyleneglycol (PEG) as determined by flow cytometry. These findings were then tested *in vivo*, by injecting mice with mannose, galactosamine- or PEG-coated QDs. Both glycan-coated QDs were taken up well by the liver after 2 h compared to a nonspecific pattern for the control QDs. Hepatocytes expressing ASPGR and Kupffer cells that express mannose receptors are thought to mediate the specific responses that result in these localized hotspots of glycosylated QDs in the liver.[116] Fang et al. have reported the labeling of mice, pigs and sea-urchin live sperm with CdSe/ZnS core shells QDs functionalized with β-N-

acetylglucosamine or mannose (Fig. 1.10). Acetylglucosamine-encapsulated QDs were concentrated at the sperm heads, while mannose-encapsulated QDs tended to spread over the whole sperm body, due to the different distribution of the GlcNAc and Mannose receptors on the sperm surface.[129]

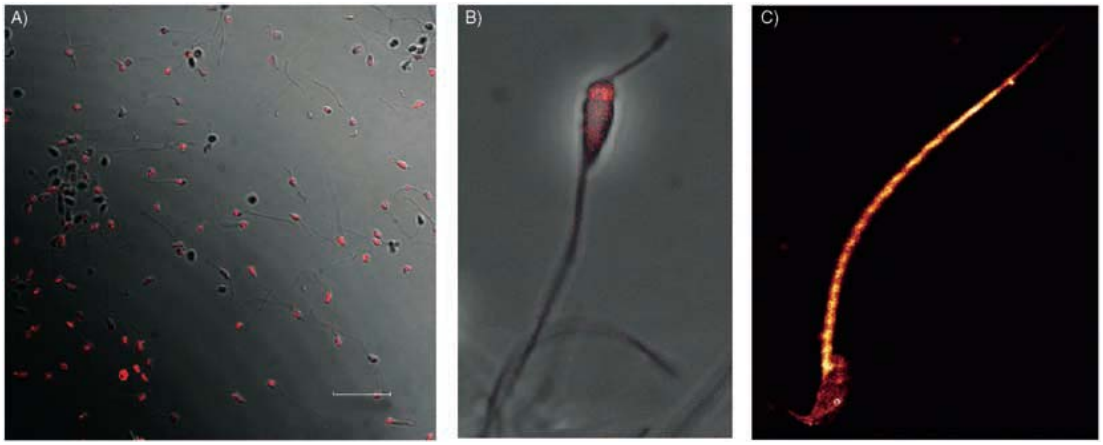

Figure 1.10. *Confocal microscope imaging for staining of sperm with glycoquantum dots: A) selective QDGLN labeling on the heads of sea-urchin sperm (scalebar=20 μm), B) close-up of QDGLN-labeled sea-urchin sperm, and C) close-up of QDMAN-labeled mouse sperm. This figure has been taken from Ref. 65.*

In general, metallic nanoparticles are extensively studied since they exhibit novel electronic, optical, and magnetic properties. Most of these new properties arise from the so-called "size effect" which affects the electronic structure, as well as from the increase of the ratio of atoms located at the surface with respect to the total number of atoms of the nanoparticle.[130, 131] GNPs are not an exception and they show very interesting physical properties. In fact, Penades et al. had reported that 1.4–1.8 nm Au GNPs functionalized with thiol derivatives exhibit a localized permanent magnetism in contrast to the metallic diamagnetism characteristic of bulk Au NPs functionalized with amminated derivatives.[132, 133]

Thus from the above observations, the number of sugar-functionalized metallic NPs and their application in investigating carbohydrate based interactions have been continually growing and it is expected to blossom in the years to come. However, selecting and synthesizing sugar containing ligand plays important role, as this is the first step before they can be decorated on nanoparticle surfaces and their biological applications can be evaluated.

1.5 Objective of this thesis

We have realized the importance of metal and metal oxide GNPs from their application point of view in different fields. Survey of various methods of synthesis has been described in earlier sections. Apart from this, we have also taken into account the role of ligand in the synthesis of GNPs as stabilizing agent, and as reducing entity.

In this thesis we concentrate on the effect of glycosyl ligand on the stability of GNPs and glycosyl ligand stability when we use then in the biological applications. We have also studied lectin (Concanavalin A) binding studies and anti bacterial activities of GNPs. Subsequently we demonstrated the aggregation of GNPs with lectin irrespective of their inorganic core. We have also demonstrated the dual characteristics of ligand that act as reducing agent and as capping moiety.

1.6 Outline of the thesis

Brief background of the work carried out in the thesis has been described in above section**.**

Chapter 2 deals with the synthesis of five different α/β-12-*C*-glycosyl acids. These 12-*C*-glycosyl acids were then used as capping and as well as reducing agent in the synthesis of Ag GNPs. Furthermore, the stability of Ag GNPs formed with 12-*C*-glycosyl acids were monitored by UV-visible spectroscopy and TEM analysis. The formation of stable Ag GNPs were observed when we use capping agent as 12-α-*C*-glycosyl acids compare to 12-β-*C*-glycosyl acids.

Chapter 3 illuminates the synthesis of Ag GNPs decorated with mannose and glucose sugar moieties. These Ag GNPs were used to study the lectin (Concanavalin A) binding by using fluorescence spectroscopy, UV-visible spectroscopy and TEM analysis. Furthermore, the specific binding of mannose coated Ag GNPs towards the type 1 pili of *E coli* demonstrated by performing antibacterial activity of Ag GNPs against *E coli* (DH5α cells).

Chapter 4 deals with the synthesis of mannose and glucose containing long chain terminal alkyne, which are clicked with silica azide by using CuAAC click reaction to get mannose and glucose coated silica GNPs. These silica GNPs were used to study the Concanavalin A binding by fluorescence spectroscopy. From the TEM

analysis, the aggregation of GNPs (Ag and SiO_2) with concanvalin A was observed in the case of mannose and glucose coating and independent of the core material.

Chapter 5 summarises the work carried out in this thesis by highlighting the prominent feature of the work. Here, we also give the possible future directions of our work.

1.7 References

1. S. Link and M. A. El-Sayed, *Int. Rev. Phys. Chem.*, 2000, **19**, 409-453.
2. M.-C. Daniel and D. Astruc, *Chem. Rev.* , 2004, **104**, 293-346.
3. M. Brust and C. J. Kiely, *Colloids Surf., A*, 2002, **202**, 175-186.
4. D. Zanchet, H. Tolentino, A. M. C. Martins, O. L. Alves and D. Ugarte, *Chem. Phys. Lett.*, 2000, **323**, 167-172.
5. N. Moran, *Nat. Biotechnol.*, 2006, **24**, 121.
6. N. L. Rosi and C. A. Mirkin, *Chem. Rev.* , 2005, **105**, 1547-1562.
7. H. Yang and Y. Xia, *Adv. Mater.* , 2007, **19**, 3085-3087.
8. S. G. Penn, L. He and M. J. Natan, *Curr. Opin. Chem. Biol.*, 2003, **7**, 609-615.
9. B. Paivanranta, P. K. Sahoo, E. Tocce, V. Auzelyte, Y. Ekinci, H. H. Solak, C.-C. Liu, K. O. Stuen, P. F. Nealey and C. David, *ACS Nano*, 2011, **5**, 1860-1864.
10. M. Acik and G. Sonmez, *Polym. Adv. Technol.*, 2006, **17**, 697-699.
11. T. Liu, C. Burger and B. Chu, *Prog. Polym. Sci.*, 2002, **28**, 5-26.
12. S. Obata and Y. Shimoi, *Phys. Chem. Chem. Phys.*, 2013, **15**, 9265-9270.
13. W.-F. Kuan, R. Roy and T. H. Epps, III, *Polym. Prepr.*, 2012, **53**, 467-468.
14. P. Posocco, Z. Posel, M. Fermeglia, M. Lisal and S. Pricl, *J. Mater. Chem.*, 2010, **20**, 10511-10520.
15. R. G. Gilbert, *Macromolecules*, 2006, **39**, 4256-4258.
16. B. J. Tighe, *Macromol. Chem. (London)*, 1984, **3**, 375-386.
17. S. Tonzani, *J. Appl. Polym. Sci.*, **129**, 527.
18. E. Simanek, *Mol. Pharmaceutics*, 2010, **7**, 921.
19. S. Wang and K. S. Schanze, *ACS Appl. Mater. Interfaces*, 2013, **5**, 4487.
20. J. F. Mena, A. Neira-Carrillo, M. Y. Pedram and M. J. Kogan, *J. Biomater. Tissue Eng.*, 2013, **3**, 135-140.
21. D. Pal, T. De and A. Baral, *PHARMANEST*, 2013, **4**, 54-65.
22. S. L. Kuan, Y. Wu and T. Weil, *Macromol. Rapid Commun.*, 2013, **34**, 380-392.
23. Y. Ohya, A. Takahashi and K. Nagahama, *Adv. Polym. Sci.*, 2012, **247**, 65-114.
24. R. A. Sperling, G. P. Rivera, F. Zhang, M. Zanella and W. J. Parak, *Chem. Soc. Rev.*, 2008, **37**, 1896-1908.

25. R. Wilson, *Chem. Soc. Rev.*, 2008, **37**, 2028-2045.
26. P. Mulvaney, *Langmuir*, 1996, **12**, 788-800.
27. R. Liu, R. Liew, J. Zhou and B. Xing, *Angew. Chem., Int. Ed.*, 2007, **46**, 8799-8803.
28. R. Elghanian, J. J. Storhoff, R. C. Mucic, R. L. Letsinger and C. A. Mirkin, *Science* 1997, **277**, 1078-1080.
29. C.-C. Lin, Y.-C. Yeh, C.-Y. Yang, G.-F. Chen, Y.-C. Chen, Y.-C. Wu and C.-C. Chen, *Chem. Commun.*, 2003, 2920-2921.
30. M.-C. Bowman, T. E. Ballard, C. J. Ackerson, D. L. Feldheim, D. M. Margolis and C. Melander, *J. Am. Chem. Soc.*, 2008, **130**, 6896-6897.
31. M. Ozkan, *Drug Discovery Today*, 2004, **9**, 1065-1071.
32. J. Hu, L.-s. Li, W. Yang, L. Manna, L.-w. Wang and A. P. Alivisatos, *Science* 2001, **292**, 2060-2063.
33. M. Nirmal and L. Brus, *Acc. Chem. Res.*, 1999, **32**, 407-414.
34. M. Bruchez, Jr., M. Moronne, P. Gin, S. Weiss and A. P. Alivisatos, *Science* 1998, **281**, 2013-2016.
35. W. C. W. Chan, D. J. Maxwell, X. Gao, R. E. Bailey, M. Han and S. Nie, *Curr. Opin. Biotechnol.*, 2002, **13**, 40-46.
36. D. J. Norris and M. G. Bawendi, *Phys. Rev. B: Condens. Matter*, 1996, **53**, 16338-16346.
37. S. D. Sung, I. Lim, P. Kang, C. Lee and W. I. Lee, *Chem. Commun.*, 2013, **49**, 6054-6056.
38. Z. Han, L. Wei, L. Tang, C. Chen, H. Pan and J. Chen, *J. Power Sources*, 2013, **239**, 546-552.
39. S. Horoz, L. Lu, Q. Dai, J. Chen, B. Yakami, J. M. Pikal, W. Wang and J. Tang, *Appl. Phys. Lett.*, 2012, **101**, 223902/223901-223902/223904.
40. J. Yan, Q. Ye, X. Wang, B. Yu and F. Zhou, *Nanoscale*, 2012, **4**, 2109-2116.
41. D. I. Son, B. W. Kwon, J. D. Yang, D. H. Park, B. Angadi and W. K. Choi, *J. Mater. Chem.*, 2012, **22**, 816-819.
42. X.-Y. Yu, J.-Y. Liao, K.-Q. Qiu, D.-B. Kuang and C.-Y. Su, *ACS Nano*, 2011, **5**, 9494-9500.
43. A.-H. Lu, E. L. Salabas and F. Schuth, *Angew. Chem., Int. Ed.*, 2007, **46**, 1222-1244.

44. A. K. Gupta and M. Gupta, *Biomaterials*, 2005, **26**, 3995-4021.
45. S. Laurent, D. Forge, M. Port, A. Roch, C. Robic, E. L. Vander and R. N. Muller, *Chem. Rev.*, 2008, **108**, 2064-2110.
46. P. Tartaj, M. d. P. Morales, S. Veintemillas-Verdaguer, T. Gonzalez-Carreno and C. J. Serna, *J. Phys. D: Appl. Phys.*, 2003, **36**, R182-R197.
47. Y.-w. Jun, J.-w. Seo and J. Cheon, *Acc. Chem. Res.*, 2008, **41**, 179-189.
48. A. K. Gupta, R. R. Naregalkar, V. D. Vaidya and M. Gupta, *Nanomedicine* 2007, **2**, 23-39.
49. B. Bonnemain, *J. Drug Targeting*, 1998, **6**, 167-174.
50. M.-S. Martina, J.-P. Fortin, C. Menager, O. Clement, G. Barratt, C. Grabielle-Madelmont, F. Gazeau, V. Cabuil and S. Lesieur, *J. Am. Chem. Soc.*, 2005, **127**, 10676-10685.
51. C. G. Hadjipanayis, M. J. Bonder, S. Balakrishnan, X. Wang, H. Mao and G. C. Hadjipanayis, *Small*, 2008, **4**, 1925-1929.
52. S. Giri, B. G. Trewyn, M. P. Stellmaker and V. S. Y. Lin, *Angew. Chem., Int. Ed.*, 2005, **44**, 5038-5044.
53. T.-J. Yoon, J. S. Kim, B. G. Kim, K. N. Yu, M.-H. Cho and J.-K. Lee, *Angew. Chem., Int. Ed.*, 2005, **44**, 1068-1071.
54. J. Dobson, *Drug Dev. Res.*, 2006, **67**, 55-60.
55. B. Polyak and G. Friedman, *Expert Opin. Drug Delivery*, 2009, **6**, 53-70.
56. A. Jordan, R. Scholz, P. Wust, H. Fahling and R. Felix, *J. Magn. Magn. Mater.*, 1999, **201**, 413-419.
57. M. Johannsen, U. Gneveckow, L. Eckelt, A. Feussner, N. Waldofner, R. Scholz, S. Deger, P. Wust, S. A. Loening and A. Jordan, *Int J Hyperthermia*, 2005, **21**, 637-647.
58. A. Ito, M. Shinkai, H. Honda and T. Kobayashi, *Cancer Gene Ther.*, 2001, **8**, 649-654.
59. P. A. Liberti, C. G. Rao and L. W. M. M. Terstappen, *J. Magn. Magn. Mater.*, 2001, **225**, 301-307.
60. S. Morisada, N. Miyata and K. Iwahori, *J. Microbiol. Methods*, 2002, **51**, 141-148.
61. K. El-Boubbou, C. Gruden and X. Huang, *J. Am. Chem. Soc.*, 2007, **129**, 13392-13393.

62. C. Xu, K. Xu, H. Gu, R. Zheng, H. Liu, X. Zhang, Z. Guo and B. Xu, *J. Am. Chem. Soc.*, 2004, **126**, 9938-9939.

63. T. Sasaki, N. Iwasaki, K. Kohno, M. Kishimoto, T. Majima, S.-I. Nishimura and A. Minami, *J. Biomed. Mater. Res., Part A*, 2008, **86A**, 969-978.

64. A. Frey, K. T. Giannasca, R. Weltzin, P. J. Giannasca, H. Reggio, W. I. Lencer and M. R. Neutra, *J. Exp. Med.*, 1996, **184**, 1045-1059.

65. J. Rojo, V. Diaz, l. F. J. M. De, I. Segura, A. G. Barrientos, H. H. Riese, A. Bernad and S. Penades, *ChemBioChem*, 2004, **5**, 291-297.

66. l. F. J. M. de and S. Penades, *Biochim. Biophys. Acta, Gen. Subj.*, 2006, **1760**, 636-651.

67. S. Cecioni, V. Oerthel, J. Iehl, M. Holler, D. Goyard, J.-P. Praly, A. Imberty, J.-F. Nierengarten and S. Vidal, *Chem.-Eur. J*, 2011, **17**, 3252-3261.

68. W. Song, C. Xiao, L. Cui, Z. Tang, X. Zhuang and X. Chen, *Colloids Surf., B*, 2012, **93**, 188-194.

69. S. Bian, J. He, K. B. Schesing and A. B. Braunschweig, *Small*, **8**, 2000-2005, S2000/2001-S2000/2017.

70. J. Iehl and J.-F. Nierengarten, *Chem.--Eur. J.*, 2009, **15**, 7306-7309, S7306/7301-S7306/7328.

71. J. Iehl and J.-F. Nierengarten, *Chem. Commun.* , 2010, **46**, 4160-4162.

72. R. Kikkeri, X. Liu, A. Adibekian, Y.-H. Tsai and P. H. Seeberger, *Chem. Commun.*, 2010, **46**, 2197-2199.

73. C.-C. Lin, Y.-C. Yeh, C.-Y. Yang, C.-L. Chen, G.-F. Chen, C.-C. Chen and Y.-C. Wu, *J. Am. Chem. Soc.*, 2002, **124**, 3508-3509.

74. l. F. J. M. de, A. G. Barrientos, T. C. Rojas, J. Rojo, J. Canada, A. Fernandez and S. Penades, *Angew. Chem., Int. Ed.*, 2001, **40**, 2258-2261.

75. A. G. Barrientos, l. F. J. M. de, T. C. Rojas, A. Fernandez and S. Penades, *Chem. Eur. J.*, 2003, **9**, 1909-1921.

76. R. Ojeda, P. J. L. De, A. G. Barrientos, M. Martin-Lomas and S. Penades, *Carbohydr. Res.*, 2007, **342**, 448-459.

77. J.-F. Lutz, *Angew. Chem., Int. Ed.*, 2007, **46**, 1018-1025.

78. W. H. Binder and R. Sachsenhofer, *Macromol. Rapid Commun.*, 2007, **28**, 15-54.

79. M. Meldal, *Macromol. Rapid Commun.*, 2008, **29**, 1016-1051.

80. J.-F. Lutz and Z. Zarafshani, *Adv. Drug Delivery Rev.*, 2008, **60**, 958-970.
81. J.-F. Lutz and H. G. Boerner, *Prog. Polym. Sci.*, 2008, **33**, 1-39.
82. Y. L. Angell and K. Burgess, *Chem. Soc. Rev.*, 2007, **36**, 1674-1689.
83. D. C. Kennedy, C. S. McKay, L.-L. Tay, Y. Rouleau and J. P. Pezacki, *Chem. Commun.* , 2011, **47**, 3156-3158.
84. D. Grunstein, M. Maglinao, R. Kikkeri, M. Collot, K. Barylyuk, B. Lepenies, F. Kamena, R. Zenobi and P. H. Seeberger, *J. Am. Chem. Soc.*, 2011, **133**, 13957-13966.
85. R. Kikkeri, I. Garcia-Rubio and P. H. Seeberger, *Chem. Commun.* , 2009, 235-237.
86. D. L. Huber, *Small*, 2005, **1**, 482-501.
87. S. Mornet, S. Vasseur, F. Grasset and E. Duguet, *J. Mater. Chem.*, 2004, **14**, 2161-2175.
88. Q. A. Pankhurst, J. Connolly, S. K. Jones and J. Dobson, *J. Phys. D: Appl. Phys.*, 2003, **36**, R167-R181.
89. l. F. J. M. De, D. Alcantara, P. Eaton, P. Crespo, T. C. Rojas, A. Fernandez, A. Hernando and S. Penades, *J. Phys. Chem. B*, 2006, **110**, 13021-13028.
90. J. Gallo, I. Garcia, N. Genicio, D. Padro and S. Penades, *Biomaterials*, 2011, **32**, 9818-9825.
91. J. Gallo, I. Garcia, D. Padro, B. Arnaiz and S. Penades, *J. Mater. Chem.*, 2010, **20**, 10010-10020.
92. L. Polito, D. Monti, E. Caneva, E. Delnevo, G. Russo and D. Prosperi, *Chem. Commun.*, 2008, 621-623.
93. Q. Wang, T. R. Chan, R. Hilgraf, V. V. Fokin, K. B. Sharpless and M. G. Finn, *J. Am. Chem. Soc.*, 2003, **125**, 3192-3193.
94. H. Gleiter, *Adv. Mater. (Weinheim, Fed. Repub. Ger.)*, 1992, **4**, 474-481.
95. W. C. Chan and S. Nie, *Science*, 1998, **281**, 2016-2018.
96. H. Mattoussi, J. M. Mauro, E. R. Goldman, G. P. Anderson, V. C. Sundar, F. V. Mikulec and M. G. Bawendi, *J. Am. Chem. Soc.*, 2000, **122**, 12142-12150.
97. l. F. J. M. de, M. Fandel, C. C. Berry, M. Riehle, L. Cronin, G. Aitchison and A. S. G. Curtis, *ChemBioChem*, 2005, **6**, 989-991.
98. J. O. Winter, T. Y. Liu, B. A. Korgel and C. E. Schmidt, *Adv. Mater.*, 2001, **13**, 1673-1677.

99. M. E. Akerman, W. C. W. Chan, P. Laakkonen, S. N. Bhatia and E. Ruoslahti, *Proc. Natl. Acad. Sci. U. S. A.*, 2002, **99**, 12617-12621.

100. G. Spreitzer, J. M. Whitling, J. D. Madura and D. W. Wright, *Chem. Commun.*, 2000, 209-210.

101. S. Sapra, J. Nanda, D. D. Sarma, E.-A. F. Abed and G. Hodes, *Chem. Commun.* , 2001, 2188-2189.

102. E. R. Goldman, E. D. Balighian, H. Mattoussi, M. K. Kuno, J. M. Mauro, P. T. Tran and G. P. Anderson, *J. Am. Chem. Soc.*, 2002, **124**, 6378-6382.

103. X. Wu, H. Liu, J. Liu, K. N. Haley, J. A. Treadway, J. P. Larson, N. Ge, F. Peale and M. P. Bruchez, *Nat. Biotechnol.*, 2003, **21**, 41-46.

104. J. K. Jaiswal, H. Mattoussi, J. M. Mauro and S. M. Simon, *Nat. Biotechnol.*, 2003, **21**, 47-51.

105. B. Dubertret, P. Skourides, D. J. Norris, V. Noireaux, A. H. Brivanlou and A. Libchaber, *Science* 2002, **298**, 1759-1762.

106. R. Mahtab, J. P. Rogers and C. J. Murphy, *J. Am. Chem. Soc.*, 1995, **117**, 9099-9100.

107. D. Gerion, W. J. Parak, S. C. Williams, D. Zanchet, C. M. Micheel and A. P. Alivisatos, *J. Am. Chem. Soc.*, 2002, **124**, 7070-7074.

108. D. J. Maxwell, J. R. Taylor and S. Nie, *J. Am. Chem. Soc.*, 2002, **124**, 9606-9612.

109. S. J. Rosenthal, I. Tomlinson, E. M. Adkins, S. Schroeter, S. Adams, L. Swafford, J. McBride, Y. Wang, L. J. DeFelice and R. D. Blakely, *J. Am. Chem. Soc.*, 2002, **124**, 4586-4594.

110. S. Westenhoff and N. A. Kotov, *J. Am. Chem. Soc.*, 2002, **124**, 2448-2449.

111. I. Potapova, R. Mruk, S. Prehl, R. Zentel, T. Basche and A. Mews, *J. Am. Chem. Soc.*, 2003, **125**, 320-321.

112. Y. Chen, T. Ji and Z. Rosenzweig, *Nano Lett.*, 2003, **3**, 581-584.

113. X.-L. Sun, W. Cui, C. Haller and E. L. Chaikof, *ChemBioChem*, 2004, **5**, 1593-1596.

114. l. F. J. M. de and S. Penades, *Tetrahedron: Asymmetry*, 2005, **16**, 387-391.

115. R. Kikkeri, P. Laurino, A. Odedra and P. H. Seeberger, *Angew. Chem., Int. Ed.*, 2010, **49**, 2054-2057, S2054/2051-S2054/2057.

116. R. Kikkeri, B. Lepenies, A. Adibekian, P. Laurino and P. H. Seeberger, *J. Am. Chem. Soc.*, 2009, **131**, 2110-2112.

117. P. Laurino, R. Kikkeri and P. H. Seeberger, *Nat. Protoc.*, 2011, **6**, 1209-1220.

118. I. Garcia, M. Marradi and S. Penades, *Nanomedicine* 2010, **5**, 777-792.

119. M. Marradi, M. Martin-Lomas and S. Penades, *Adv. Carbohydr. Chem. Biochem.*, 2010, **64**, 211-290.

120. l. F. J. M. De, P. Eaton, A. G. Barrientos, M. Menendez and S. Penades, *J. Am. Chem. Soc.*, 2005, **127**, 6192-6197.

121. C.-C. Lin, Y.-C. Yeh, C.-Y. Yang, G.-F. Chen, Y.-C. Chen, Y.-C. Wu and C.-C. Chen, *Chem. Commun. (Cambridge, U. K.)*, 2003, 2920-2921.

122. l. F. J. M. de and S. Penades, *Glycoconjugate J.*, 2004, **21**, 149-163.

123. N. Kojima and S. Hakomori, *J. Biol. Chem.*, 1989, **264**, 20159-20162.

124. S. H. Rouhanifard, R. Xie, G. Zhang, X. Sun, X. Chen and P. Wu, *Biomacromolecules*, 2012, **13**, 3039-3045.

125. N. P. Pera, A. Kouki, S. Haataja, H. M. Branderhorst, R. M. J. Liskamp, G. M. Visser, J. Finne and R. J. Pieters, *Org. Biomol. Chem.*, 2010, **8**, 2425-2429.

126. J.-h. Lee, M. J. Jung, Y. H. Hwang, Y. J. Lee, S. Lee, D. Y. Lee and H. Shin, *Biomaterials*, 2012, **33**, 4861-4871.

127. C.-H. Lai, C.-Y. Lin, H.-T. Wu, H.-S. Chan, Y.-J. Chuang, C.-T. Chen and C.-C. Lin, *Adv. Funct. Mater.*, 2010, **20**, 3948-3958.

128. M. Moros, B. Hernaez, E. Garet, J. T. Dias, B. Saez, V. Grazu, A. Gonzalez-Fernandez, C. Alonso and l. F. J. M. de, *ACS Nano*, 2012, **6**, 1565-1577.

129. A. Robinson, J.-M. Fang, P.-T. Chou, K.-W. Liao, R.-M. Chu and S.-J. Lee, *ChemBioChem*, 2005, **6**, 1899-1905.

130. A. P. Alivisatos, *Science* 1996, **271**, 933-937.

131. I. Coulthard, S. Degen, Y. J. Zhu and T. K. Sham, *Can. J. Chem.*, 1998, **76**, 1707-1716.

132. C. Lopez-Cartes, T. C. Rojas, R. Litran, D. Martinez-Martinez, l. F. J. M. De, S. Penades and A. Fernandez, *J. Phys. Chem. B*, 2005, **109**, 8761-8766.

133. P. Crespo, R. Litran, T. C. Rojas, M. Multigner, l. F. J. M. de, J. C. Sanchez-Lopez, M. A. Garcia, A. Hernando, S. Penades and A. Fernandez, *Phys. Rev. Lett.*, 2004, **93**, 087204/087201-087204/087204.

Chapter 2

Synthesis of Silver glyconanoparticles with *C*-glycosyl acids and their stability

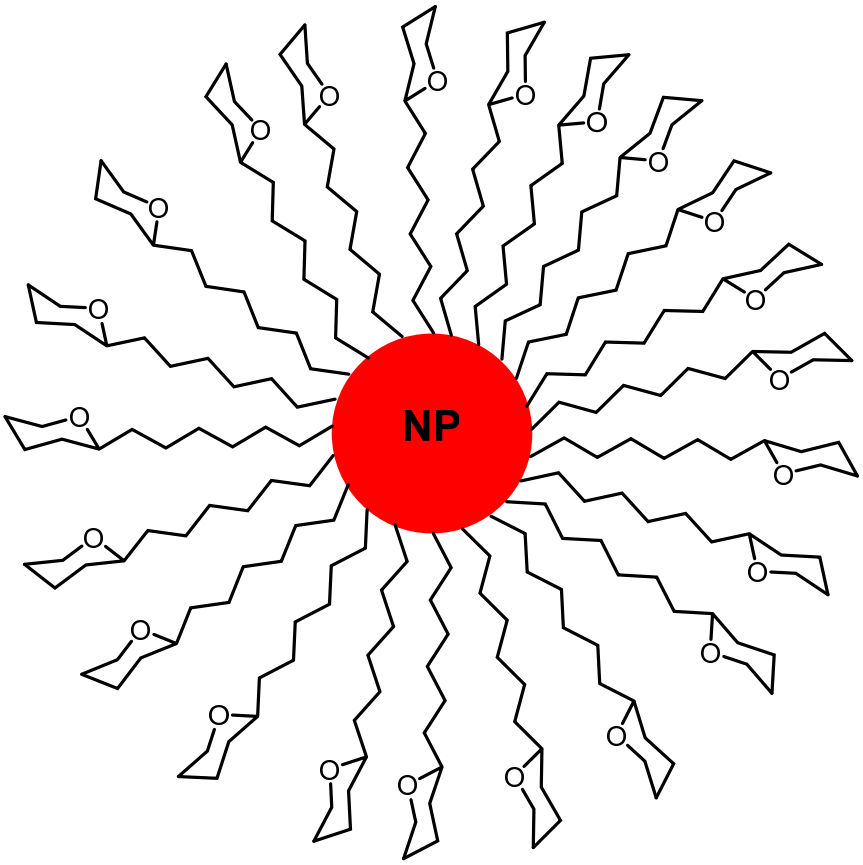

2.1 Introduction

Carbohydrates are important molecules for life together with nucleic acids and proteins.[1-3] While the structure, interactions and function of nucleic acids and proteins in biological processes are reasonably well understood, the role of carbohydrates in the cell is less clear. In many cases cell surface is mostly covered densely by various glycoconjugates such as glycolipids, glycoproteins and proteoglycans which are well-known as glycocalyx.[4] It is known that these glycocalyx are involved in the control of many normal and pathological processes.[5-7]

An interesting feature of the biological interactions where carbohydrates are involved is their extreme low affinity. To overcome this problem, nature utilizes multivalent interactions between the cell surface ligands (oligosaccharides) and their biological receptors (e.g., lectins).[8, 9] Functionalized inorganic nanoparticles with carbohydrate containing molecules are known as glyconanoparticles (GNPs). GNPs are emerging as new tools facilitating the study and understanding of carbohydrate-mediated interactions. These GNPs are mimics of glycocalyx and can be employed to evaluate carbohydrate–carbohydrate and carbohydrate–protein interactions[10-12] because protein-carbohydrate interactions regulate many important biological processes, like cell-cell communication, trafficking, tumor genesis, progression, immune responses, fertilization, apoptosis, and infection.[13-18]

After Penades *et al.* highlighted the application of gold glyconanoparticles to study the self aggregation of Le^x trisaccharide in the presence of calcium in 2001,[19] several research groups have developed different strategies to prepare and apply nanoparticles functionalized with biologically relevant oligosaccharides to study carbohydrate interactions or to intervene in carbohydrate-mediated biological processes.[20-27] At present, there are enough results to indicate that similar to proteins, peptides and DNA, carbohydrates are important partners of inorganic nanomaterials to study/manipulate biological processes.[28-30]

There are different strategies that can be used to access these GNPs. As mentioned previously two methods that are popular in this regard include incubating the glycolipids with appropriate functional groups with preformed nanoparticles or synthesizing nanoparticles in presence of these glycolipids. Typically, gold and silver nanoparticles are obtained by chemical reduction of respective metal salts.[31-33] However, this conventional approach is based on the use of external chemical

reductants that often produce undesired side products. In recent times researchers working in the area of nanoparticle synthesis have developed new methods of synthesis where in the capping agent itself acts as a reducing agent.[34] Therefore, a series of functionalizing agents for noble metal nanoparticles has recently been developed that display a dual role of effective reducing agents and stabilizing agent.[35] These reducing/stabilizing agents apart from carrying out the reduction step, also provide a robust coating to noble metal nanoparticles, within a unique reaction step. Seven different types of these reducing/capping agents were investigated to date: microorganisms and bacteria,[36] plants extracts[37] and physiological molecules, inorganic reagents and metal complexes,[38] organic molecules,[39] organic acids[40] and salts,[41] liposomes, and polymers (Fig. 2.1).[42, 43] In this context we have envisaged that glycosyl acids which have carboxylate as one end-functional group and sugar at another end can act as capping as well as reducing agents in the synthesis of Ag/Au nanoparticles. One such class of compounds are sugars. Sugars are known to be reducing agents and sugar mediated reduction of noble metal ions to noble metal nanoparticles have been well documented. Our group has worked in this area extensively some of the earlier results from our group included the preparation of silver and gold nanoparticles using gellan gum,[37, 44] sophorolipids[45, 46] etc, as capping and reducing agents.

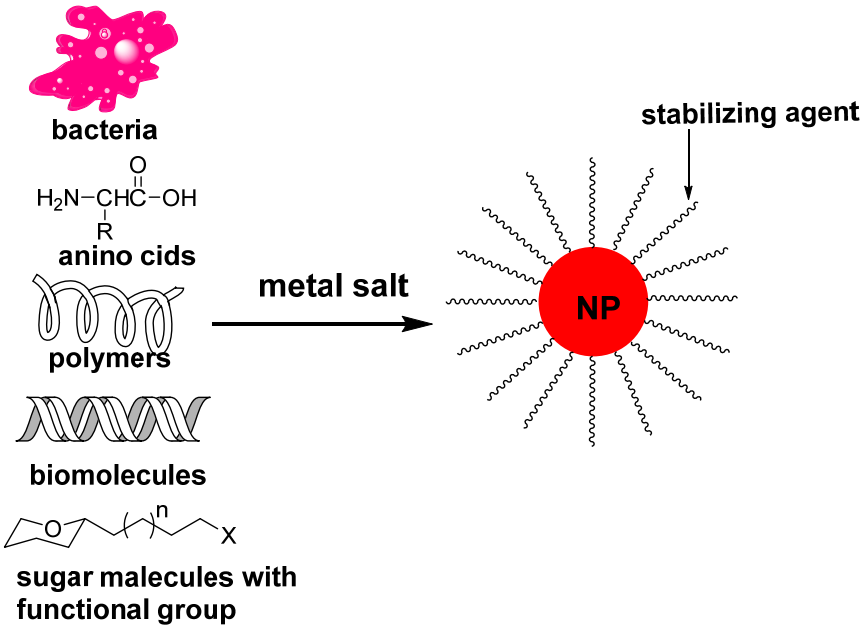

Figure 2.1. *Schematic representation of nanoparticle synthesis by using different molecules as capping/reducing agent.*

2.2 Present work

So far in the literature, GNPs, derived from the surface modification of metal nanoparticles by molecules connected with sugar residues through *O*-glycoside linkages, have been utilized as novel tools to investigate carbohydrate recognition processes[19, 47-51]. However, if the in vivo applications of the GNPs are to be considered, the enzymatic degradation of the *O*-glycoside linkage in these GNPs becomes a great concern. It is in this premise that *C*-glycosides assume greater importance. *C*-glycosides with methylene substitution for the anomeric oxygen, are isosteric mimics of their *O*-glycoside counterparts, and offer a great deal of stability without substantial conformational amendment.[52-55] *C*-glycoside have been known to be potential carbohydrate analogs resistant to metabolic processes. Though the application of *C*-glycosylated long chain alkanes has been explored in liquid crystals and as surfactants,[56] their use in GNPs synthesis has been very sparse and has been unveiled only recently in our group earlier.[57] Expanding this, in this chapter we report our investigations on the synthesis of different 12-*C*-glycosyl long chain acids and their utility as capping/reducing agents during the synthesis of silver nanoparticles. We also investigated the stabilization of silver nanoparticles which were obtained by the reaction of different 12-C-glycosyl long chain acids as capping and reducing agents (Fig 2.2).

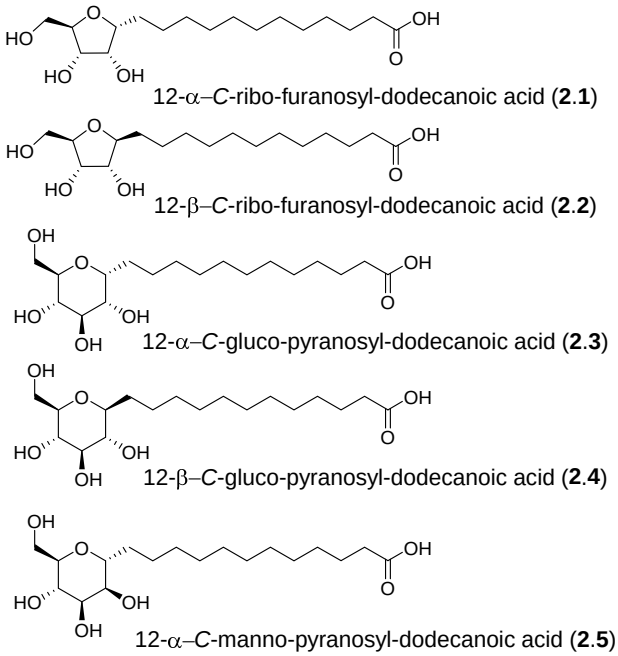

Figure 2.2. *C-glycosides of dodecanoic acid: new capping/reducing agents for glyconanoparticle synthesis*

2.2.1 Retrosynthesis

Considering the fact that the simple monosaccharides in biological systems can exist either in furanose or in pyranose forms, five compounds **2.1-2.5** were selected as representatives of α and β pentoaldofuranose (D-ribo), α and β hexoaldopyranose (D-gluco) and α-D-mannopyranose respectively to carry out this study. The designed retrosynthetic strategy for the *C*-glycosyl acids **2.1-2.5** is based upon the cross-metathesis[58] of the corresponding peracetylated *C*-allyl glycosides **2.22-2.26** with 10-undecene-1-ol (**2.21**) followed by hydrogenation, oxidation and deprotection (Fig 2.3).

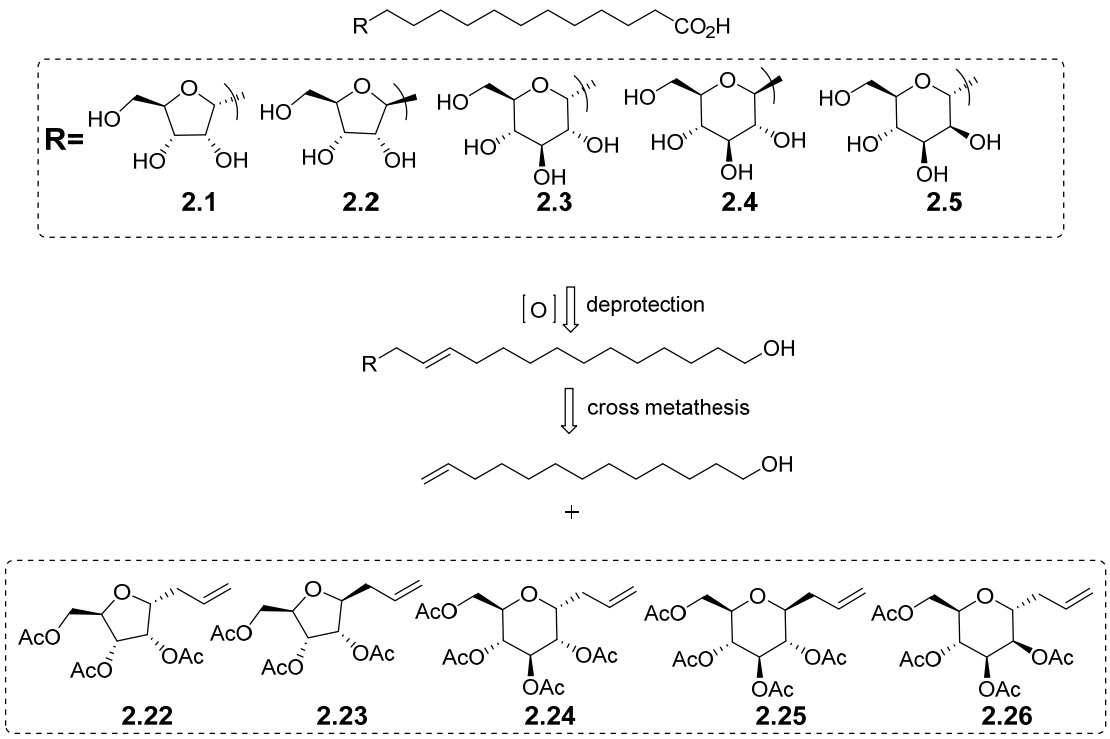

Figure 2.3. *Selected 12-C-glycosylated dodecanoic acids* ***1-5*** *and the retrosynthetic strategy*

2.2.2 Synthesis

The synthesis of differently protected α-*C*-allylribofuranosides[59, 60], β-*C*-allylribofuranosides,[61] α-*C*-allylglucopyranosides,[62, 63] β-*C*-allylglucopyranosides,[64] and α-*C*-allylmannopyranosides[62] (**22-26**) was accomplished following well established procedures.

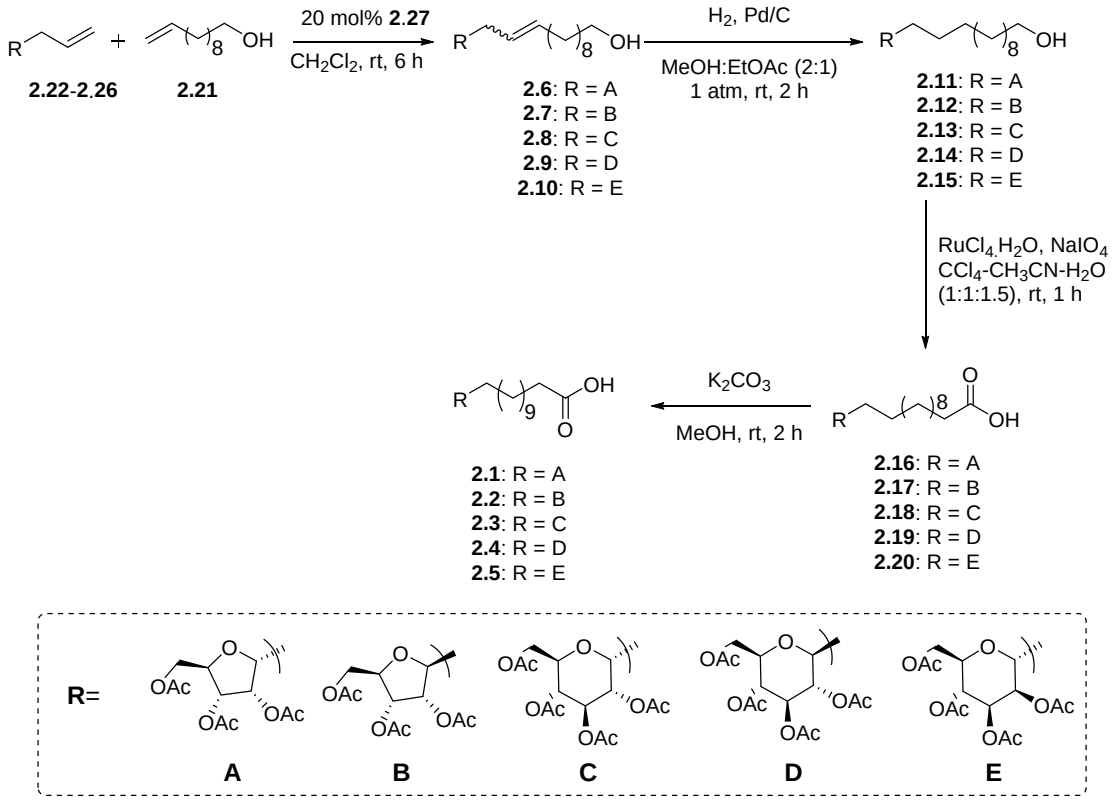

Scheme 2.1. *Synthesis of 12-C-glycosyl-dodecanoic acids* ***2.1-2.5***

Scheme 2.1 depicts the general strategy followed for the synthesis of 12 -*C*-glycosyl dodecanoic acids **2**.**1-2**.**5**, employing cross-metathesis of *C*-allyl derivatives **2**.**22–2**.**26** with 10-undecene-1-ol (**2**.**21**). The *C*-allyl sugar derivative was subjected to cross-metathesis with 10-undecene-1-ol using Grubbs' 1st generation catalyst (**2**.**27**) (20 mol%) to afford inseparable mixture of trans/cis olefins **2**.**6-2**.**10**, along with the 10-undecene-1-ol dimer. The olefin mixture was hydrogenated with 5% Pd/C in methanol:ethyl acetate (1:2) to yield saturated alcohols **2**.**11-2**.**15**. Oxidation of the hydroxyl group to acid with $RuCl_3.H_2O$ and $NaIO_4$ (**2**.**16-2**.**20**) followed by deacetylation completed the synthesis of 12-*C*- glycosyldodecanoic acids **2**.**1-2**.**5** in overall yields of 46%, 51%, 50%, 49% and 48% respectively (synthesis and characterization details are provided in section 2.5).

2.3 Synthesis of Ag-glyconanoparticles and their stability

After synthesizing the desired *C*-glycosyl acids **2**.**1-2**.**5**, the next objective was to use them as capping/reducing agents for the synthesis of silver glyconanoparticles (Ag GNPs). It has already been established that 12-α-*C*-glycosyl acid can be used as

capping and reducing agents for Ag GNPs.[57] Utilizing similar strategy, the synthesis of Ag GNPs using 12-*C*-glycosyl acids **2.1-2.5** were accomplished. A typical synthesis of Ag GNPs was accomplished in the following manner. Equimolar quantities of silver nitrate (10^{-4} M) and 12-*C*-glycosyl acid **2.1-2.5** (10^{-4} M) were heated (~50-60 °C) in dilute alkaline solution.[65] The reduction of Ag^{+1} to Ag^{0} was instantaneous and the Ag GNPs could be isolated as stable powder by simple centrifugation. The Ag nanoparticles synthesized using the different molecules **2.1-2.5** will be abbreviated as Ag GNPs-**2.1**, Ag GNPs-**2.2**, Ag GNPs-**2.3**, Ag GNPs-**2.4** and Ag GNPs-**2.5** respectively. Figure 2.3 shows the UV-vis spectrum of Ag GNPs capped by 12-*C*-glycosyl acids (**2.1-2.5**) at different time intervals after their formation. As it was mentioned the reduction of Ag^{+1} to Ag^{0} with all the acids was instantaneous and within 5 min a well defined peak at λ_{max} at 412 nm developed. This peak is attributed to the surface plasmon resonance and is characteristic of Ag GNPs formation. These synthesized Ag GNPs were kept dispersed in water and the UV-vis spectra were recorded at different time intervals. The UV-vis spectra of Ag NPs reduced/capped by molecule **2.1** (Fig. 2.4 A), **2.3** (Fig. 2.4 C) and **2.5** (Fig. 2.4 E) display no change in the λ_{max} and peak width even after 2 days. However, in the case of Ag GNPs-**2.2** (Fig. 2.4 B) and Ag GNPs-**2.4** (Fig. 2.4 D) the UV-vis spectra shows a gradual red shift in the λ_{max}. The peak width becomes broad and the intensity also gradually decreases. All these are indications of aggregation of nanoparticles. In fact in these two cases most of the Ag NPs were indeed found at the bottom of vials.

From all the above observations we could conclude that Ag NPs reduced/capped with α-*C*-glycosyl acids were forming stable NPs, whereas in the case of β-*C*-glycosyl acids reduced/capped Ag NPs were getting agglomerated over time.

Figure 2.5 shows TEM images of the Ag GNPs-**2.1** to Ag GNPs-**2.5**. Figure 2.5 (A, C and E) are images of Ag GNPs reduced/capped with **2.1, 2.3** and **2.5** respectively. Here one could see that particles are spherical and polydispersed, with a size distribution of ~10-20 nm. In the case of Ag GNPs-**2.2** and Ag GNPs-**2.4** (Fig. 2.5 B and D), aggregation of particles was noticed without any control on the particle size. This result is in accordance with UV-vis results mentioned earlier. High-resolution electron micrograph of Ag GNPs-**2.3** (Fig. 2.5 F) reveals that the particles are single crystalline in nature. The fringe spacing between two crystal layers of silver is about 0.23 nm, which is consistent with the (1 1 1) facet of fcc Ag metal. Thus from

the above results it can be concluded that, all the different *C*-glycosides can affect the reduction of Ag^{+} ions to Ag NPs. However, the particles obtained with the **2.1**, **2.3** and **2.5** have well defined size and shape and are also more stable.

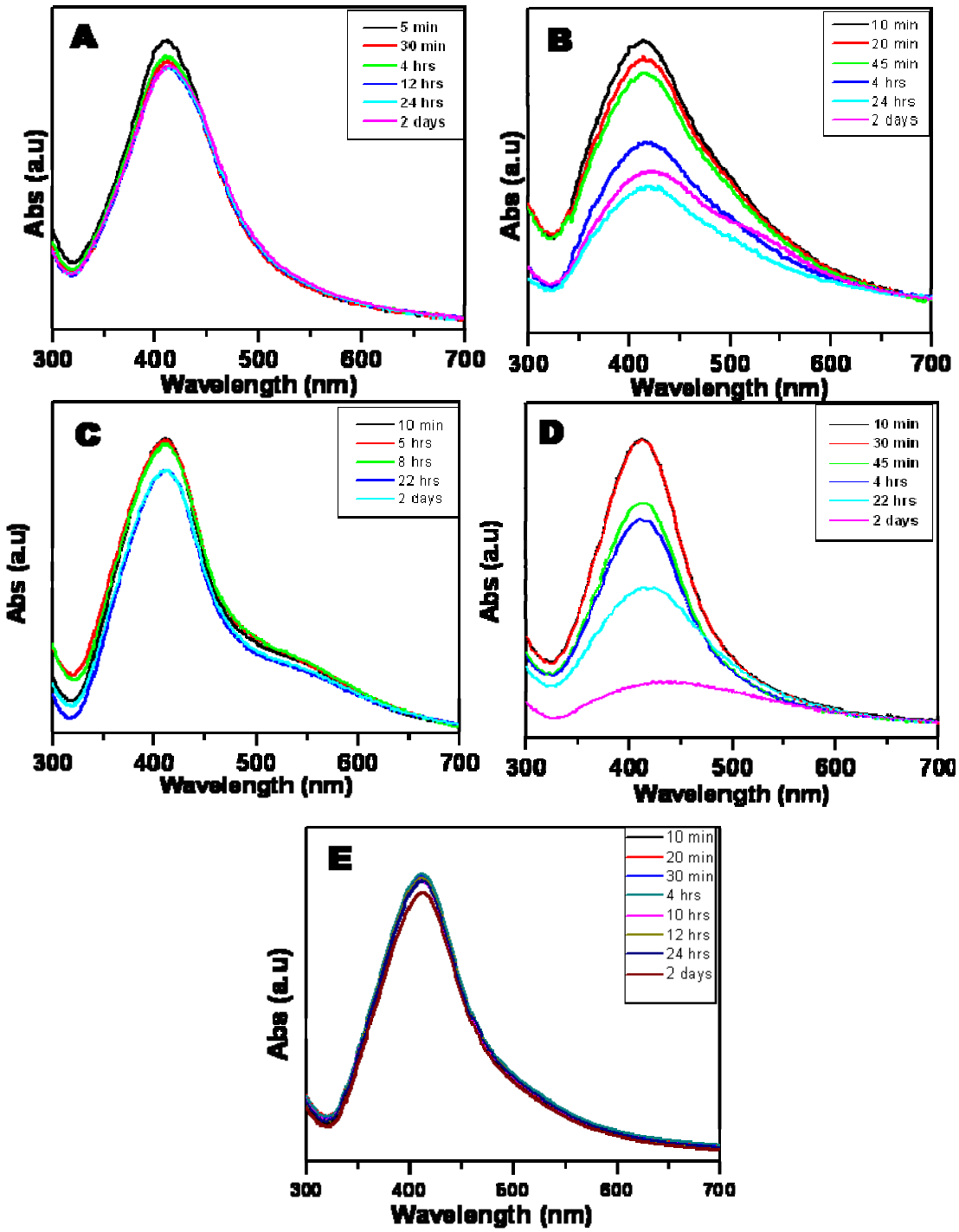

Figure 2.4. *UV-vis spectrum of Ag GNPs at different time intervals after their formation (A) Ag GNPs-**2.1** (B) Ag GNPs-**2.2** (C) Ag GNPs-**2.3** (D) Ag GNPs-**2.4** and (E) Ag GNPs-**2.5***

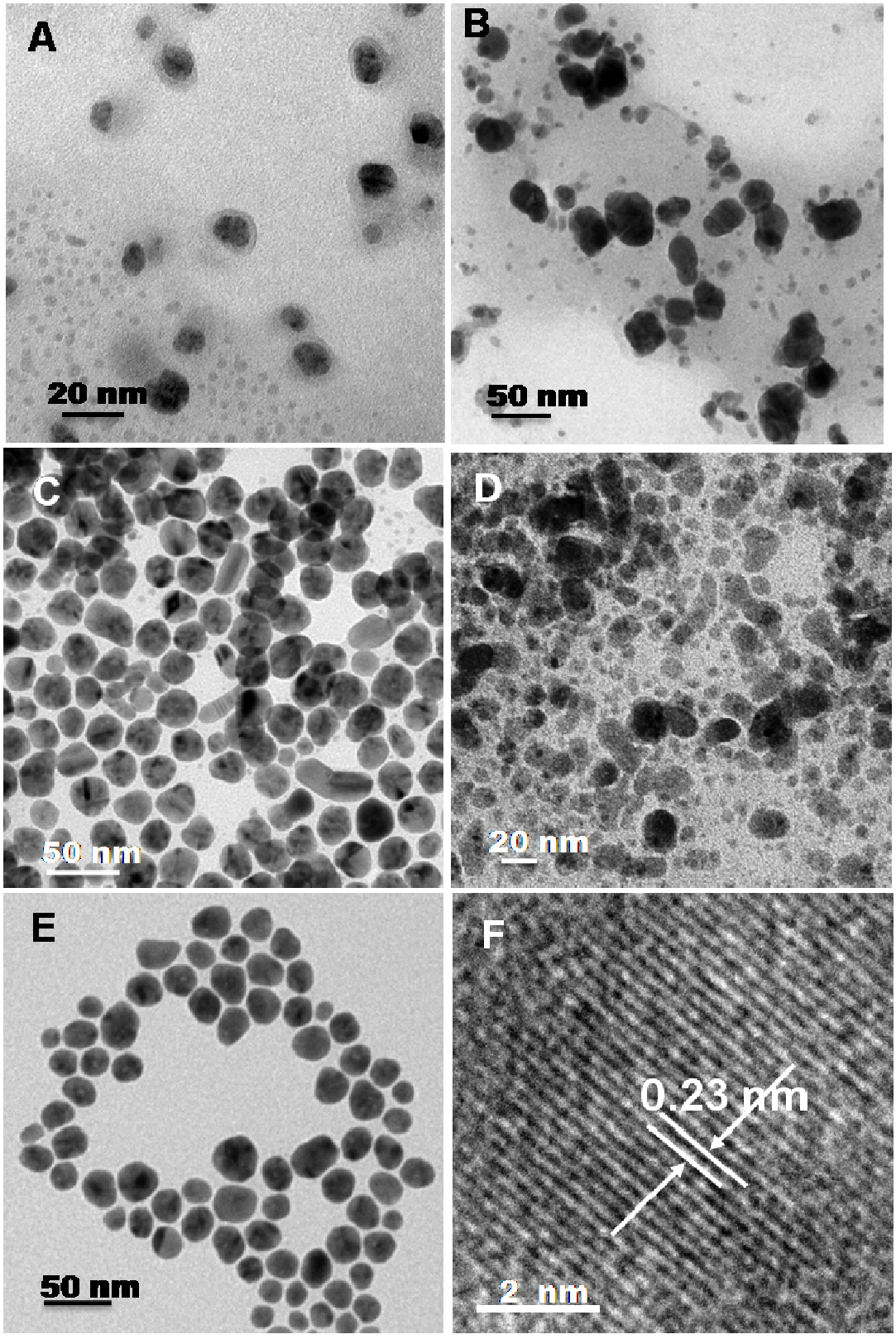

Figure 2.5**. TEM images of (A) Ag GNPs-**2.1**, (B) Ag GNPs-**2.2**, (C) Ag GNPs-**2.3**, (D) Ag GNPs-**2.4**, (E) Ag GNPs-**2.5** and (E) HRTEM image of Ag GNPs-**2.3

2.4 Conclusions

In conclusion, 12-α/β-*C*-glycosyl dodecanoic acids containing either ribopentofuranose or glucohexopyranose motifs were synthesized, by employing cross-metathesis as the key step. Ag GNPs synthesized by using 12-α-*C*-glycosyl acid (**2.1**, **2.3** and **2.5**) as capping/reducing agent, are stable, where as Ag NPs synthesized by using 12-β-*C*-glycosyl acid (**2.2** and **2.4**) as capping/reducing agent, are agglomerated.

2.5 Experimental

1-(2,3,5-Tri-*O*-acetyl-α-D-ribofuranosyl)-12-hydroxydodec-2-ene (2.6)

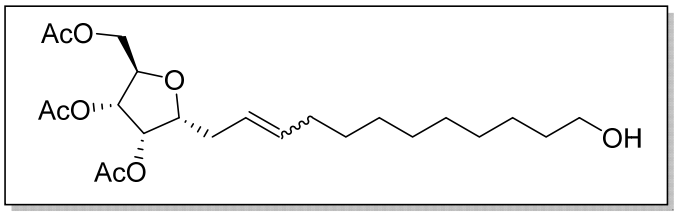

A solution of *C*-allyl derivative (200 mg, 0.67 mmol), 10-undec-1-ol (**2.21**) (567 mg, 3.3 mmol), Grubbs' Ist generation catalyst (26 mg, 0.03 mmol) in dry DCM (15 mL) was degassed with argon and heated at 40 °C (oil bath temperature) for 24 h, under inert atmosphere. The reaction mixture was cooled to room temperature and concentrated under reduced pressure. The residue was purified by column chromatography (4:1 petroleum ether/ethyl acetate) to afford inseparable mixture of *E/Z* isomers **6** [2.7:1] (110 mg, 37%) as colorless oil, 10-undec-1-ol dimer (115 mg, 55%) as a white amorphous solid. The same procedure has been followed to synthesize compounds **2.7**-**2.10**. IR ($CHCl_3$): υ 3482, 3018, 2929, 2855, 1750, 1437, 1374, 1326, 756 cm^{-1}. ^{1}H NMR (200 MHz, $CDCl_3$): δ 1.27 (m, 10H), 1.40–1.57 (m, 4H), 1.94 (dd, J = 6.6, 13.1 Hz, 2H), 2.02 (s, 3H), 2.08 (s, 3H), 2.12 (s, 3H), 2.31 (dd, J = 6.7, 13.6 Hz, 2H), 3.61 (t, J = 6.6 Hz, 2H), 4.06 (dd, J = 4.6, 11.2 Hz, 1H), 4.10–4.21 (m, 2H), 4.26 (dd, J = 2.7, 11.2 Hz, 1H), 5.22 (dd, J = 4.5, 7.8 Hz, 1H), 5.24 (ddd, J = 6.8, 11.5, 14.7 Hz, 1H), 5.39 (dd, J = 3.4, 4.5 Hz, 2H), 5.42–5.53 (m, 1H). ^{13}C NMR (50 MHz, $CDCl_3$): δ 20.3 (q), 20.4 (q), 20.6 (q), 25.6 (t), 27.2 (t), 27.3 (t), 28.9 (t), 29.1 (t), 29.3 (t), 29.4 (t), 32.4 (t), 32.6 (t), 62.6 (t), 63.6 (t), 72.0 (d), 76.5 (d), 79.1 (d), 79.3 (d), 123.8 (d), 134.1 (d), 169.5 (s), 169.6 (s), 170.4 (s) ppm. ESI-MS: *m/z* 465.2 (100%, $[M+Na]^+$). Anal. Calcd for $C_{23}H_{38}O_8$: C, 62.42; H, 8.65. Found: C, 62.39; H, 8.60.

12-(2,3,5-Tri-*O*-acetyl-α-D-ribofuranosyl)-dodecane (2.11)

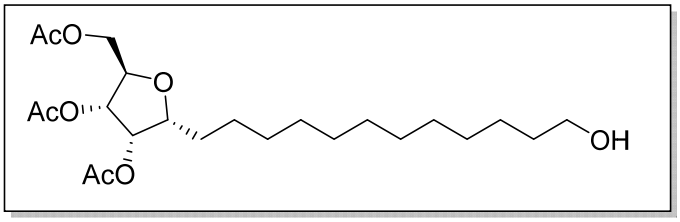

To a solution of alcohol **2.6** (200 mg, 0.45 mmol) in MeOH:EtOAc (1:2), 5% Pd-C (10 mg) was added. The solution was stirred under hydrogen atmosphere at room temperature for 2 h. Reaction mixture was filtered through a short pad of celite and washed with methanol. The combined filtrate was concentrated and the crude residue was purified by column chromatography (4:1 petroleum ether/ethylacetate) to furnish the alcohol **2.11** (159 mg, 79%) as a colorless liquid. The same procedure has been followed to synthesize the compounds **2.12**-**2.15**. $[\alpha]_D^{25}$ = +32.0 (*c* 1.0, $CHCl_3$). IR ($CHCl_3$): υ 3404, 3019, 2928, 2855, 1745, 1216, 1046, 757, 668 cm^{-1}. ^1H NMR (200 MHz, $CDCl_3$): δ 1.24 (s, 18H), 1.45–1.60 (m, 4H), 2.02 (s, 3H), 2.08 (s, 3H), 2.12 (s, 3H), 3.61 (t, *J* = 6.5 Hz, 2H), 4.06 (dd, *J* = 4.8, 10.9 Hz, 1H), 4.11 (dd, *J* = 1.8, 3.3 Hz, 1H), 4.15 (dd, *J* = 4.5, 7.6 Hz, 1H), 4.26 (dd, *J* = 2.3, 10.9 Hz, 1H), 5.22 (dd, *J* = 4.5, 7.6 Hz, 1H), 5.39 (dd, *J* = 3.3, 4.5 Hz, 1H). ^{13}C NMR (50 MHz, $CDCl_3$): δ 20.2 (q), 20.3 (q), 20.6 (q), 25.3 (t), 25.6 (t), 29.0 (t), 29.2 (t), 29.3 (t), 29.3 (t), 29.3 (t), 29.4 (t), 29.4 (t), 32.6 (t), 62.5 (t), 63.6 (t), 72.2 (d), 72.3 (d), 76.2 (d), 79.4 (d), 169.4 (s), 169.7 (s), 170.3 (s) ppm. ESI-MS: *m/z* 467.2 (100%, $[M+Na]^+$). Anal. Calcd for $C_{23}H_{40}O_8$: C, 62.14; H, 9.07. Found: C, 62.19; H, 9.11.

1-(2,3,5-Tri-*O*-acetyl-α-D-ribofuranosyl)-12-dodecanoic acid (2.16)

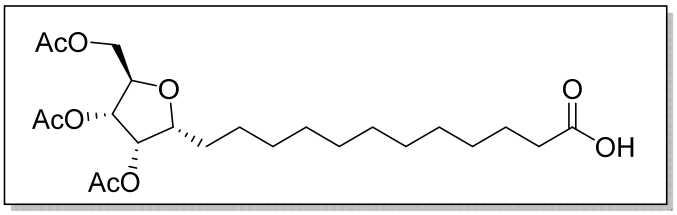

To a solution of alcohol **2.11** (150 mg, 0.3 mmol) in CCl_4 (2 mL)-CH_3CN (2 mL)-H_2O (3 mL), $NaIO_4$ (288 mg, 1.3 mmol) and $RuCl_4.H_2O$ (1.8 mg, 0.007 mmol) were added. The biphasic suspension was stirred vigorously for 1 h. The color was changed from wine red to pale brown. Reaction mixture was extracted with DCM (3 x 25 mL). The combined organic layer was dried, (Na_2SO_4), filtered and concentrated. To it diethyl ether (20 mL) was added, filtered through a celite pad to remove metal

impurities, the filtrate was concentrated at reduced pressure and purified by column chromatography (3:1 petroleum ether/acetone) to furnish the triacetate acid **2.16** (126 mg, 81%) as a colorless liquid. Same procedure has been followed to synthesize the compounds **2.17-2.20**. $[\alpha]_D^{25}$ = +21.1 (*c* 1.0, $CHCl_3$). IR ($CHCl_3$): υ 3400, 3020, 2929, 1744, 1711, 1215, 1046, 668 cm^{-1}. ^1H NMR (200 MHz, $CDCl_3$): δ 1.25 (s, 16H), 1.49–1.70 (m, 4H), 2.03 (s, 3H), 2.08 (s, 3H), 2.12 (s, 3H), 2.32 (t, *J* = 7.4 Hz, 2H), 4.04–4.19 (m, 3H), 4.26 (dd, *J* = 2.3, 11.1 Hz, 1H), 5.22 (dd, *J* = 4.5, 7.6 Hz, 1H), 5.39 (dd, *J* = 3.3, 4.5, Hz, 1H). ^{13}C NMR (50 MHz, $CDCl_3$): δ 20.1 (q), 20.2 (q), 20.4 (q), 24.4 (t), 25.3 (t), 28.8 (t), 28.9 (t, 2C), 29.0 (t), 29.1 (t), 29.2 (t), 29.2 (t), 33.7 (t), 63.5 (t, 2C), 72.2 (d), 72.2 (d), 76.2 (d), 79.3 (d), 169.4 (s), 169.6 (s), 170.3 (s), 178.7 (s) ppm. ESI-MS: *m/z* 481.1 (100%, $[M+Na]^+$). Anal. Calcd for $C_{23}H_{38}O_9$: C, 60.24; H, 8.35. Found: C, 60.30; H, 8.39.

1-(α-D-Ribofuranosyl)-12-dodecanoic acid (2.1)

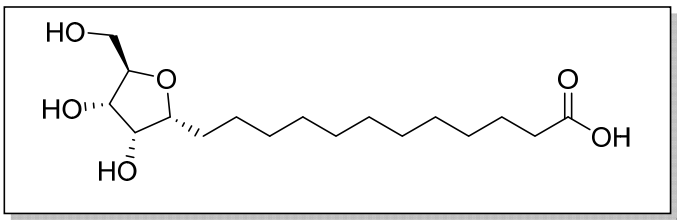

1-(α-D-Ribofuranosyl)-12-dodecanoic acid (2.1): To a solution of acid **2.16** (100 mg, 0.2 mmol) in 5 mL of dry methanol, K_2CO_3 (90 mg, 0.6 mmol) was added. The suspension was stirred at room temperature for 1 h. The reaction mixture was filtered through a celite pad, washed with methanol and combined filtrate was concentrated at reduced pressure. Crude mass was purified by column chromatography (8:1:1 of $CHCl_3$/MeOH/AcOH) to furnish the *C*-glycosyl acid **2.1** (69 mg, 95%) as a white hygroscopic solid. Same procedure has been followed to synthesize the compounds **2.2-2.5**. $[\alpha]_D^{25}$ = +9.0 (*c* 1.0, MeOH). IR ($CHCl_3$): υ 3439, 3258, 2923, 2852, 1709, 1462, 1377 cm^{-1}. ^1H NMR (400 MHz, $CDCl_3$): δ 1.32 (s, 16H), 1.59–1.71 (m, 4H), 2.26 (t, *J* = 7.3 Hz, 2H), 3.58 (dd, *J* = 4.8, 11.8 Hz, 1H), 3.74 (dd, *J* = 2.8, 11.8 Hz, 1H), 3.79 (ddd, *J* = 2.8, 4.5, 7.5 Hz, 1H), 3.91 (dt, *J* = 2.8, 6.8 Hz, 1H), 3.96 (dd, *J* = 3.0, 4.3 Hz, 1H), 4.11 (dd, *J* = 4.5, 8.0 Hz, 1H). ^{13}C NMR (100 MHz, $CDCl_3$): δ 26.4 (t), 27.0 (t), 30.4 (t), 30.5 (t), 30.6 (t), 30.7 (t), 30.8 (t), 31.0 (t), 35.8 (t), 63.5 (t), 73.8 (d), 74.0 (d), 82.6 (d), 82.9 (d), 178.8 (s) ppm. ESI-MS: *m/z* 355.1 (100%, $[M+Na]^+$). Anal. Calcd for $C_{17}H_{32}O_6$: C, 61.42; H, 9.70. Found: C, 61.46; H, 9.73.

1-(2,3,5-Tri-*O*-acetyl-β-D-ribofuranosyl)-12-hydroxydodec-2-ene (2.7)

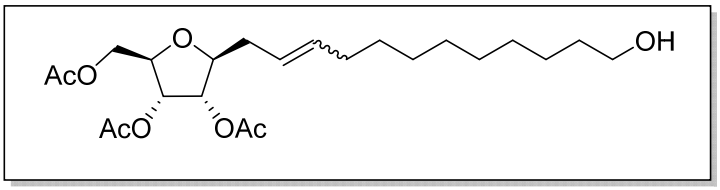

$[\alpha]_D^{25}$ = + 9.33 (*c* 1.0, $CHCl_3$). IR ($CHCl_3$): υ 3434, 2923, 2852, 1749, 1374, 1231, 1047, 666 cm^{-1}. ^1H NMR (500 MHz, $CDCl_3$): δ 1.24 (br s, 14H), 1.50–1.56 (m, 2H), 1.94–2.0 (m, 2H), 2.04 (s, 6H), 2.07 (s, 3H), 2.24–2.41 (m, 1H), 3.60 (t, 2H), 3.97–4.02 (m, 1H), 4.05–4.12 (m, 3H), 4.27–4.31 (m, 1H), 4.93–4.97 (m, 1H), 5.33–5.39 (m, 1H), 5.49–5.54 (m, 1H). ^{13}C NMR (125 MHz, MeOH-d_4): δ 20.5 (q), 20.6 (q), 20.8 (q), 25.6 (m), 32.6 (m), 32.7 (m), 36.0 (m), 60.4 (t), 62.9 (t), 63.6 (d), 71.4 (t), 71.5 (t), 73.4 (t), 73.5 (t), 78.7 (q), 78.8 (q), 80.9 (q), 81.0 (q), 122.8 (q), 123.6 (q), 133.5 (q), 134.7 (q), 169.7 (s), 169.8 (s), 170.6 (s) ppm. ESI-MS: *m/z* 465.8 (100%, $[M+Na]^+$). Anal. Calcd for $C_{23}H_{38}O_8$: C, 62.42; H, 8.65. Found: C, 62.39; H, 8.63.

12-(2,3,5-Tri-*O*-acetyl-β-D-ribofuranosyl)-dodecan-1-ol (2.12)

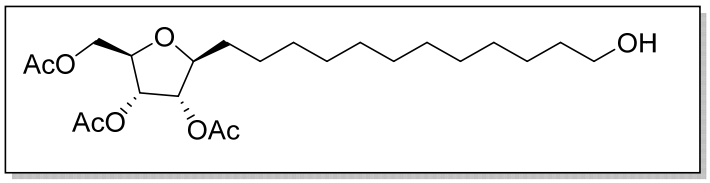

$[\alpha]_D^{25}$ = + 4.33 (*c* 1.0, $CHCl_3$). IR ($CHCl_3$): υ 3482, 3021, 2929, 2856, 1749, 1369, 1216, 1034, 757, 668 cm^{-1}. ^1H NMR (400 MHz, $CDCl_3$): δ 1.22 (br s, 18H), 1.49–1.58 (m, 4H), 2.04 (s, 3H), 2.05 (s, 3H), 2.06 (s, 3H), 3.60 (t, *J* = 6.7 Hz, 2H), 3.92 (q, *J* = 5.5 Hz, 1H), 4.04–4.11 (m, 2H), 4.26-4.31 (m, 1H), 4.92 (t, *J* =5.5 Hz, 1H), 5.09 (t, *J* = 5.5 Hz, 1H). ^{13}C NMR (50 MHz, $CDCl_3$): δ 20.5 (q), 20.6 (q), 20.8 (q), 25.2 (t), 25.7 (t), 29.3 (t) , 29.4 (t), 29.5 (t, 3C), 29.5 (t , 2C), 32.7 (t), 33.2 (t), 62.9 (t), 63.6 (t), 71.6 (d), 74.2 (d), 78.7 (d), 81.2 (d), 169.8 (q), 169.9(q), 170.6 (q) ppm. ESI-MS: *m/z* 467.4 (100%, $[M +Na]^+$). Anal. Calcd for $C_{23}H_{40}O_8$: C, 62.14; H, 9.07. Found: C, 62.17; H, 9.10.

1-(2,3,5-Tri-*O*-acetyl-β-D-ribofuranosyl)-12-dodecanoic acid (2.17)

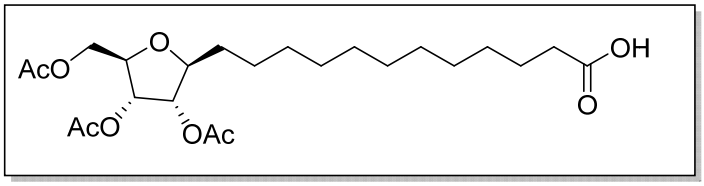

$[\alpha]_D^{25}$ = +4.31 (*c* 1.2, $CHCl_3$). IR ($CHCl_3$): υ 3482, 3021, 2929, 2856, 1749, 1369, 1216, 1034, 757, 668 cm^{-1}. ^1H NMR (400 MHz, $CDCl_3$): δ 1.24 (br s, 16H), 1.53–1.85 (m, 4H), 2.06 (s, 3H), 2.07 (s, 3H), 2.08 (s, 3H), 2.33 (t, *J* = 7.5 Hz , 3H), 3.94 (q, *J* = 5.5 Hz, 1H), 4.06–4.13 (m, 2H), 4.93 (t, *J* = 5.7 Hz, 1H), 5.10 (t, *J* = 5.5 Hz, 1H). ^{13}C NMR (100 MHz, $CDCl_3$): δ 20.6 (q), 20.6 (q), 20.8 (q), 24.7 (t), 25.2 (t), 29.0 (t), 29.2 (t), 29.34 (t), 29.5 (br t, 4C), 33.3 (t), 33.8 (t), 63.6 (t), 71.7 (d), 74.2 (d), 78.7 (d), 81.2 (d), 169.9 (s), 169.9 (s), 170.7 (s), 178.8 (s) ppm. ESI-MS: *m/z* 481.2 (100%, $[M+Na]^+$). Anal. Calcd for $C_{23}H_{38}O_9$: C, 60.24; H, 8.35. Found: C, 60.28; H, 8.38.

1-(β-D-Ribofuranosyl)-12-dodecanoic acid (2.2)

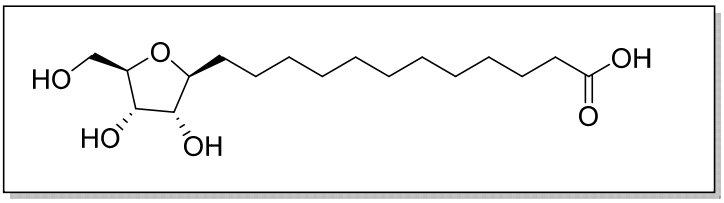

$[\alpha]_D^{25}$ = -1.19 (*c* 1.0, MeOH). IR ($CHCl_3$): υ 3429 (broad), 2881, 2830, 1709,1641,1559, 1414, 1346 cm^{-1}. ^1H NMR (500 MHz, MeOH-d_4): δ 1.20 (br s, 15H), 1.37–1.45 (m, 2H), 1.49 (br s, 3H), 1.83 (s, 4H), 2.10 (t, *J* = 6.6 Hz, 2H), 3.46 (dd, *J* = 5.5, 11.9 Hz , 1H), 3.56–3.63 (m, 3H), 3.67 (dd, *J* = 4.8, 8.8 Hz, 1H), 3.79 (t, *J* = 5 Hz, 1H). ^{13}C NMR (125 MHz, MeOH-d_4): δ 25.6 (t), 26.0 (t), 29.2 (t), 29.3 (br t, 6), 29.4 (t), 33.4 (t), 62.4 (t), 71.5 (d), 74.9 (d), 83.0 (d), 84.0 (d), 177.8 (s) ppm. MS: *m/z* 355.5 (100%, $[M+Na]^+$). Anal. Calcd for $C_{17}H_{32}O_6$: C, 61.42; H, 9.70. Found: C, 61.44; H, 9.72.

1-(2,3,4,6-Tetra-*O*-acetyl-α-D-glucopyranosyl)-12-hydroxydodec-2-ene (2.8)

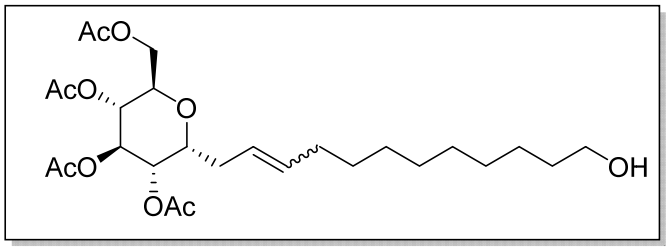

$[\alpha]_D^{25}$ = +15.23 (*c* 1.2, $CHCl_3$). IR ($CHCl_3$): υ 3410, 3020, 2929, 1743, 1750, 1215, 1034, 758, 668 cm^{-1}. ^1H NMR (200 MHz, $CDCl_3$): δ 1.20–1.40 (m, 12H), 1.50–1.65 (m, 4H), 2.03 (s, 3H), 2.04 (s, 3H), 2.05 (s, 3H), 2.09 (s, 3H), 2.21–2.37 (m, 1H), 2.41–2.60 (m, 1H), 3.63 (t, *J* = 6.6 Hz, 2H), 3.75–3.87 (m, 1H), 3.99–4.09 (m, 1H), 4.15–4.27 (m, 2H), 4.93–5.11 (m, 2H), 5.31 (dt, *J* = 3.4, 9.0 Hz, 2H), 5.45–5.61 (m, 1H). ^{13}C NMR (50 MHz, $CDCl_3$): δ 20.3 (q), 20.4 (q), 23.8 (t), 25.5 (t), 27.3 (t), 28.8 (t), 29.0 (t), 29.1 (t), 29.2 (t), 29.3 (t), 32.4 (t), 32.5 (t), 61.9 (t), 62.3 (t), 68.3 (d), 68.5 (d), 70.0 (d), 72.0 (d), 72.2 (d), 132.4 (d), 133.7 (d), 169.1 (s), 169.2 (s), 169.7 (s), 169.8 (s), 170.2 (s) ppm. ESI-MS: *m/z* 537.6 (100%, $[M+Na]^+$). Anal. Calcd for $C_{26}H_{42}O_{10}$: C, 62.42; H, 8.65. Found: C, 62.39; H, 8.60.

1-(2,3,4,6-Tetra-*O*-acetyl-α-D-glucopyranosyl)-12-hydroxydodecane (2.13)

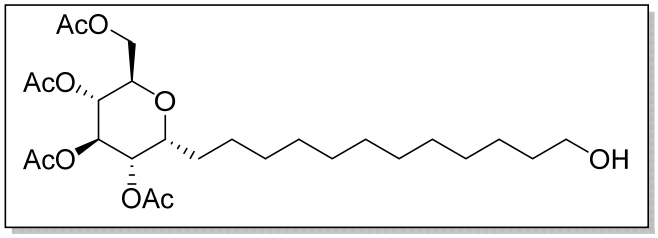

$[\alpha]_D^{25}$ = +15.2 (*c* 1.2, $CHCl_3$). IR ($CHCl_3$): υ 3482, 3021, 2929, 1749, 1369, 1216, 1034, 757, 668 cm^{-1}. ^1H NMR (200 MHz, $CDCl_3$): δ 1.24 (br s, 18H), 1.53–1.90 (m, 4H), 2.03 (s, 3H), 2.03 (s, 3H), 2.05 (s, 3H), 2.09 (s, 3H), 3.63 (t, *J* = 6.5 Hz, 1H), 3.79 (ddd, *J* = 2.3, 5.1, 9.2 Hz, 1H), 4.06 (dd, *J* = 2.6, 12.0 Hz, 2H), 4.22 (dd, *J* = 5.1, 12.0 Hz, 2H), 4.96 (dd, *J* = 9.1, 9.4 Hz, 1H), 5.05 (dd, *J* = 5.8, 9.6 Hz, 1H), 5.29 (dd, *J* = 9.1. 9.4 Hz, 1H). ^{13}C NMR (50 MHz, $CDCl_3$): δ 20.4 (br q, 2C), 20.5 (br q, 2C), 24.8 (t), 25.0 (t), 25.6 (t), 29.1 (t), 29.3 (t), 29.4 (t, 4C), 29.4 (t), 32.6 (t), 62.2 (t), 62.6 (t), 68.3 (d), 68.8 (d), 70.4 (d), 72.4 (d), 169.3 (s), 169.3 (s), 169.9 (s, 2C), 170.3 (s) ppm. ESI-MS: *m/z* 539.6 (100%, $[M+Na]^+$). Anal. Calcd for $C_{26}H_{44}O_{10}$ C, 60.45; H, 8.58. Found: C, 60.39; H, 8.54.

1-(2,3,4,6-Tetra-*O*-acetyl-α-D-glucopyranosyl)-12-dodecanoic acid (2.18)

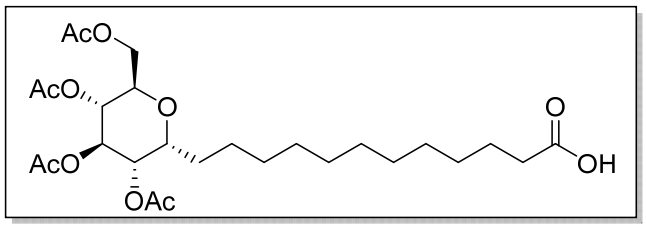

$[\alpha]_D^{25}$ = +54.4 (*c* 1.1, $CHCl_3$). IR ($CHCl_3$): υ 3401, 2929, 1748, 1710, 1368, 1216, 1034, 756 cm^{-1}. ^1H NMR (400 MHz, $CDCl_3$): δ 1.27 (br s, 16H), 1.45–1.51 (m, 2H), 1.63 (qui, *J* = 7.3, 14.5 Hz, 2H), 1.73–1.81 (m, 2H), 2.03 (s, 3H), 2.04 (s, 3H), 2.05 (s, 3H), 2.09 (s, 3H), 2.35 (t, *J* = 7.5 Hz, 2H), 3.81 (ddd, *J* = 2.2, 5.3, 8.8 Hz, 1H), 4.09 (dd, *J* = 2.3, 12.0 Hz, 1H), 4.16 (ddd, *J* = 2.2, 5.3, 8.8 Hz, 1H), 4.23 (dd, *J* = 5.3, 12.0 Hz, 1H), 4.98 (dd, *J* = 9.1. 9.3 Hz, 1H), 5.07 (dd, *J* = 5.8, 9.5 Hz, 1H), 5.33 (dd, *J* = 9.1. 9.3 Hz, 1H). ^{13}C NMR (100 MHz, $CDCl_3$): δ 20.5 (q), 20.6 (q, 3C), 24.6 (t), 24.8 (t), 25.1 (t), 28.9 (t), 29.1 (t), 29.1 (t), 29.2 (t), 29.4 (t), 29.4 (t, 2C), 29.5 (t), 62.3 (t), 68.4 (d), 68.9 (d), 70.4 (d, 2C), 72.5 (d), 169.5 (s), 169.6 (s), 170.2 (s), 170.6 (s), 179.3 (s) ppm. ESI-MS: *m/z* 553.3 (100%, $[M+Na]^+$). Anal. Calcd for $C_{26}H_{42}O_{11}$: C, 58.85; H, 7.98. Found: C, 58.80; H, 8.02.

1-(α-D-Glucopyranosyl)-12-dodecanoic acid (2.3)

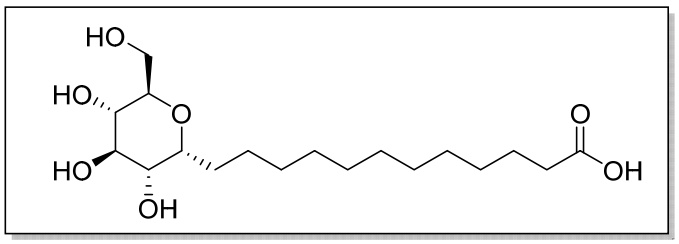

$[\alpha]_D^{25}$ = +46.5 (*c* 4.0, MeOH). IR ($CHCl_3$): υ 3365, 2853, 1709, 1569, 1455, 1377, 1032, 721 cm^{-1}. ^1H NMR (400 MHz, MeOH-d_4): δ 1.30 (br s, 16H), 1.59–1.65 (m, 4H), 2.22 (t, *J* = 7.3 Hz, 2H), 3.25 (dd, *J* = 8.5, 9.3 Hz, 1H), 3.39 (ddd, *J* = 2.2, 5.3, 8.0 Hz, 1H), 3.52 (t, *J* = 8.8 Hz, 1H), 3.60 (dd, *J* = 5.5, 9.5 Hz, 1H), 3.63 (dd, *J* = 5.3, 11.5 Hz, 1H), 3.77 (dd, *J* = 2.5, 11.8 Hz, 1H), 3.80 (dt, *J* = 5.0, 10.0 Hz, 1H). ^{13}C NMR (100 MHz, MeOH-d_4): δ 25.4 (t), 26.7 (t), 27.0 (t), 30.6 (t), 30.6 (t), 30.7 (t), 30.7 (t, 5C), 63.1 (t), 72.4 (d), 73.1 (d), 74.3 (d), 75.3 (d), 77.3 (d) ppm. ESI-MS: *m/z* 385.4 (100%, $[M+Na]^+$). Anal. Calcd for $C_{18}H_{34}O_7$: C, 59.65; H, 9.45. Found: C, 59.69; H, 9.49.

1-(2,3,4,6-Tetra-*O*-acetyl-β-D-glucopyranosyl)-12-hydroxydodec-2-ene (2.9)

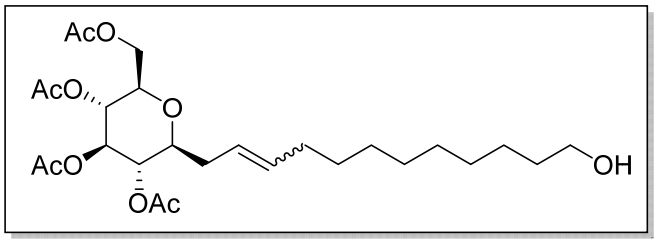

$[\alpha]_D^{25}$ = +15.23 (*c* 1.2, $CHCl_3$). IR ($CHCl_3$): υ 3410, 3020, 2929, 1743, 1750, 1215, 1034, 758, 668 cm^{-1}. ^1H NMR (200 MHz, $CDCl_3$): δ 1.25–1.28 (m, 8H), 1.32–1.33 (m, 4H), 1.54–1.59 (m, 2H), 2.00 (d, *J* = 1.4 Hz, 3H), 2.02 (br s, 3H), 2.03 (br s, 3H), 2.05 (d, *J* = 1.4 Hz, 2H), 2.09 (d, *J* = 1.1 Hz, 3H), 2.16–2.22 (m, 1H), 2.23–2.33 (m, 1H), 3.44–3.48 (m, 1H), 3.62–3.65 (dt, *J* = 1.3, 6.7 Hz, 2H), 4.11 (dd, *J* = 1.4, 7.2 Hz, 1H), 4.14 (dd, *J* = 1.4, 7.2 Hz, 1H), 4.24 (dd, *J* = 4.9, 12.1 Hz, 1H), 4.91 (dt, *J* = 1.1, 9.6 Hz, 1H), 5.05 (dt, *J* = 1.1, 9.6 Hz, 1H), 5.16 (dt, *J* = 1.4, 9.4 Hz, 1H), 5.37–5.49 (m, 2H). ^{13}C NMR (50 MHz, $CDCl_3$): δ 20.5 (q), 20.5 (q), 20.6 (q), 20.6 (q), 25.6 (t), 28.9 (t), 29.0 (t), 29.1 (t), 29.3 (t), 29.4 (t), 32.5 (t), 32.6 (t), 34.5 (t), 62.3 (t), 62.7 (t), 62.7 (d), 68.6 (d), 71.5 (d), 74.4 (d), 75.4 (d), 77.5 (d), 123.8 (d), 134.0 (d), 169.4 (s), 170.3 (s), 170.6 (s) ppm. ESI-MS: (*m/z*) 537.6 (100%, $[M+Na]^+$). Anal. Calcd for $C_{26}H_{42}O_{10}$: C, 62.42; H, 8.65. Found: C, 62.39; H, 8.60.

1-(2,3,4,6-Tetra-*O*-acetyl-β-D-glucopyranosyl)-12-hydroxydodecane (2.14)

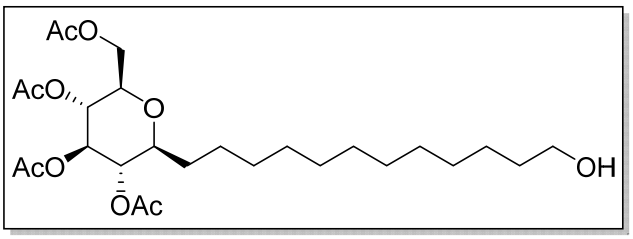

$[\alpha]_D^{25}$ = -10.0 (*c* 1.2, $CHCl_3$). IR ($CHCl_3$): υ 3482, 3021, 2929, 1749, 1369, 1216, 1034, 757, 668 cm^{-1}. ^1H NMR (200 MHz, $CDCl_3$): δ 1.26 (br s, 16H), 1.48–1.65 (m, 6H), 2.00 (s, 3H), 2.02 (s, 3H), 2.04 (s, 3H), 2.08 (s, 3H), 3.33–3.43 (m, 1H), 3.64 (t, *J* = 6.5 Hz, 3H), 4.09 (dd, *J* = 2.3, 12.3 Hz, 1H), 4.25 (dd, *J* = 2.3, 12.3 Hz, 1H), 4.87 (t, *J* = 9.4 Hz, 1H), 5.04 (t, *J* = 9.5 Hz, 1H), 5.16 (t, *J* = 9.3 Hz, 1H). ^{13}C NMR (50 MHz, $CDCl_3$): δ 19.8 (br q, 2C), 19.9 (br q, 2C), 24.3 (t), 25.1 (t), 28.6 (t), 28.7 (t, 2C), 28.8 (t, 2C), 28.8 (t, 2C), 30.5 (t), 32.0 (t), 61.7 (t), 61.8 (t), 68.1 (d), 71.4 (d), 73.8 (d), 74.9 (d), 76.0 (d), 168.8 (s), 168.9 (s), 169.6 (s), 169.9 (s) ppm. ESI-MS: (*m/z*) 539.6 (100%, $[M+Na]^+$). Anal. Calcd for $C_{26}H_{44}O_{10}$: C, 60.45; H, 8.58. Found: C, 60.39; H, 8.54.

1-(2,3,4,6-Tetra-*O*-acetyl-β-D-glucopyranosyl)-12-dodecanoic acid (2.19)

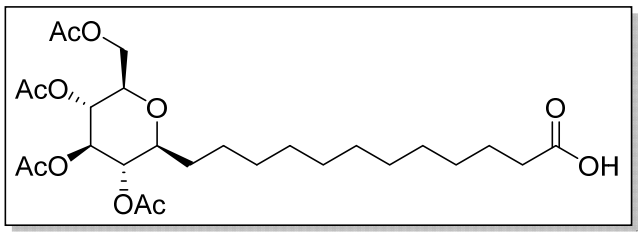

$[\alpha]_D^{29.4}$ = -13.4 (*c* 1, MeOH). IR ($CHCl_3$): υ 3401, 2929, 1748, 1710, 1368, 1216, 1034, 756 cm^{-1}. ^1H NMR (200 MHz, $CDCl_3$): δ 1.26 (br s, 12H), 1.48 (br s, 2H), 1.59–1.66 (m, 2H), 2.00 (s, 3H), 2.02 (s, 3H), 2.04 (s, 3H), 2.08 (s, 3H), 2.34 (t, *J* = 7.5 Hz, 2H), 3.04 (t, *J* = 7.5 Hz, 2H), 3.33–3.43 (m, 1H), 3.57–3.66 (m, 1H), 4.05–4.14 (m, 1H), 4.25 (dd, *J* = 5.1, 12.3 Hz, 1H), 4.87 (t, *J* = 9.3 Hz, 1H), 5.17 (dd, *J* = 9.1, 9.2 Hz, 1H). ^{13}C NMR (50 MHz, $CDCl_3$): δ 20.6 (q), 20.6 (q), 20.7 (q), 20.7 (q), 24.6 (t), 25.0 (t), 29.0 (t), 29.2 (t), 29.4 (t, 2C), 29.5 (t, 3C), 31.3 (t), 33.9 (t), 62.4 (t), 68.8 (d), 72.0 (d), 74.5 (d,), 75.6 (d), 77.8 (d), 169.5 (s), 169.7 (s, 2C), 170.5 (s), 170.8 (s), 179.0 (s) ppm. ESI-MS: (*m/z*) 533.3 (100%, $[M+Na]^+$). Anal. Calcd for $C_{26}H_{42}O_{11}$: C, 58.85; H, 7.98. Found: C, 58.80; H, 8.02.

1-(β-D-Glucopyranosyl)-12-dodecanoic acid (2.4)

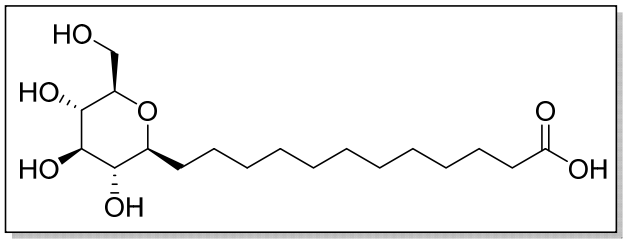

$[\alpha]_D^{29.6}$ = –7.8 (*c* 1, MeOH). IR ($CHCl_3$): υ 3365, 2853, 1709, 1569, 1455, 1377, 1032, 721 cm^{-1}. ^1H NMR (MeOH-d_4, 400 MHz): δ 1.30 (br s, 15H), 1.37–1.44 (m, 2H), 1.60 (t, *J* = 6.3 Hz, 3H), 1.78–1.86 (m, 1H), 1.94 (s, 3H), 2.22 (t, *J* = 7.3 Hz, 2H), 3.05 (d, *J* = 8.5 Hz, 1H), 3.09–3.19 (m, 1H), 3.18 (dd, *J* = 2.3, 5.8 Hz, 1H), 3.24 (d, *J* = 8.8 Hz, 1H), 3.28 (d, *J* = 3.8 Hz, 1H), 3.63 (dd, *J* = 5.5, 11.8 Hz, 1H), 3.83 (dd, *J* = 2.0, 11.8 Hz, 1H). ^{13}C NMR (MeOH-d_4, 100 MHz): δ 26.6 (t), 27.0 (t), 30.6 (t, 2C), 30.8 (t, 2C), 30.8 (t, 3C), 31.0 (t), 33.0 (t), 63.2 (t), 72.1 (d), 75.6 (d), 80.0 (d), 81.0 (d), 81.7 (d) ppm. ESI-MS: (*m/z*) 385.4 (100%, $[M+Na]^+$). Anal. Calcd for $C_{18}H_{34}O_7$: C, 59.65; H, 9.45. Found: C, 59.69; H, 9.49.

1-(2,3,4,6-Tetra-*O*-acetyl-*α*-D-mannopyranosyl)-12-hydroxydodec-2-ene (2.10)

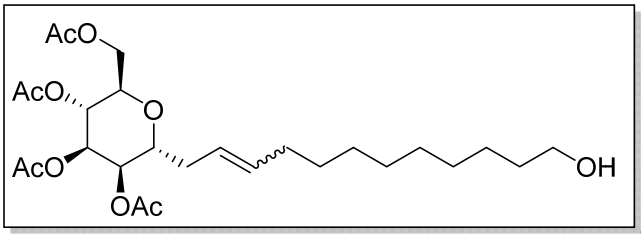

$[\alpha]_D^{25}$ = +6.48 (*c* 1.2, $CHCl_3$). IR ($CHCl_3$): ϑ 3410, 3020, 2929, 1743, 1750, 1215, 1034, 758, 668 cm^{-1}. ^1H NMR (200 MHz, $CDCl_3$): δ 1.20-1.30 (br s, 16H), 1.46–1.55 (m, 2H), 1.97 (s, 3H), 2.01 (s, 3H), 2.04 (s, 3H), 2.08 (s, 3H), 2.15–2.28 (m, 1H), 2.30–2.47 (m, 1H), 3.57 (t, *J* = 6.6 Hz, 2H), 3.80–3.87 (m, 1H), 3.90–3.97 (m, 1H), 4.02–4.08 (m, 1H), 4.26 (dd, *J* = 5.7, 12.0 Hz, 1H) 5.13–5.16 (m, 1H), 5.17–5.24 (m, 2H), 5.26–5.34 (m, 1H), 5.45–5.55 (m, 1H). ^{13}C NMR (50 MHz, $CDCl_3$): δ 20.4 (q, 3C), 20.6 (q), 25.5 (t), 28.8 (t), 28.9 (t), 29.1 (t, 3C), 29.2 (t, 2C), 32.4 (t), 62.5 (t, 2C), 66.6 (d), 68.6 (d), 69.8 (d), 70.1 (d), 74.7 (d), 123.3 (d), 134.4 (d), 169.4 (s), 169.7 (s), 170.0 (s), 170.4 (s) ppm. ESI-MS: (*m/z*) 537.6 (100%, $[M+Na]^+$). Anal. Calcd for $C_{26}H_{42}O_{10}$: C, 62.42; H, 8.65. Found: C, 62.39; H, 8.60.

1-(2,3,4,6-Tetra-*O*-acetyl-α-D-mannopyranosyl)-12-hydroxydodecane (2.15)

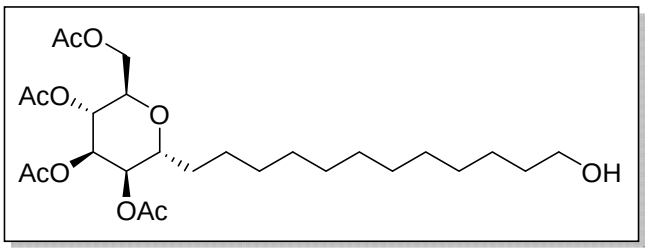

$[\alpha]_D^{25}$ = +4.67 (*c* 1.2, $CHCl_3$). IR ($CHCl_3$): ϑ 3482, 3021, 2929, 1749, 1369, 1216, 1034, 757, 668 cm^{-1}. ^1H NMR (200 MHz, $CDCl_3$): δ 1.24 (br s, 18H), 1.48–1.61 (m, 4H), 2.00 (s, 3H), 2.03 (s, 3H), 2.08 (s, 3H), 2.12 (s, 3H), 3.61 (t, *J* = 6.5 Hz, 2H), 3.75–3.85 (m, 1H), 3.88–3.98 (m, 1H), 4.75 (dd, *J* = 2.6, 9.5 Hz, 1H), 4.28 (dd, *J* = 6.1, 12.1 Hz, 1H), 5.12–5.17 (m, 1H), 5.18–5.23 (m, 2H). ^{13}C NMR (50 MHz, $CDCl_3$): δ 20.7 (q, 3C), 20.9 (q), 25.3 (t), 25.6 (t), 28.3 (t), 29.0 (t), 29.4 (t, 3C), 29.5 (t, 3C), 32.7 (t), 62.6 (t), 62.9 (t), 66.9 (d), 69.1 (d), 69.9 (d), 70.9 (d), 75.4 (d), 169.6 (s), 170.0 (s), 170.3 (s), 170.7 (s) ppm. ESI-MS: *m/z* 539.6 (100%, $[M+Na]^+$). Anal. Calcd for $C_{26}H_{44}O_{10}$ C, 60.45; H, 8.58. Found: C, 60.39; H, 8.54.

1-(2,3,4,6-Tetra-*O*-acetyl-α-D-mannopyranosyl)-12-dodecanoic acid (2.20):

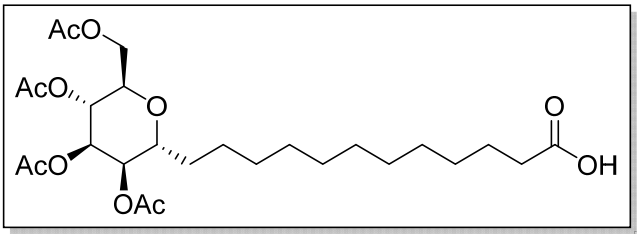

$[\alpha]_D^{25}$ = +4.83 (*c* 1.1, $CHCl_3$). IR ($CHCl_3$): ϑ 3401, 2929, 1748, 1710, 1368, 1216, 1034, 756 cm^{-1}. ^1H NMR (200 MHz, $CDCl_3$): δ 1.26 (br s, 16H), 1.55–1.70 (m, 4H), 2.00 (s, 3H), 2.02 (s, 3H), 2.10 (s, 3H), 2.14 (s, 3H), 2.35 (t, *J* = 7.4 Hz, 2H), 3.80–3.89 (m, 1H), 3.90–4.00 (m, 1H), 4.05–4.15 (m, 2H), 4.31 (dd, *J* = 6.0, 12.0 Hz, 1H), 5.16–5.20 (m, 1H), 5.21–5.25 (m, 1H). ^{13}C NMR (50 MHz, $CDCl_3$): δ 20.7 (q, 3C), 20.9 (q), 24.6 (t), 25.3 (t), 28.9 (t), 29.0 (t), 29.1 (t), 29.3 (t), 29.4 (t, 3C), 29.6 (t), 33.8 (t), 62.6 (t), 66.9 (d), 69.1 (d), 69.9 (d), 70.9 (d), 75.4 (d), 169.7 (s), 170.1 (s), 170.4 (s), 170.7 (s), 179.1 (s) ppm. ESI-MS: *m/z* 553.3 (100%, $[M+Na]^+$). Anal. Calcd for $C_{26}H_{42}O_{11}$: C, 58.85; H, 7.98. Found: C, 58.80; H, 8.02.

1-(α-D-mannopyranosyl)-12-dodecanoic acid (2.5)

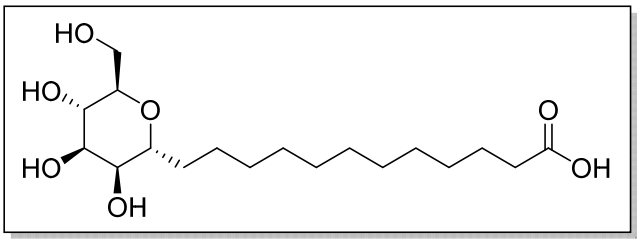

$[\alpha]_D^{25}$ = -51.87 (*c* 4.0, MeOH). IR ($CHCl_3$): ϑ 3365, 2853, 1709, 1569, 1455, 1377, 1032, 721 cm^{-1}. ^1H NMR (400 MHz, CD_3OD): δ 1.28 (br s, 16H), 1.43–1.50 (m, 2H), 1.55–1.64 (m, 2H), 2.25 (t, *J* = 7.1 Hz, 2H), 3.37–3.43 (m, 1H), 3.53–3.62 (m, 1H), 3.63–3.66 (m, 1H), 3.67–3.70 (m, 1H), 3.71–3.77 (m, 2H), 3.79–3.86 (m, 1H). ^{13}C NMR (100 MHz, MeOH-d_4): δ 20.8 (t), 23.5 (t), 24.1 (t), 26.3 (t), 26.7 (t), 27.4 (t), 27.6 (t), 27.8 (t), 27.9 (t, 2C), 30.2 (t), 60.1 (t), 66.3 (d), 69.9 (d), 70.3 (d), 72.6 (d), 76.2 (d), 174.7 (s) ppm. ESI-MS: *m/z* 385.4 (100%, $[M+Na]^+$). Anal. Calcd for $C_{18}H_{34}O_7$: C, 59.65; H, 9.45. Found: C, 59.69; H, 9.49.

2.6 NMR spectral data

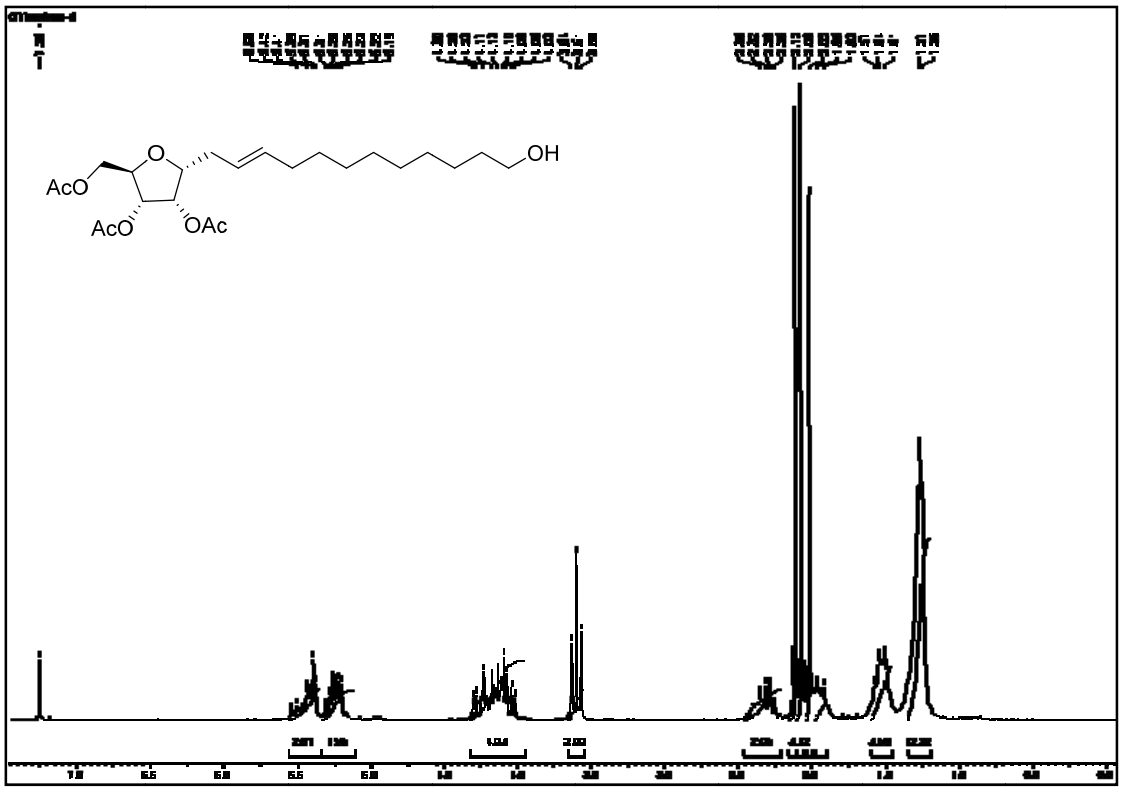

^{1}H NMR spectrum of **2.6** in $CDCl_3$

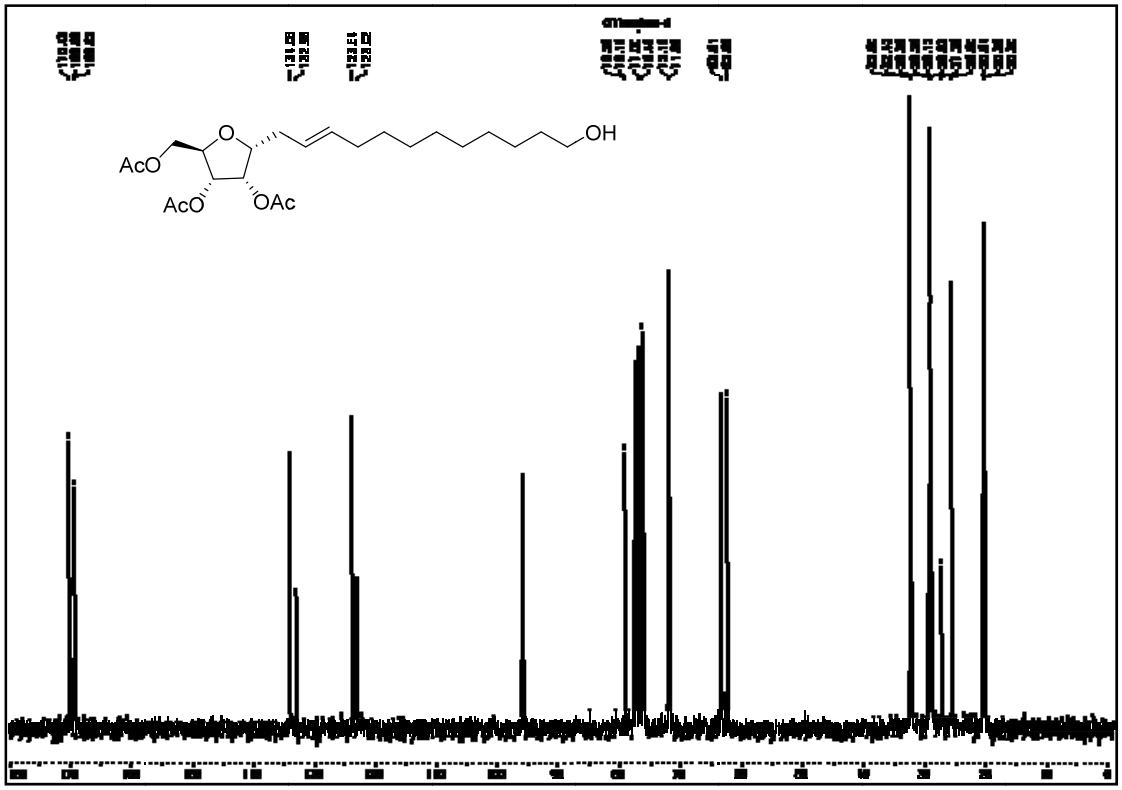

^{13}C NMR spectrum of **2.6** in $CDCl_3$

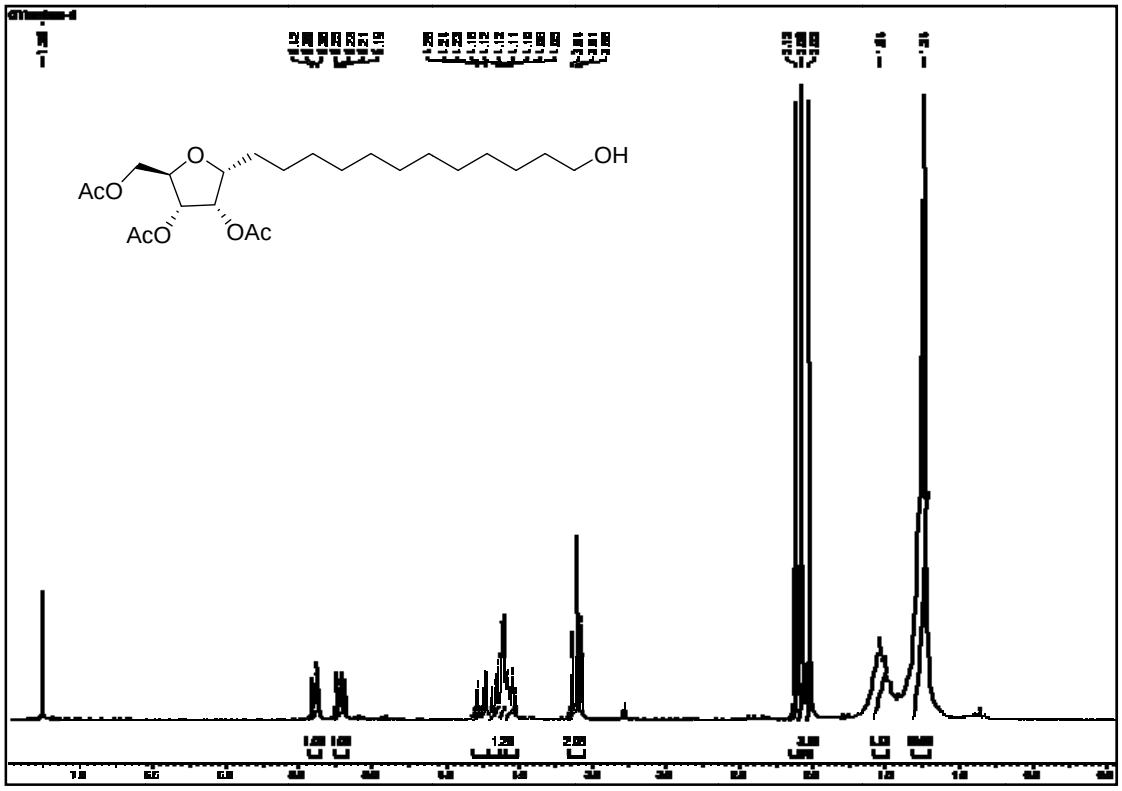

^{1}H NMR spectrum of **2.11** in $CDCl_3$

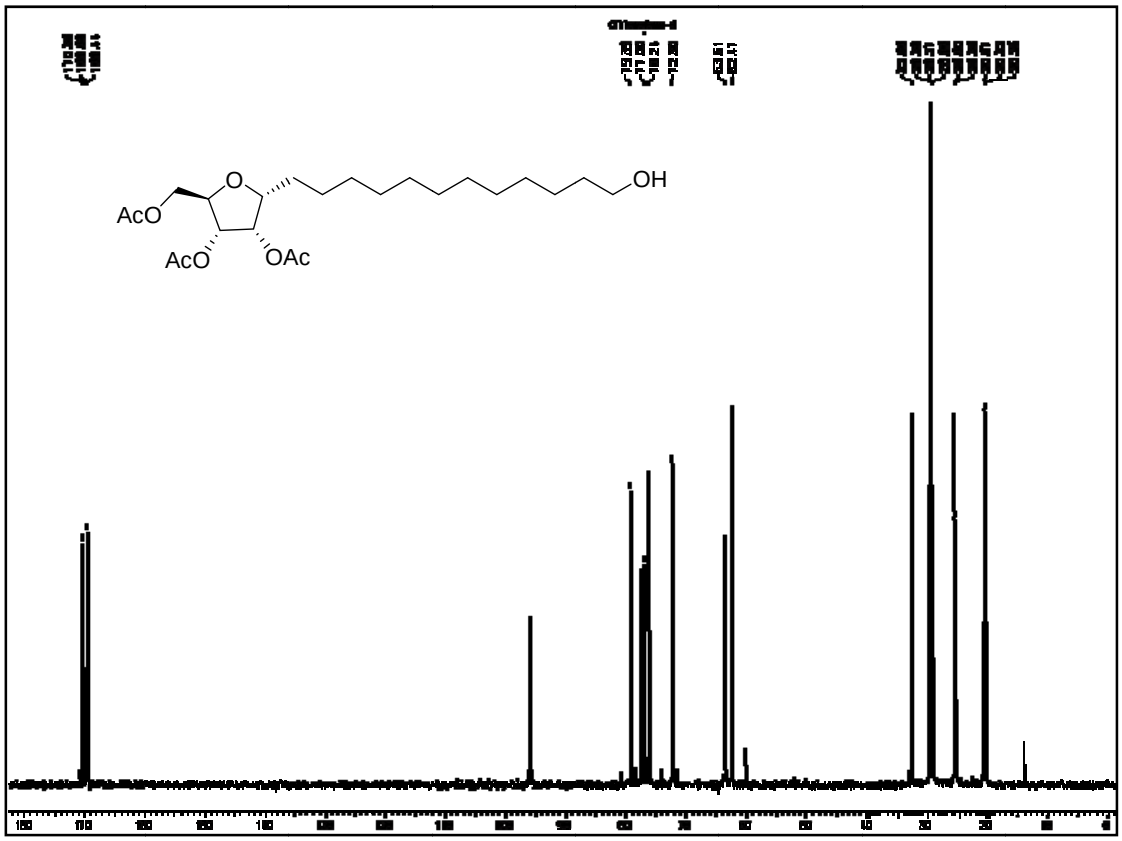

^{13}C NMR spectrum of **2.11** in $CDCl_3$

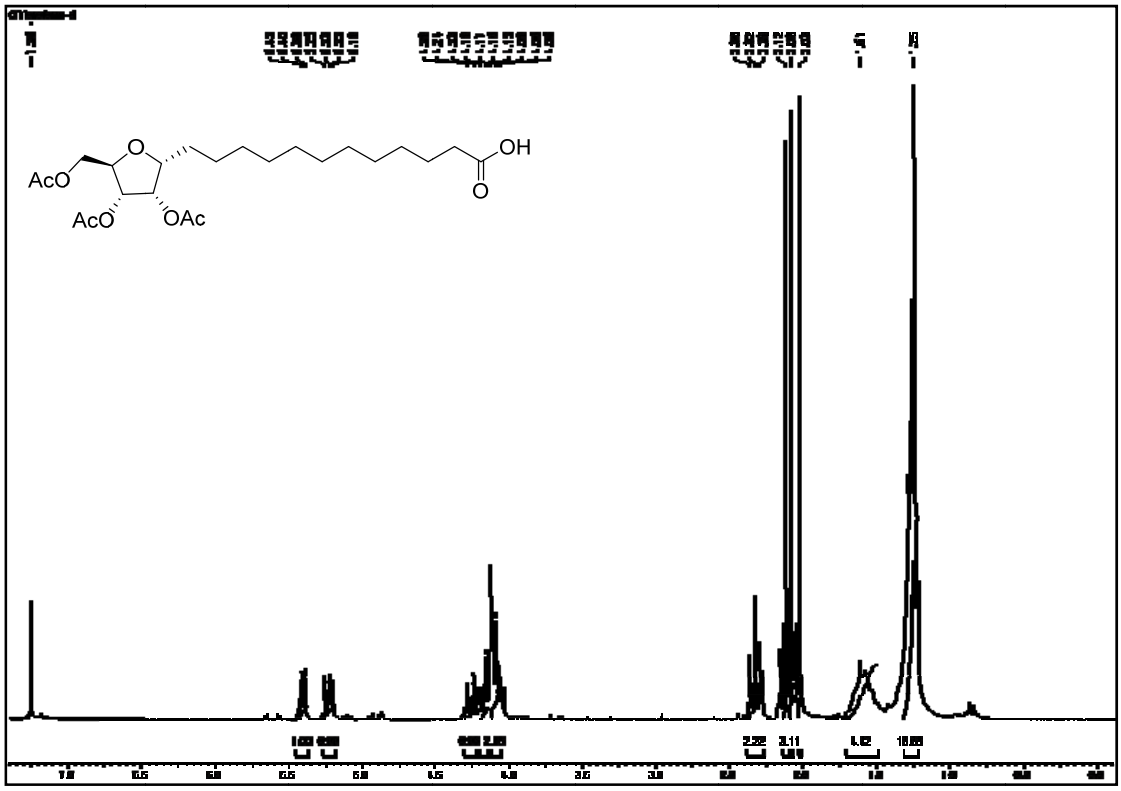

^{1}H NMR spectrum of **2.16** in $CDCl_3$

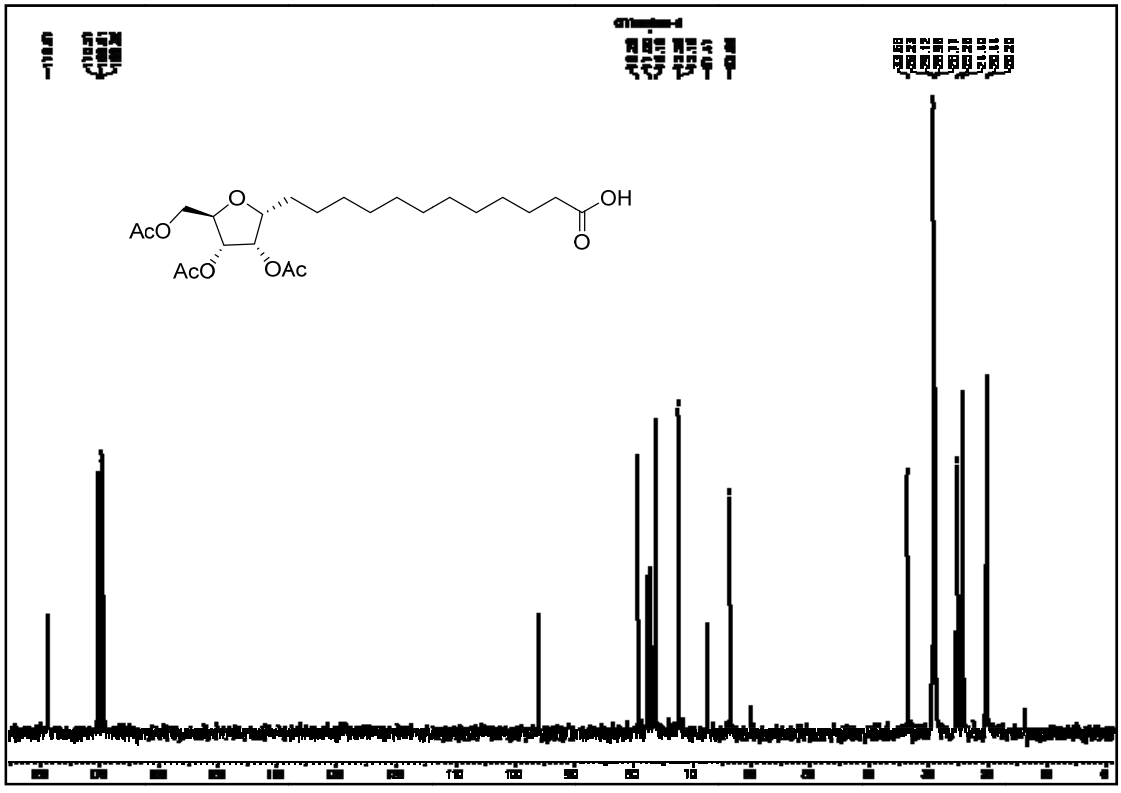

^{13}C NMR spectrum of **2.16** in $CDCl_3$

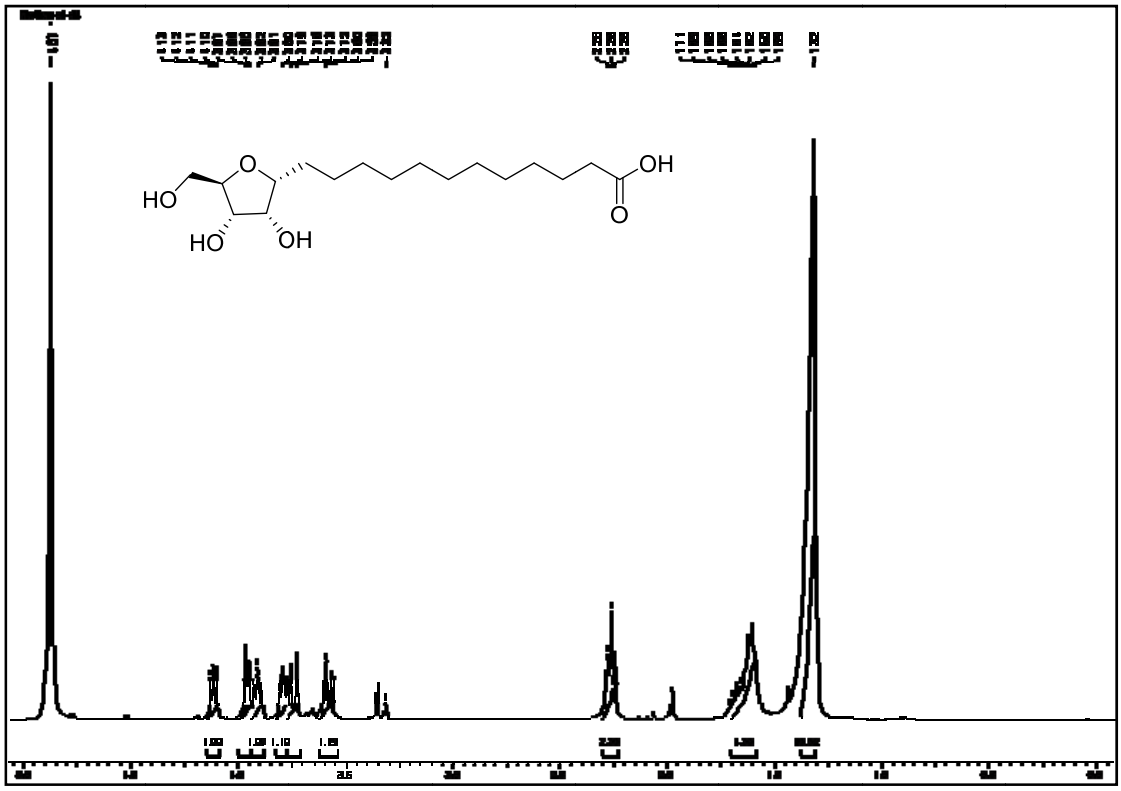

^{1}H NMR spectrum of **2.1** in MeOH-D4

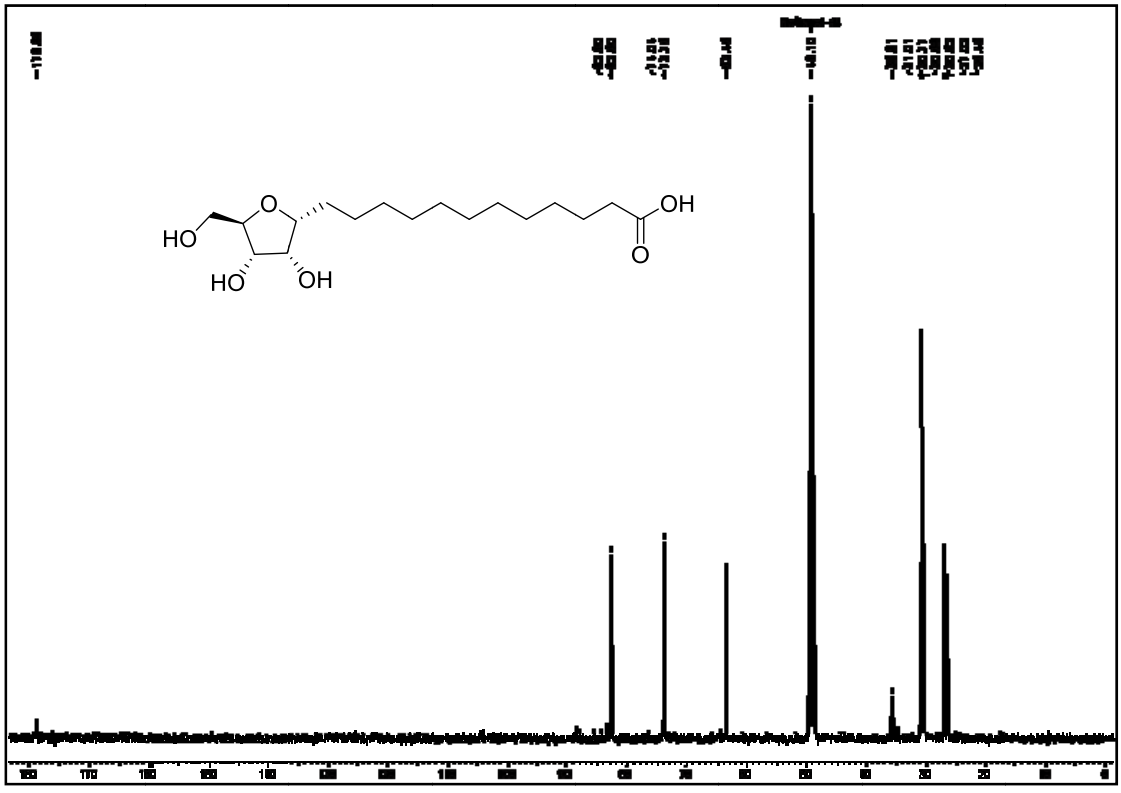

^{13}C NMR spectrum of **2.1** in MeOH-D4

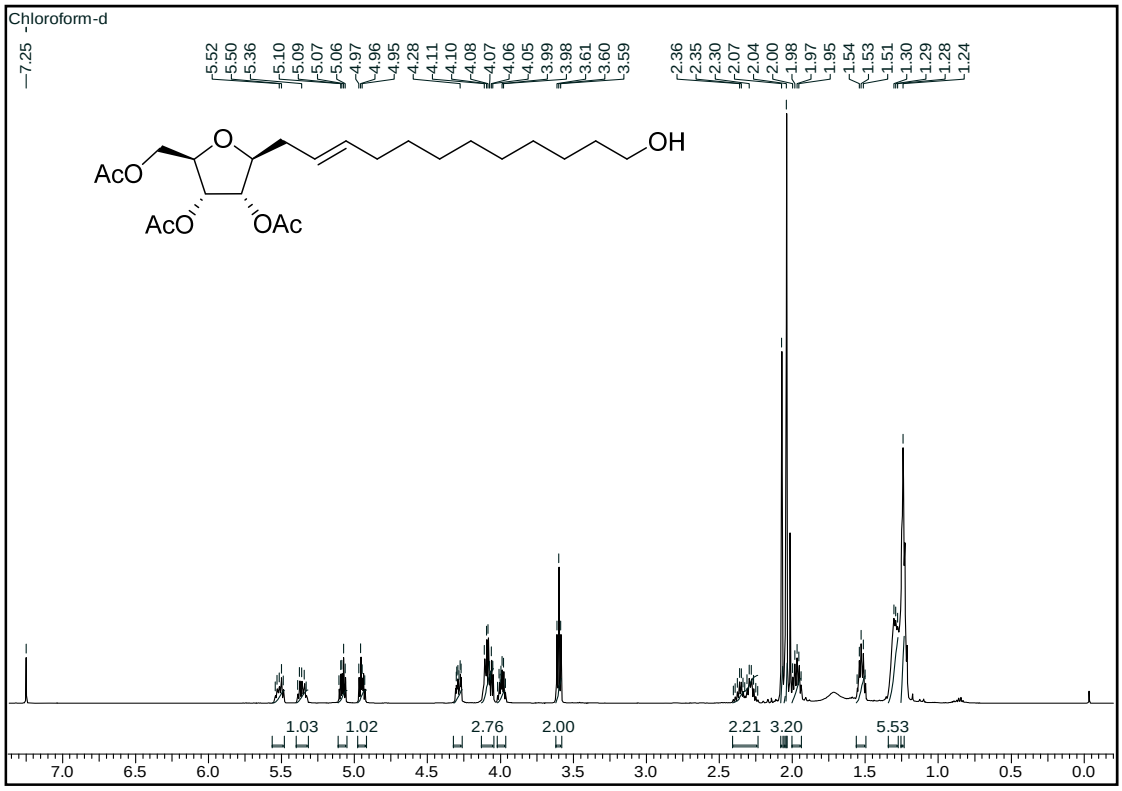

^{1}H NMR spectrum of **2.7** in $CDCl_3$

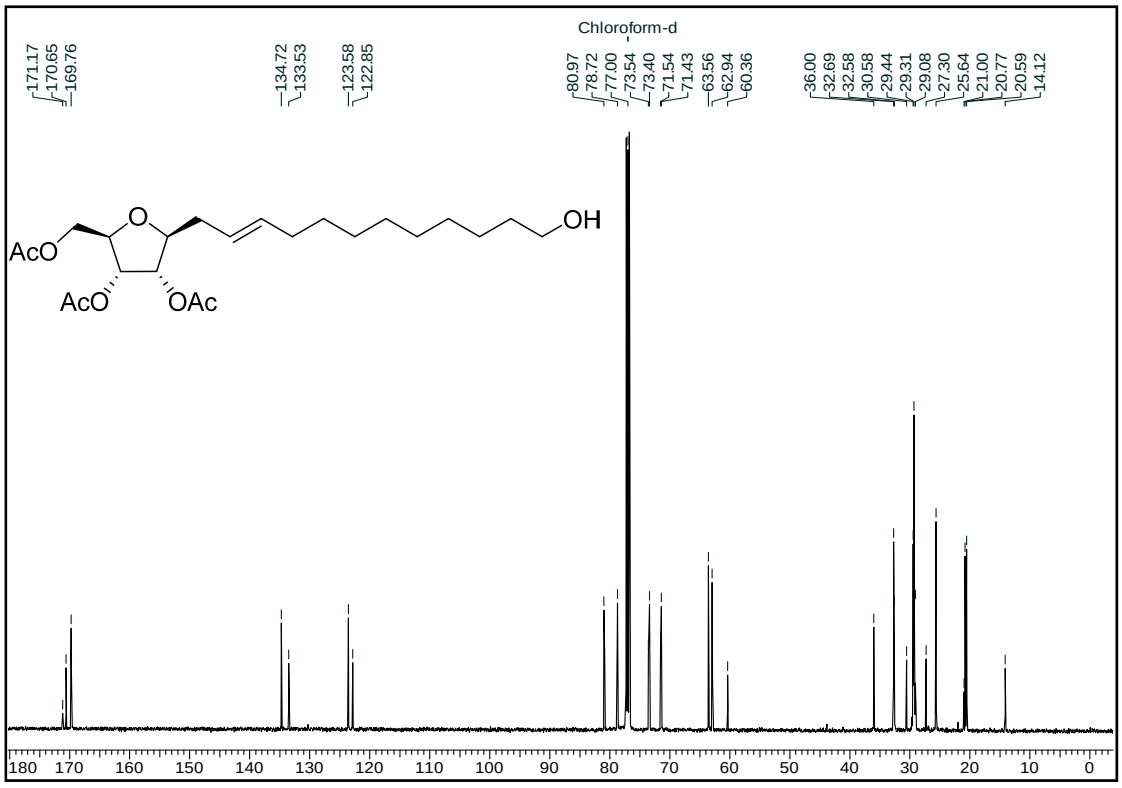

^{13}C NMR spectrum of **2.7** in $CDCl_3$

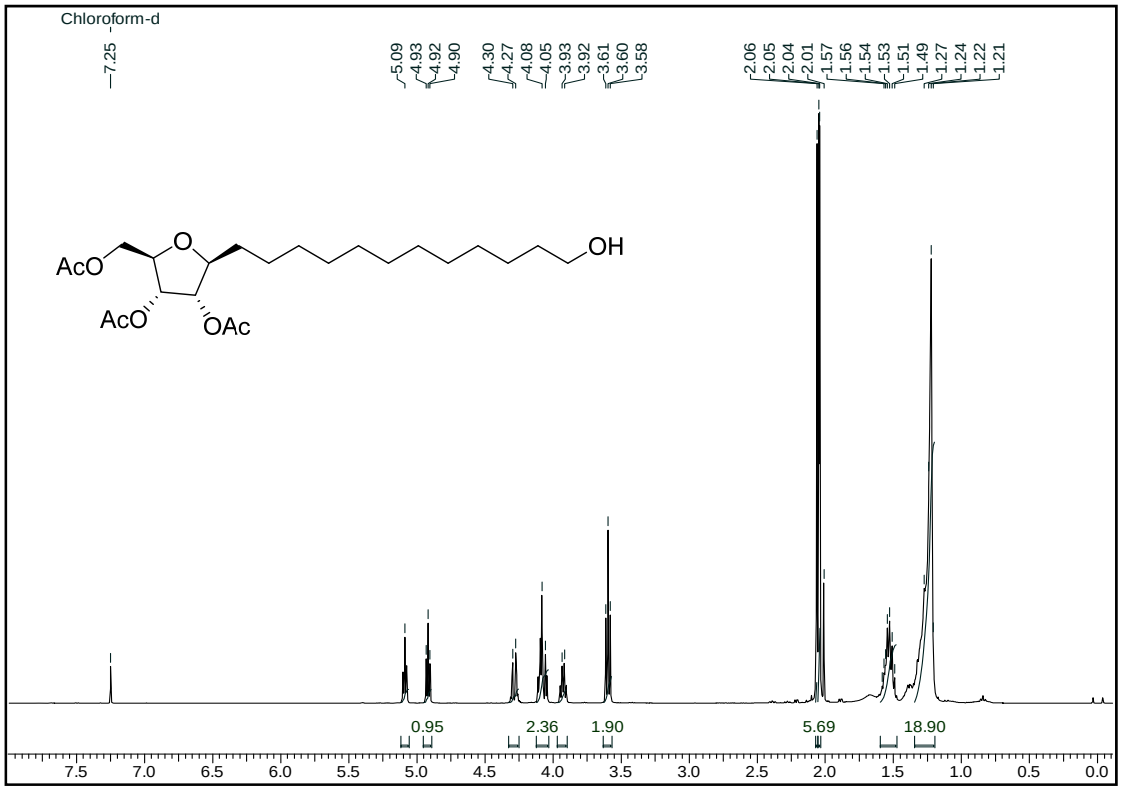

^{1}H NMR spectrum of **2.12** in $CDCl_3$

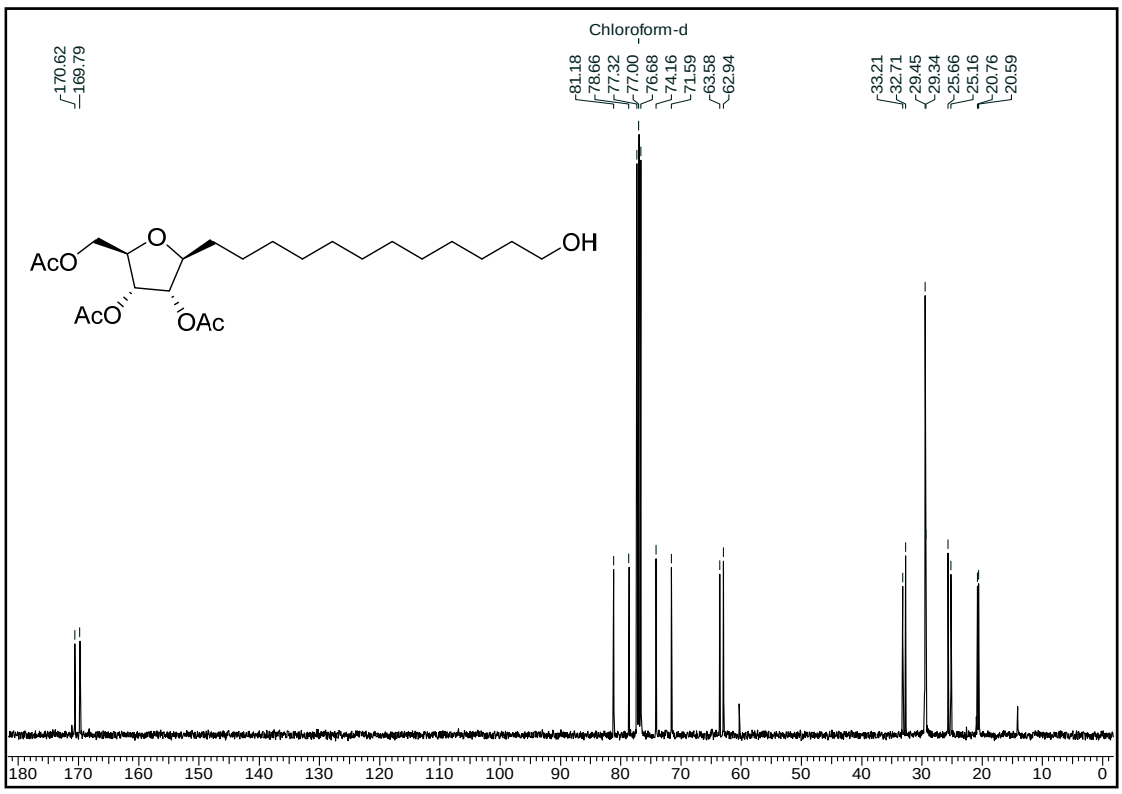

^{13}C NMR spectrum of **2.12** in $CDCl_3$

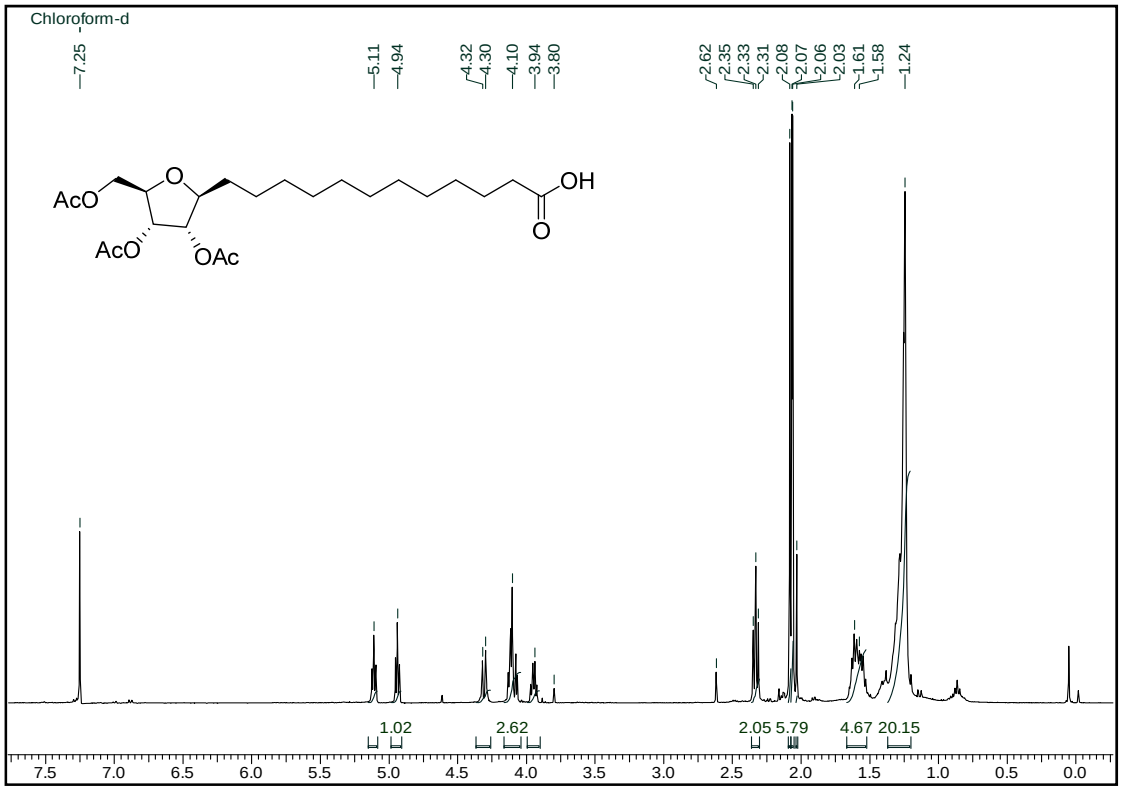

^{1}H NMR spectrum of **2.17** in $CDCl_3$

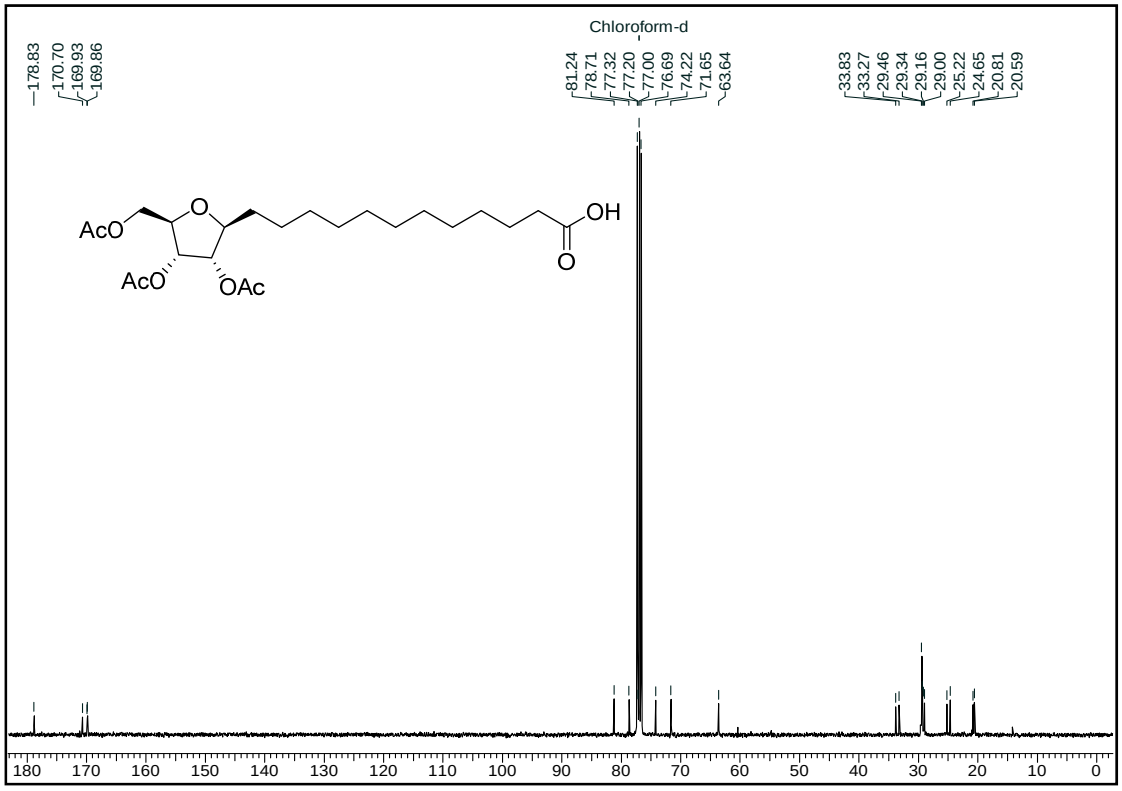

^{13}C NMR spectrum of **2.17** in $CDCl_3$

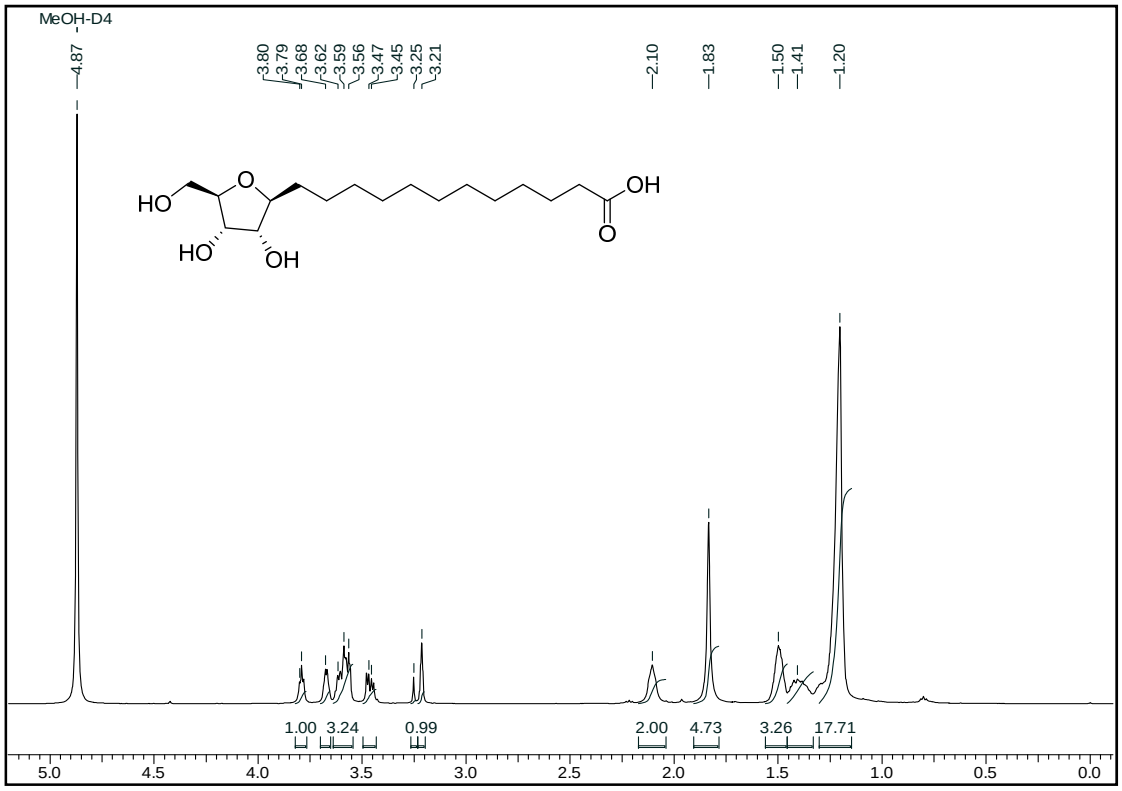

^{1}H NMR spectrum of **2.2** in MeOH-D4

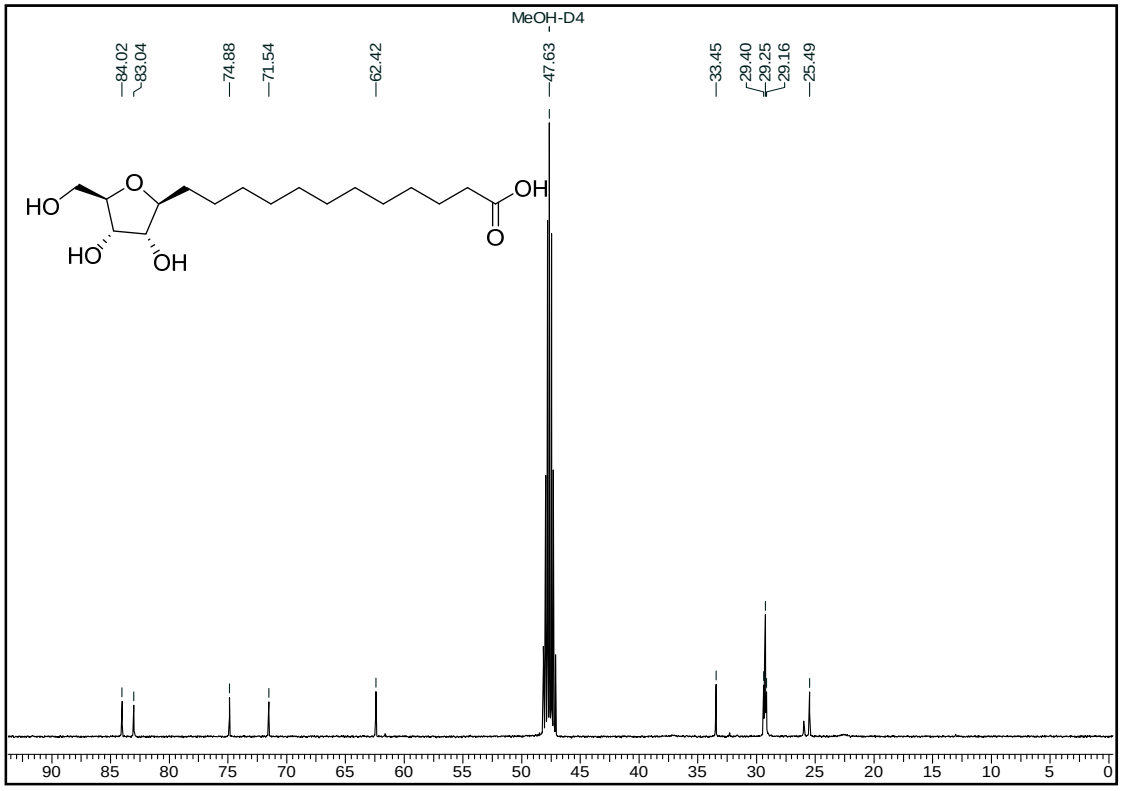

^{13}C NMR spectrum of **2.2** in MeOH-D4

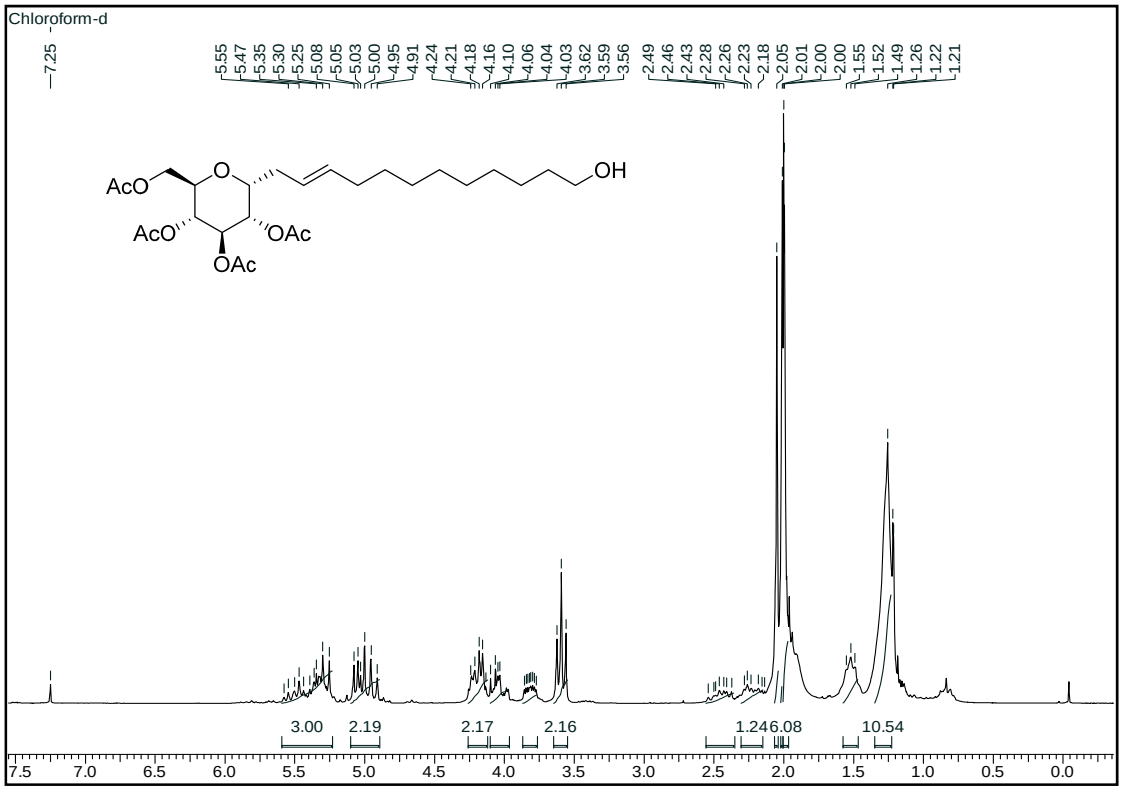

^{1}H NMR spectrum of **2.8** in $CDCl_3$

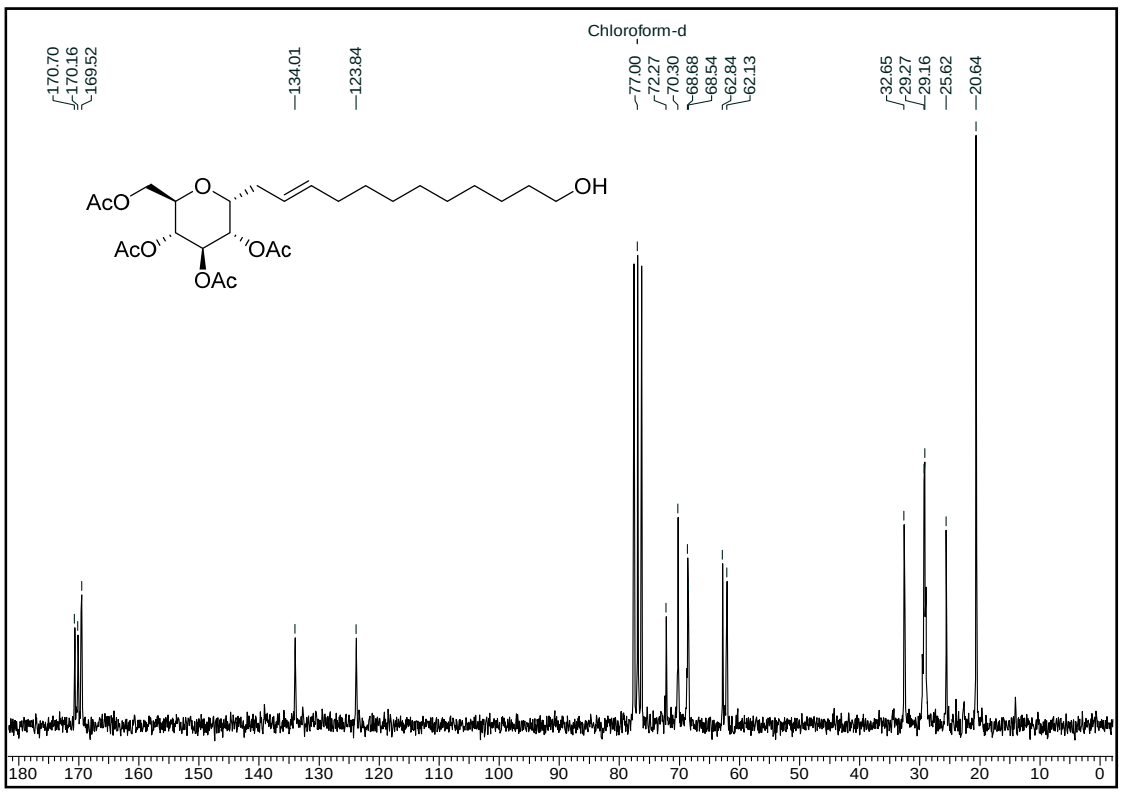

^{13}C NMR spectrum of **2.8** in $CDCl_3$

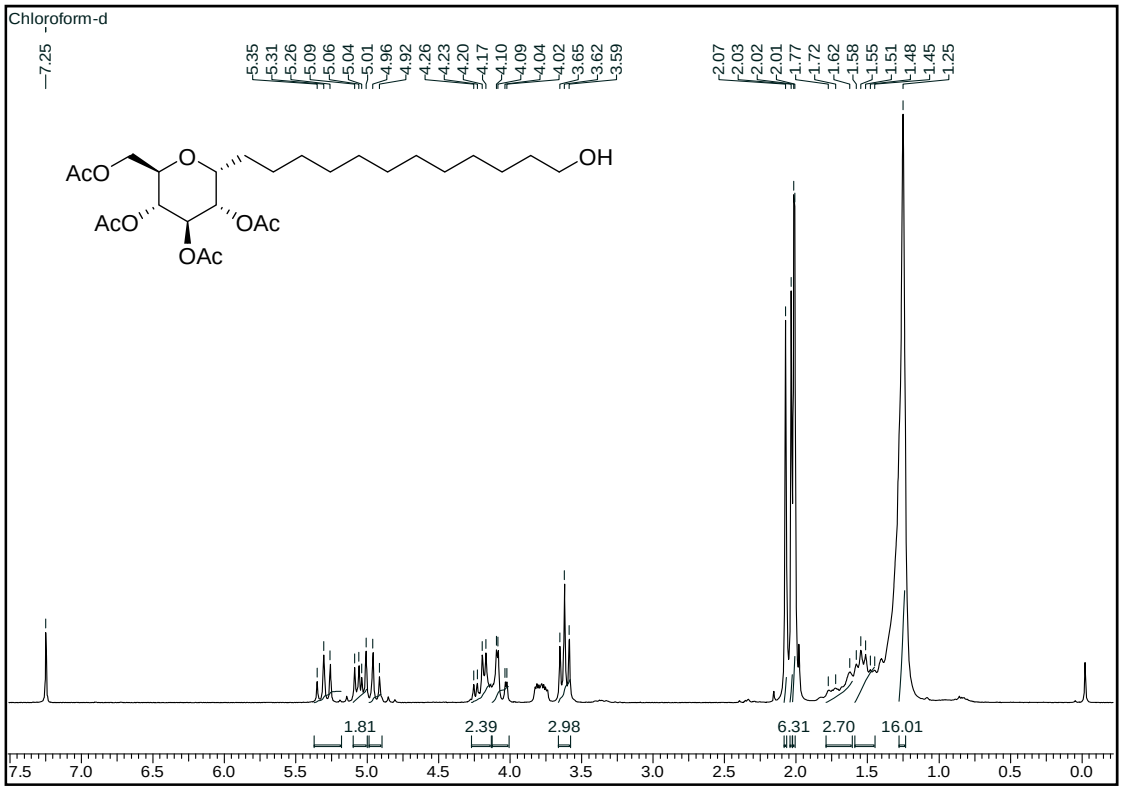

^{1}H NMR spectrum of **2.13** in $CDCl_3$

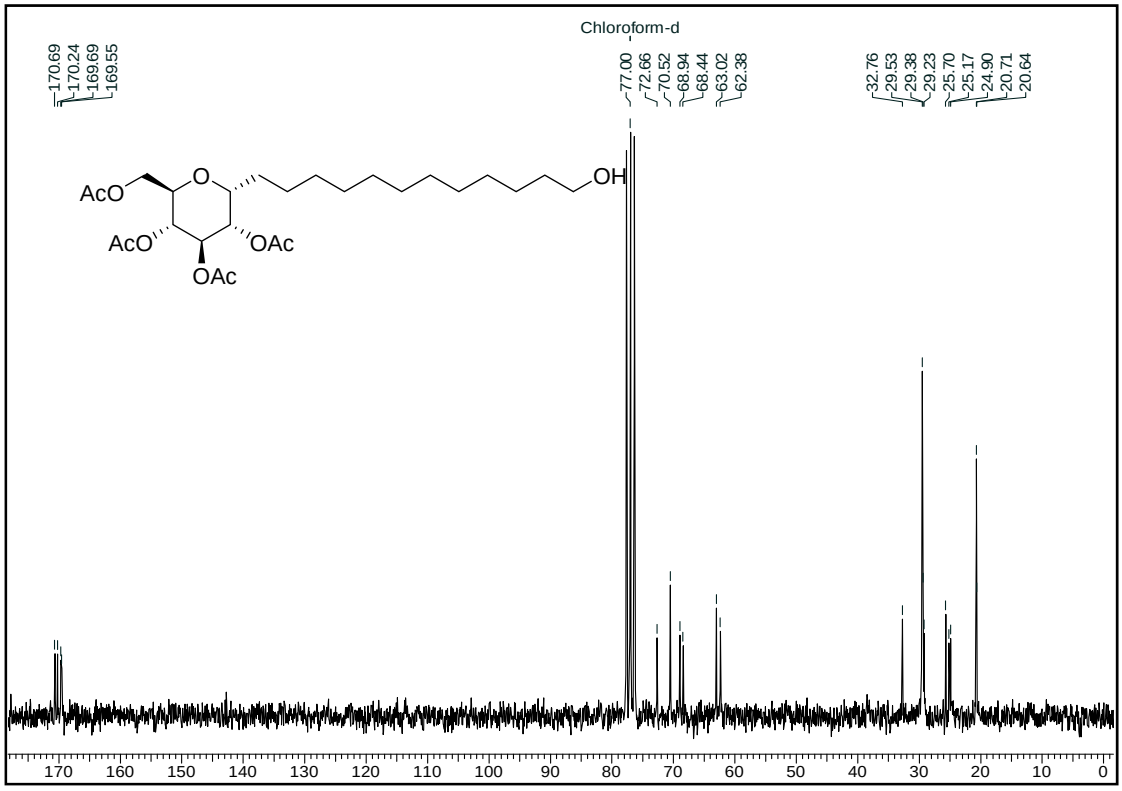

^{13}C NMR spectrum of **2.13** in $CDCl_3$

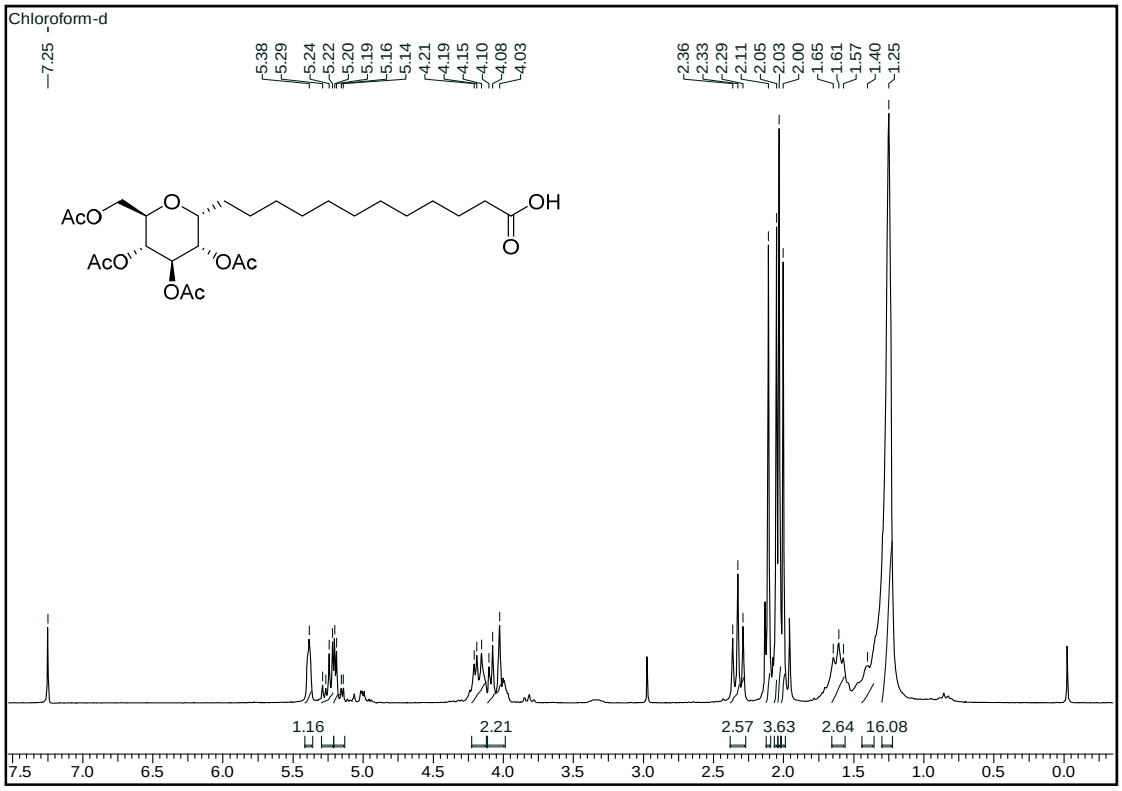

^{1}H NMR spectrum of **2.18** in $CDCl_3$

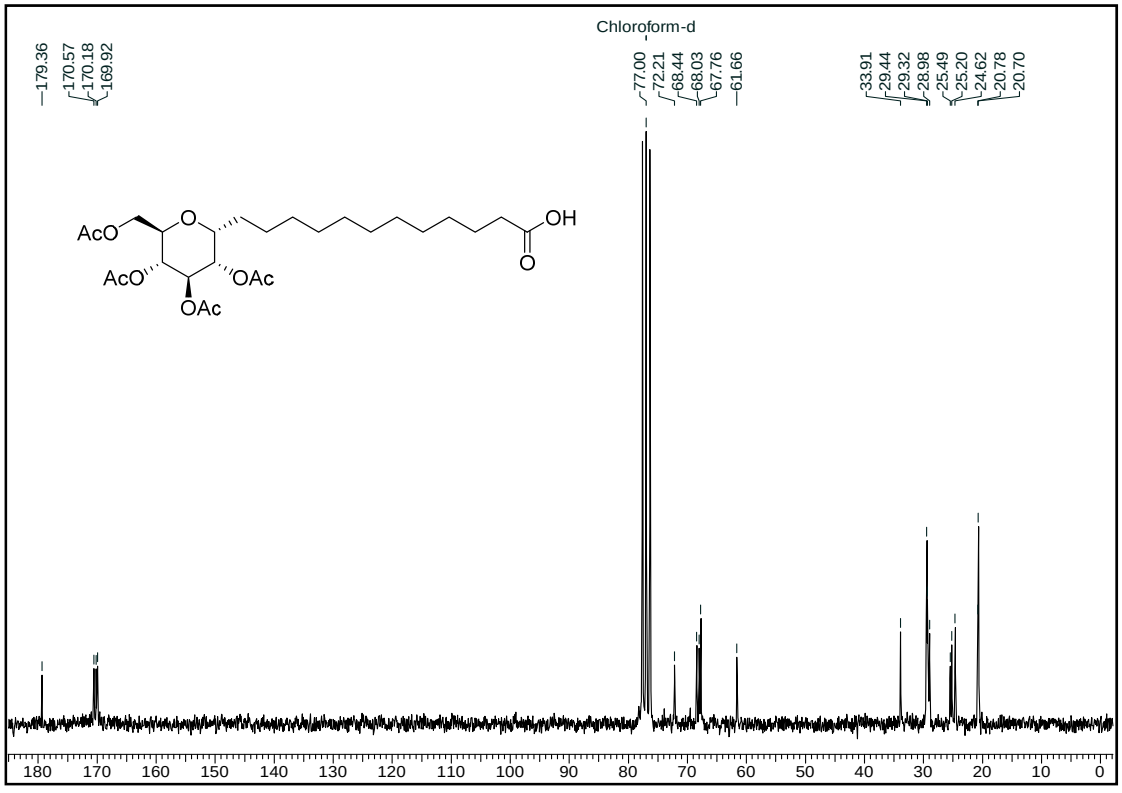

^{13}C NMR spectrum of **2.18** in $CDCl_3$

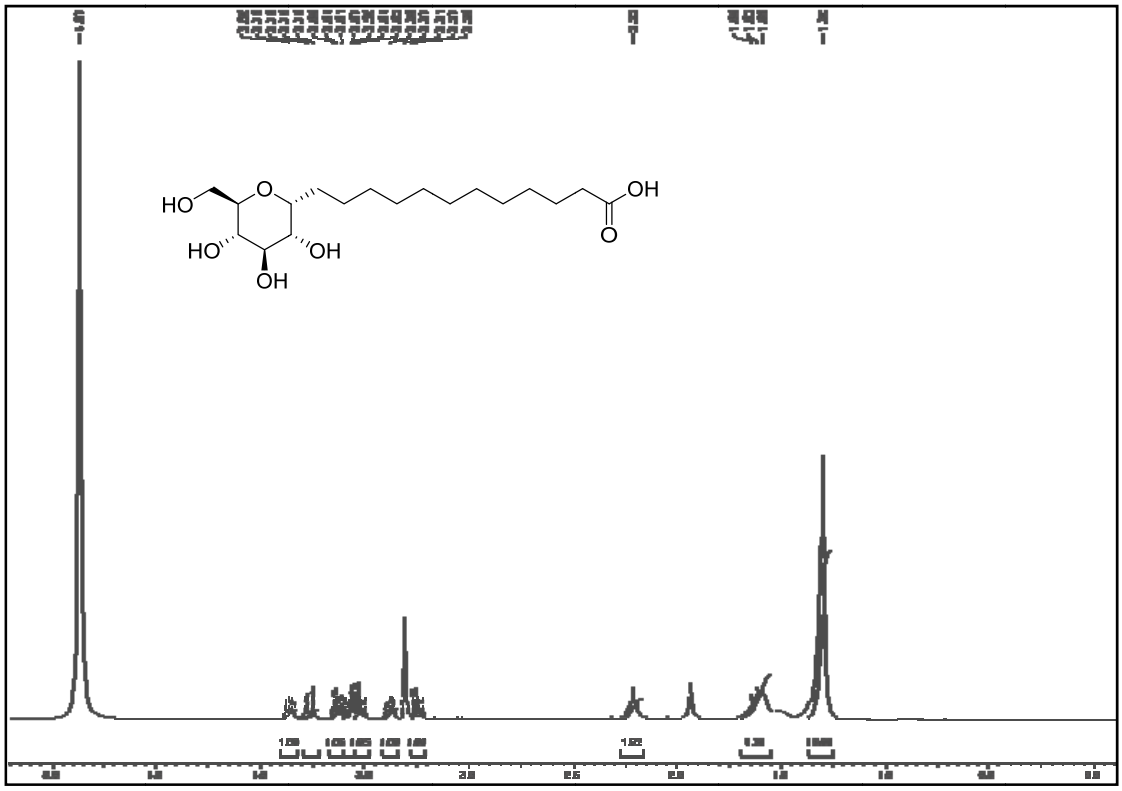

^{1}H NMR spectrum of **2.3** in MeOH-D4

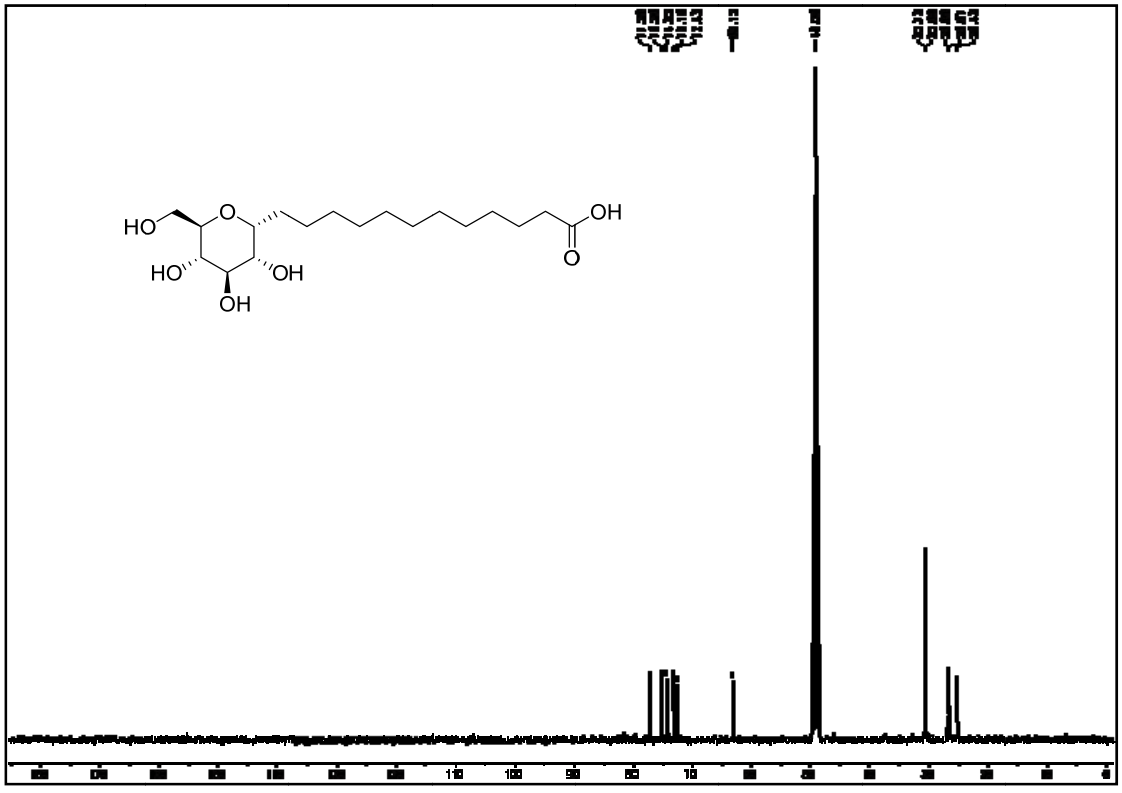

^{13}C NMR spectrum of **2.3** in MeOH-D4

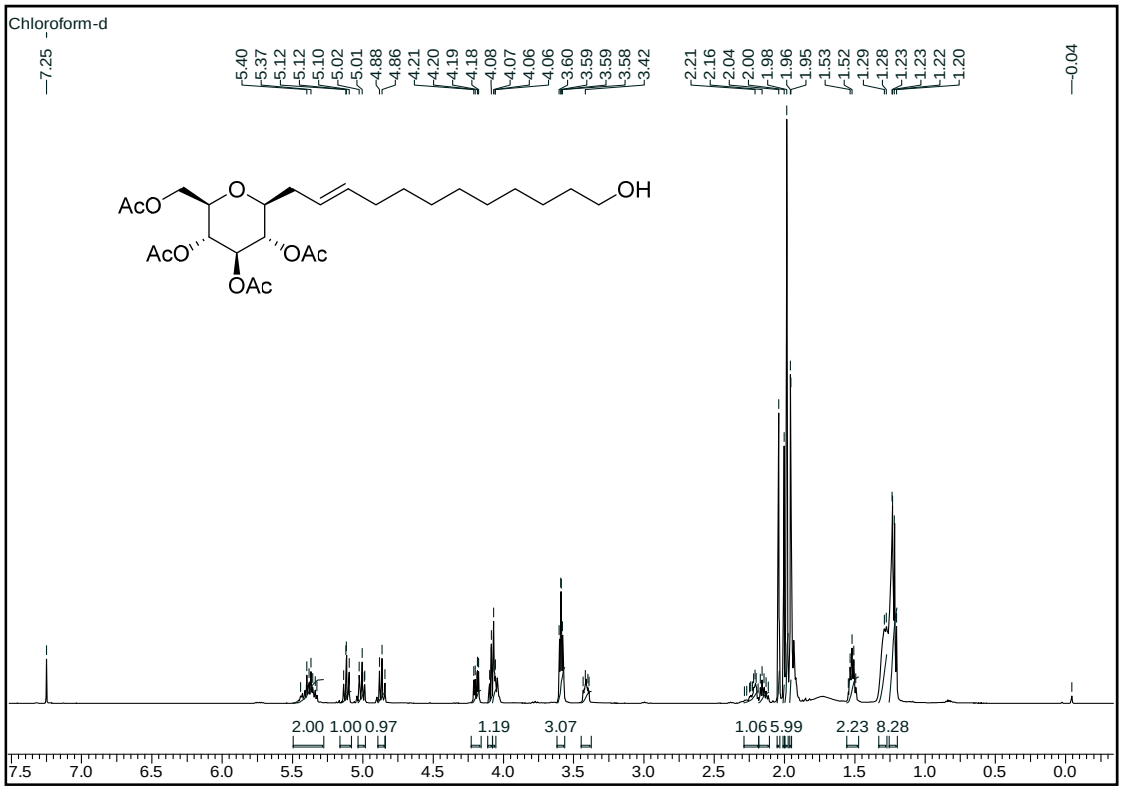

^{1}H NMR spectrum of **2.9** in $CDCl_3$

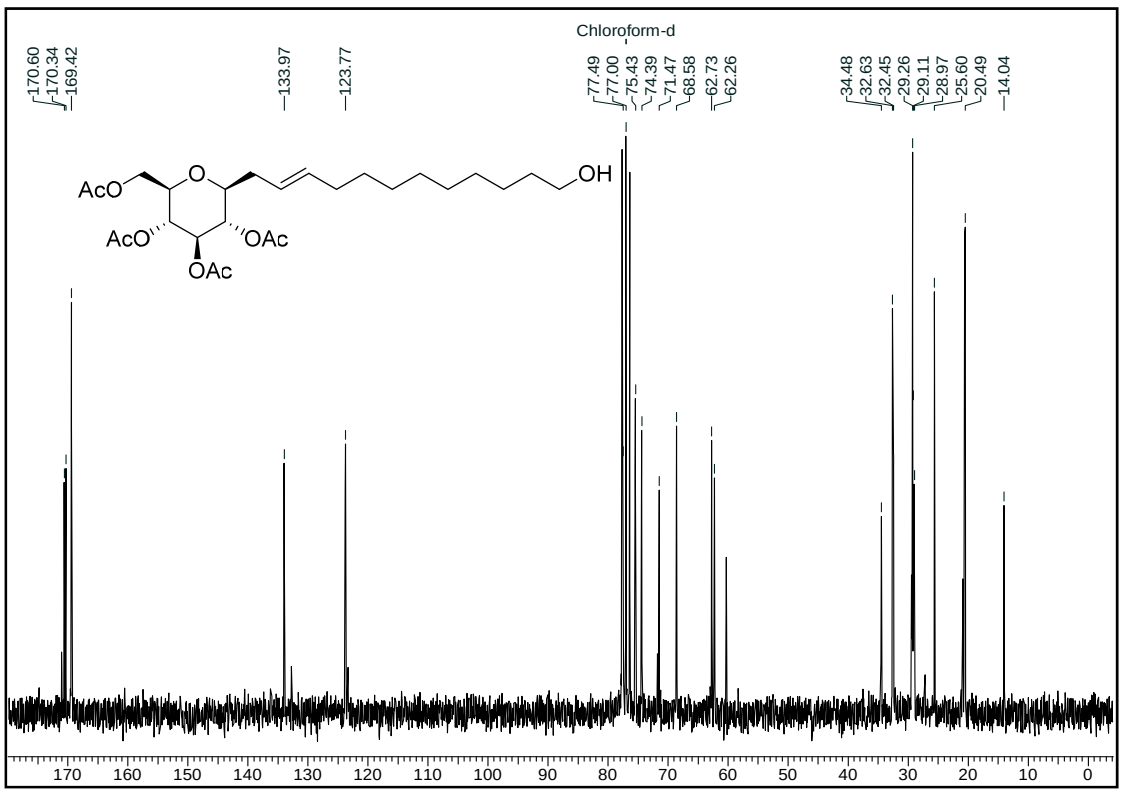

^{13}C NMR spectrum of **2.9** in $CDCl_3$

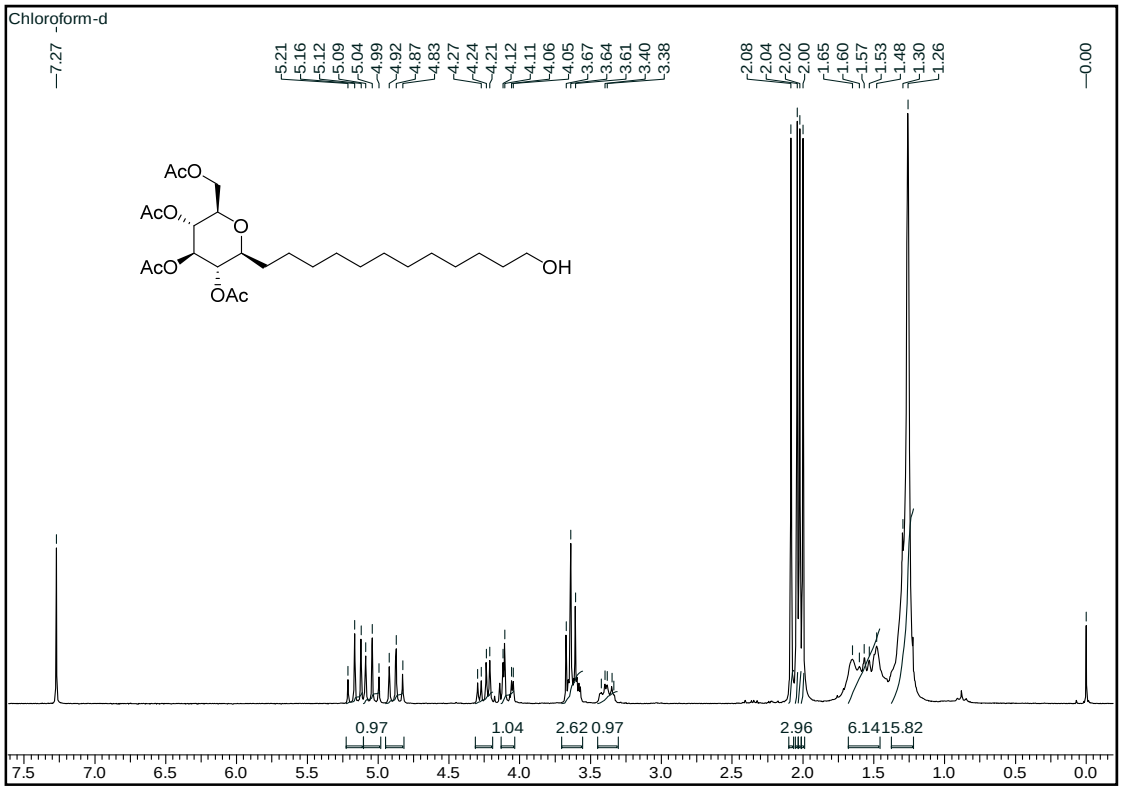

^{1}H NMR spectrum of **2.14** in $CDCl_3$

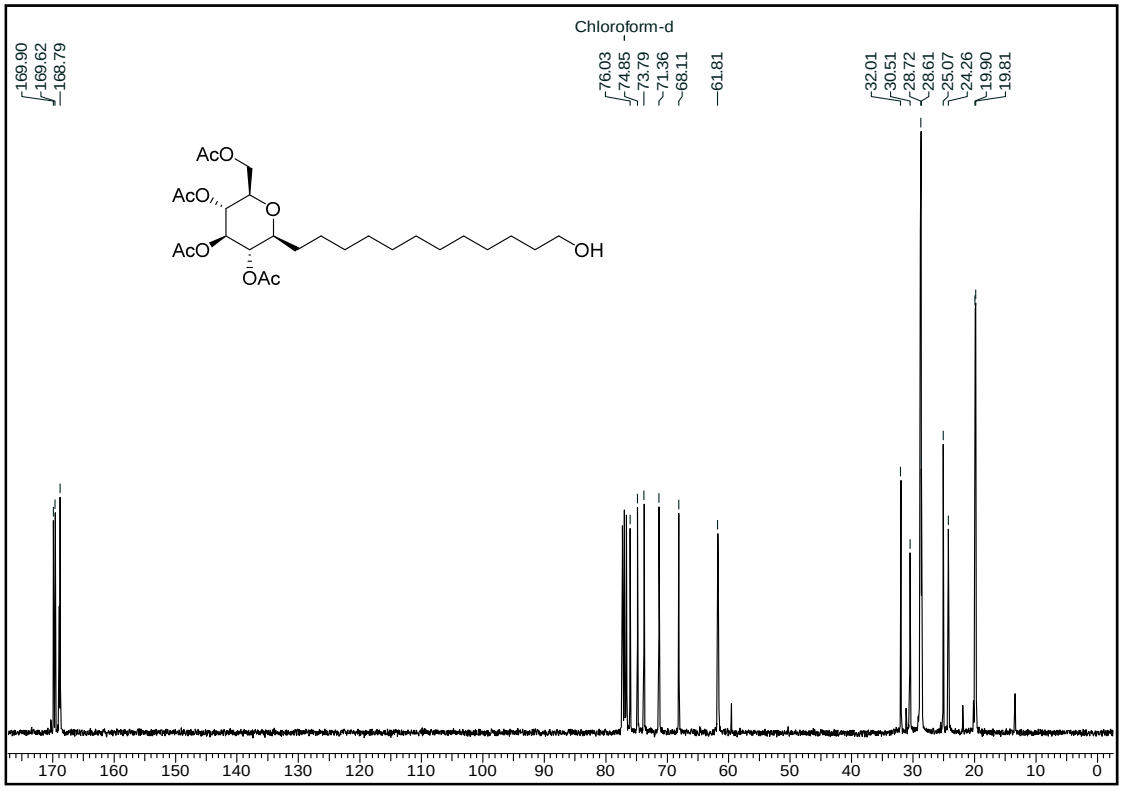

^{13}C NMR spectrum of **2.14** in $CDCl_3$

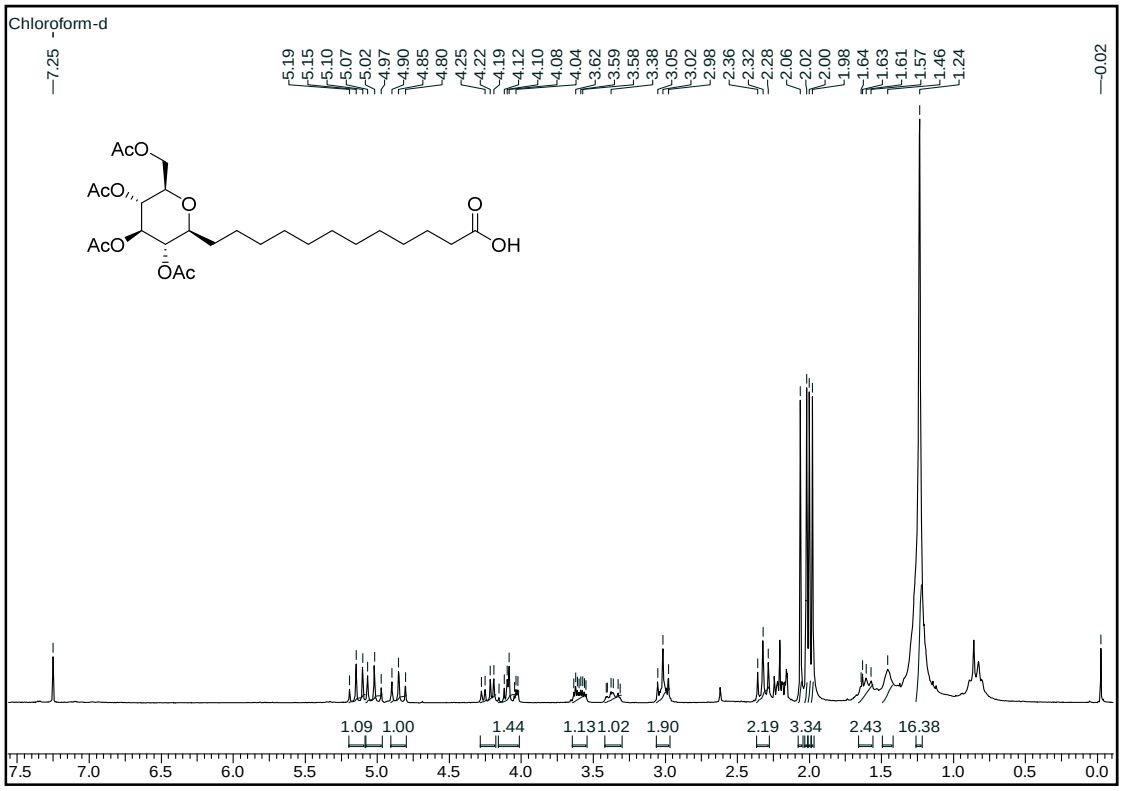

^{1}H NMR spectrum of **2.19** in $CDCl_3$

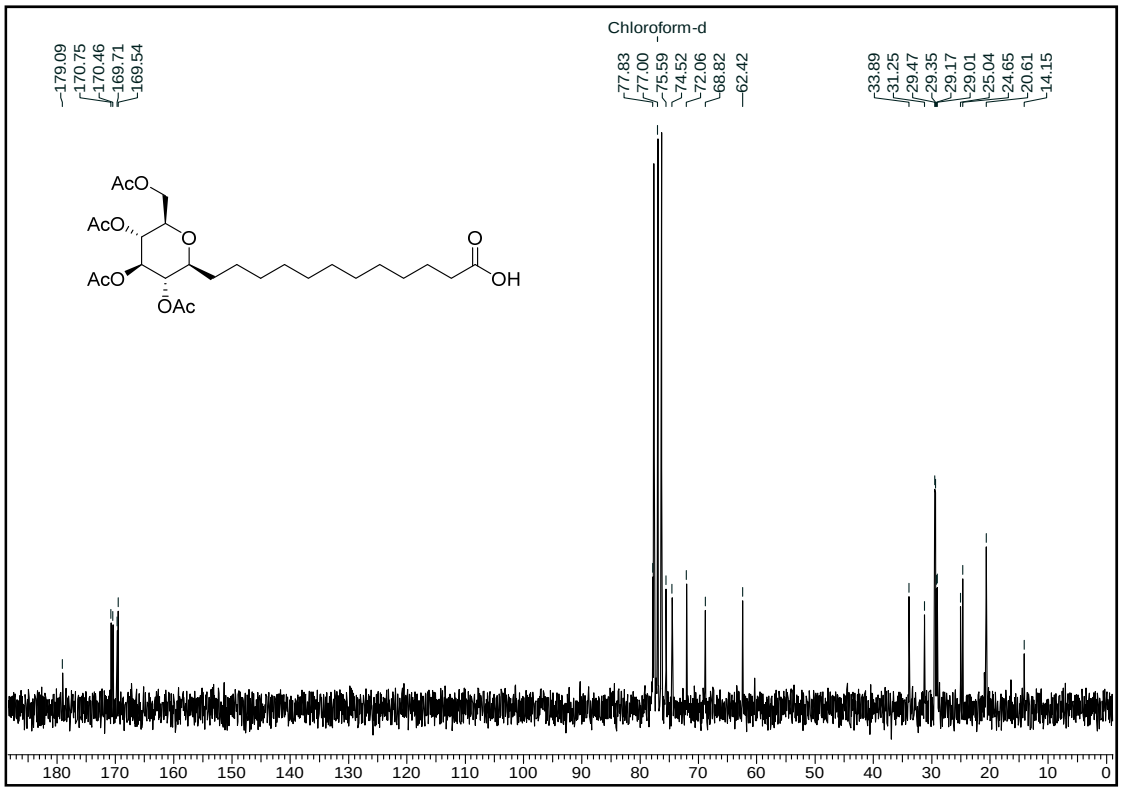

^{13}C NMR spectrum of **2.19** in $CDCl_3$

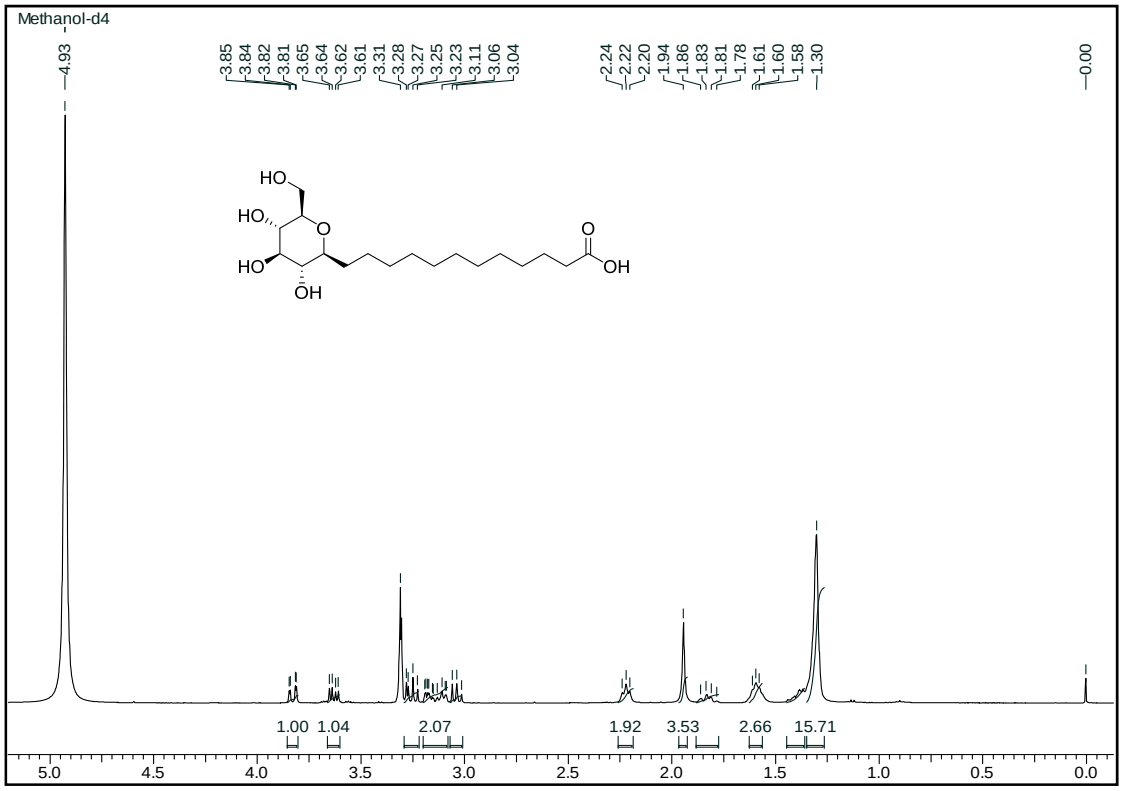

^{1}H NMR spectrum of **2.4** in $CDCl_3$

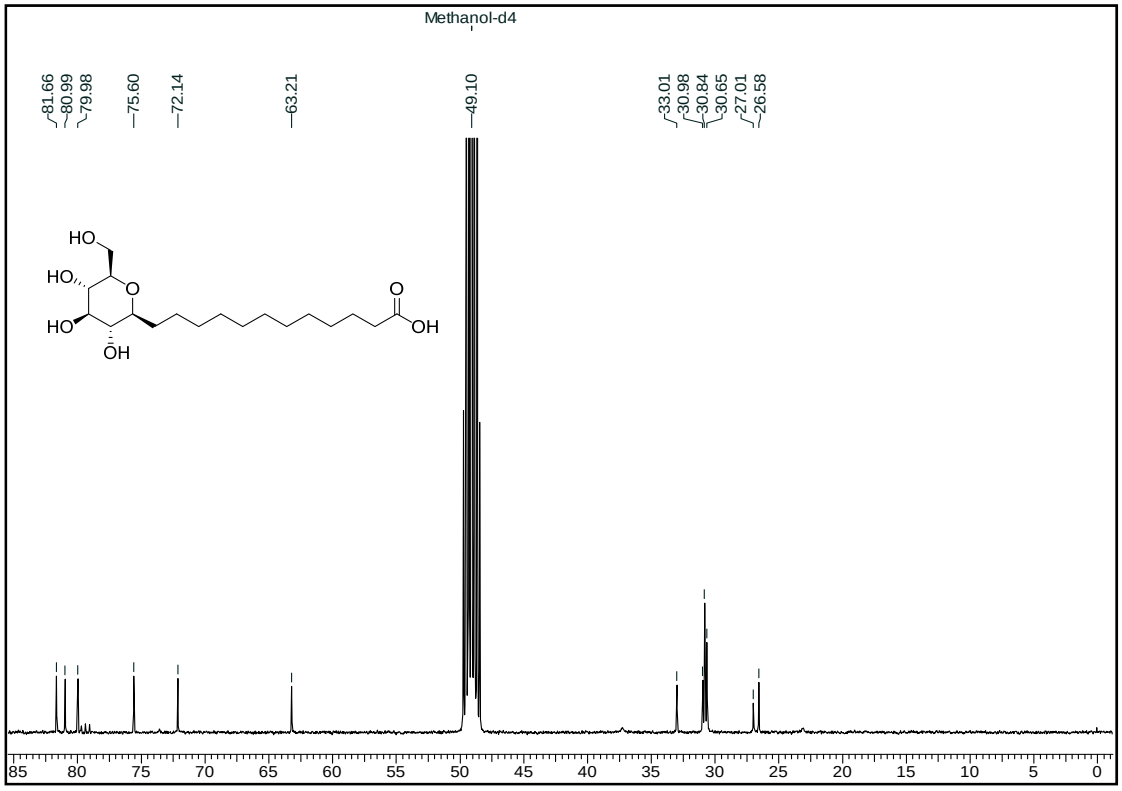

^{13}C NMR spectrum of **2.4** in $CDCl_3$

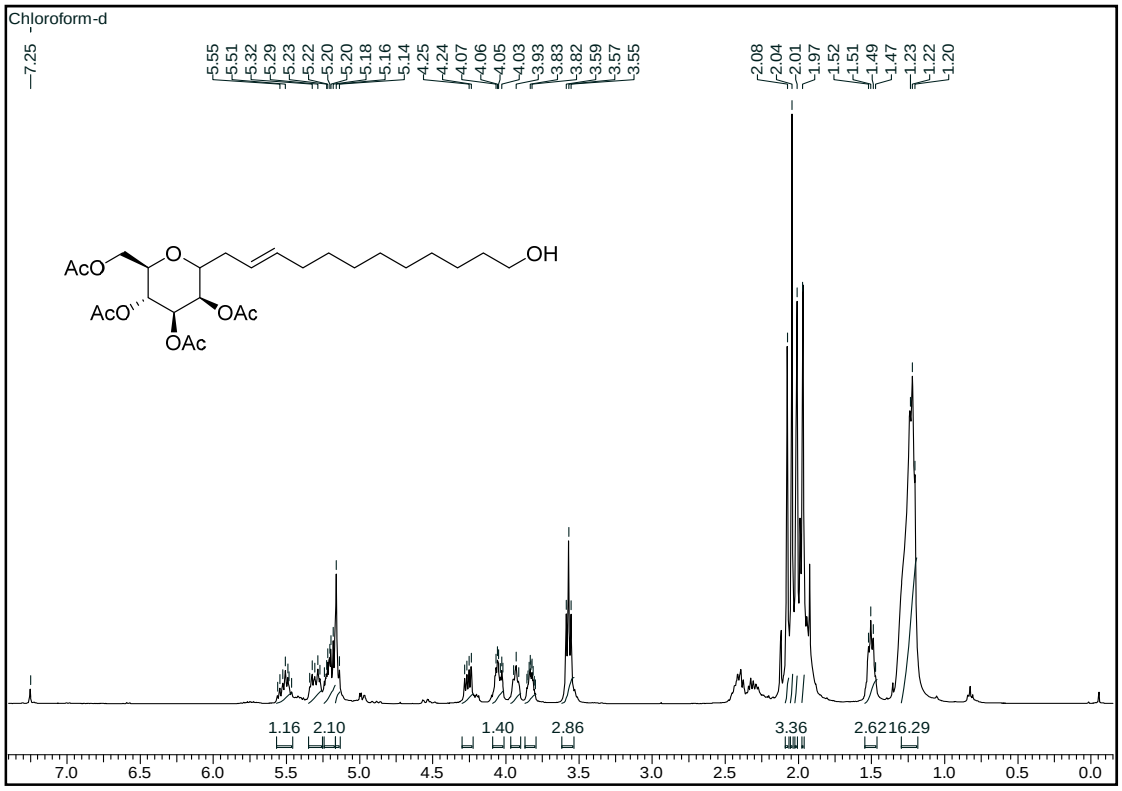

^{1}H NMR spectrum of **2.10** in $CDCl_3$

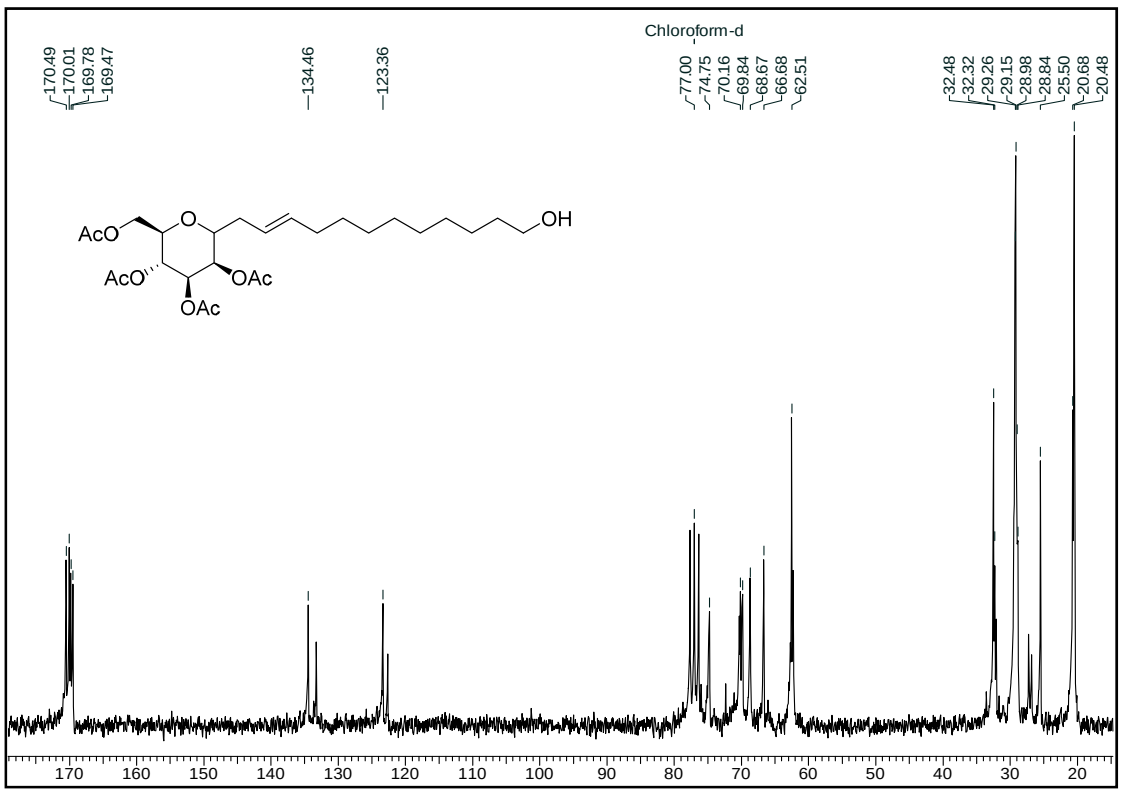

^{13}C NMR spectrum of **2.10** in $CDCl_3$

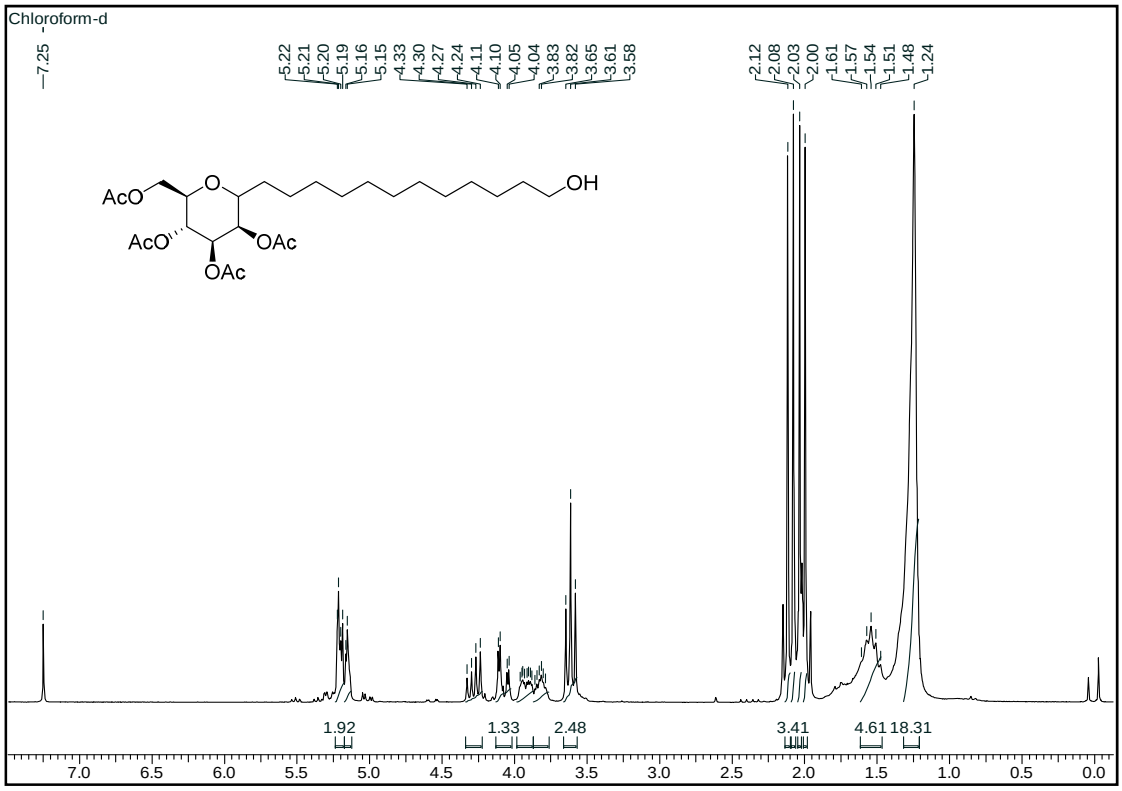

^{1}H NMR spectrum of **2.15** in $CDCl_3$

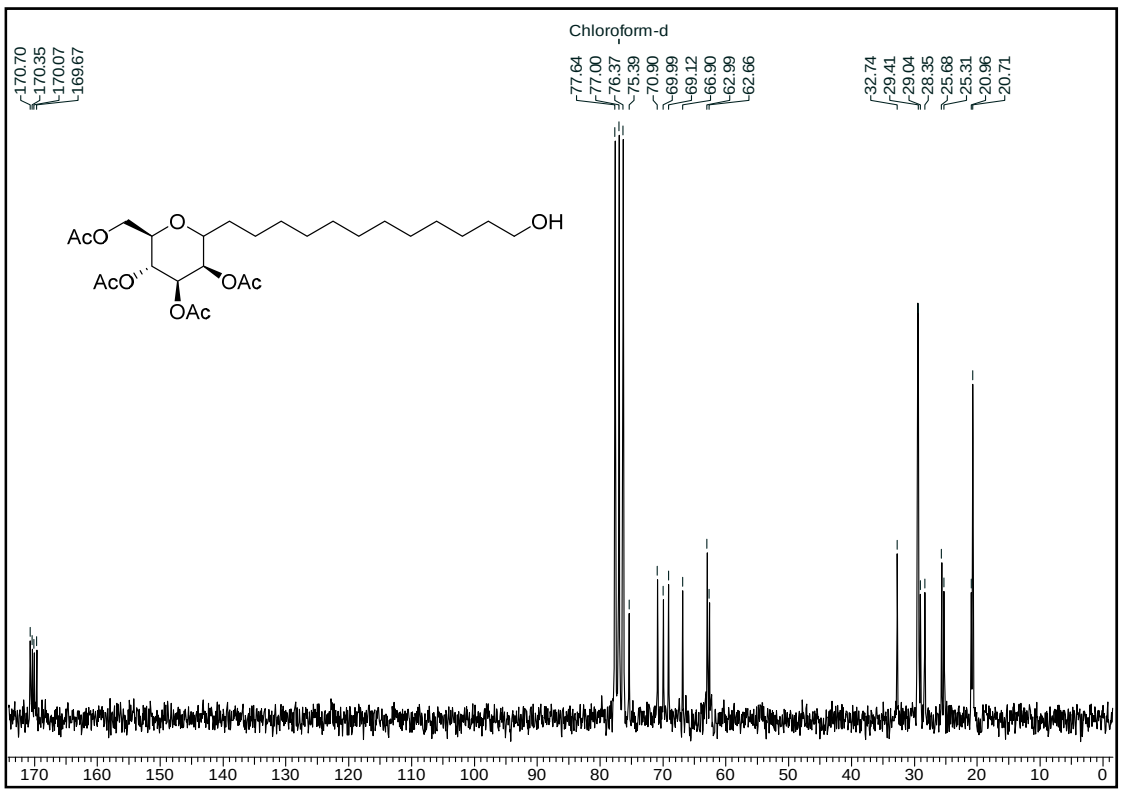

^{13}C NMR spectrum of **2.15** in $CDCl_3$

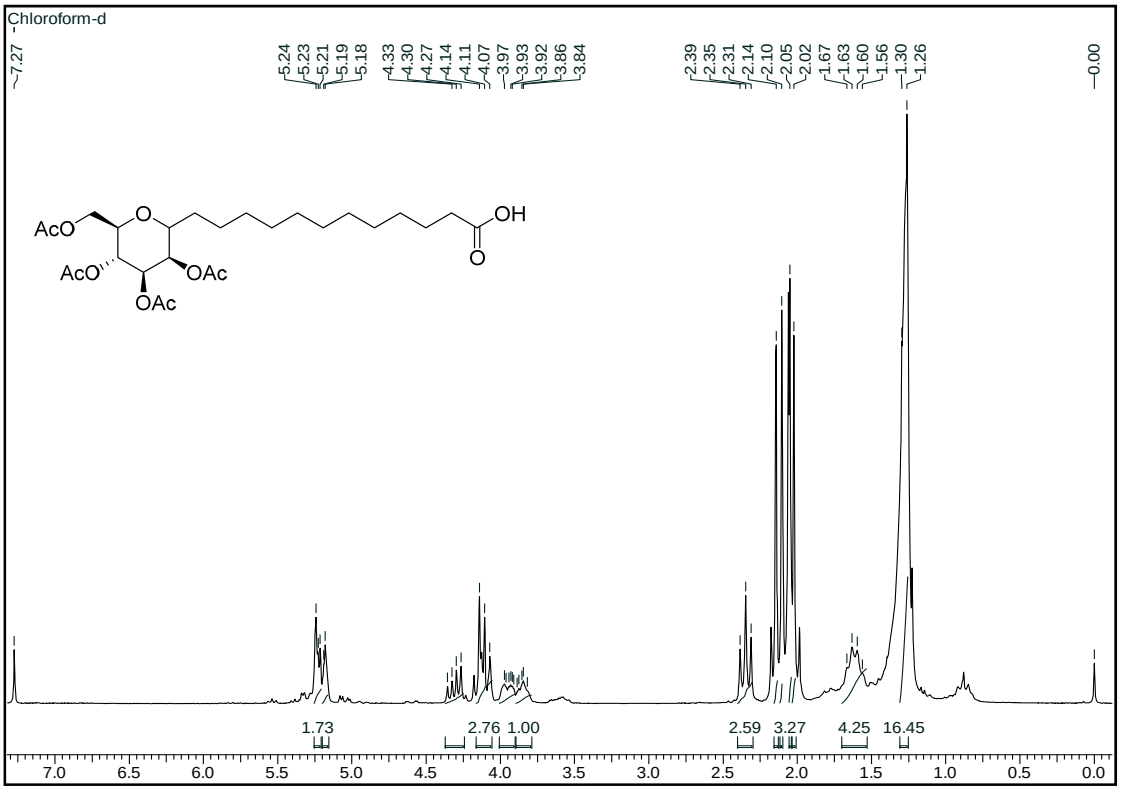

^{1}H NMR spectrum of **2.20** in $CDCl_3$

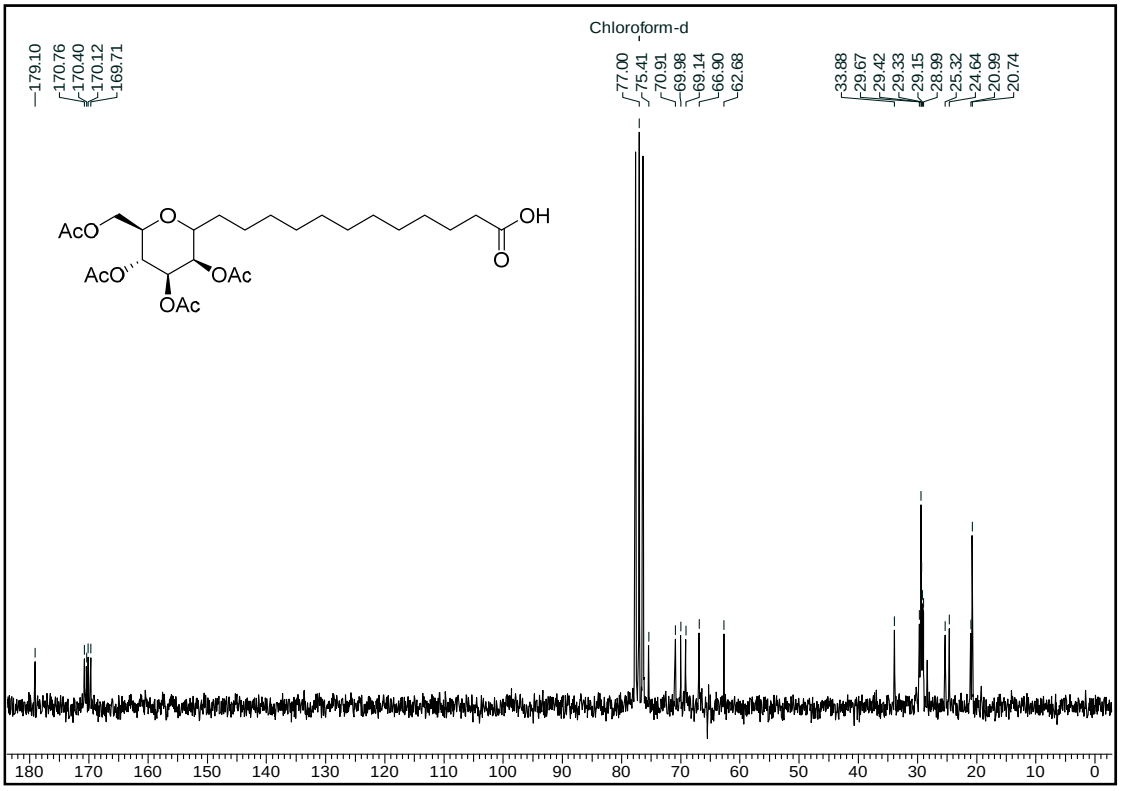

^{13}C NMR spectrum of **2.20** in $CDCl_3$

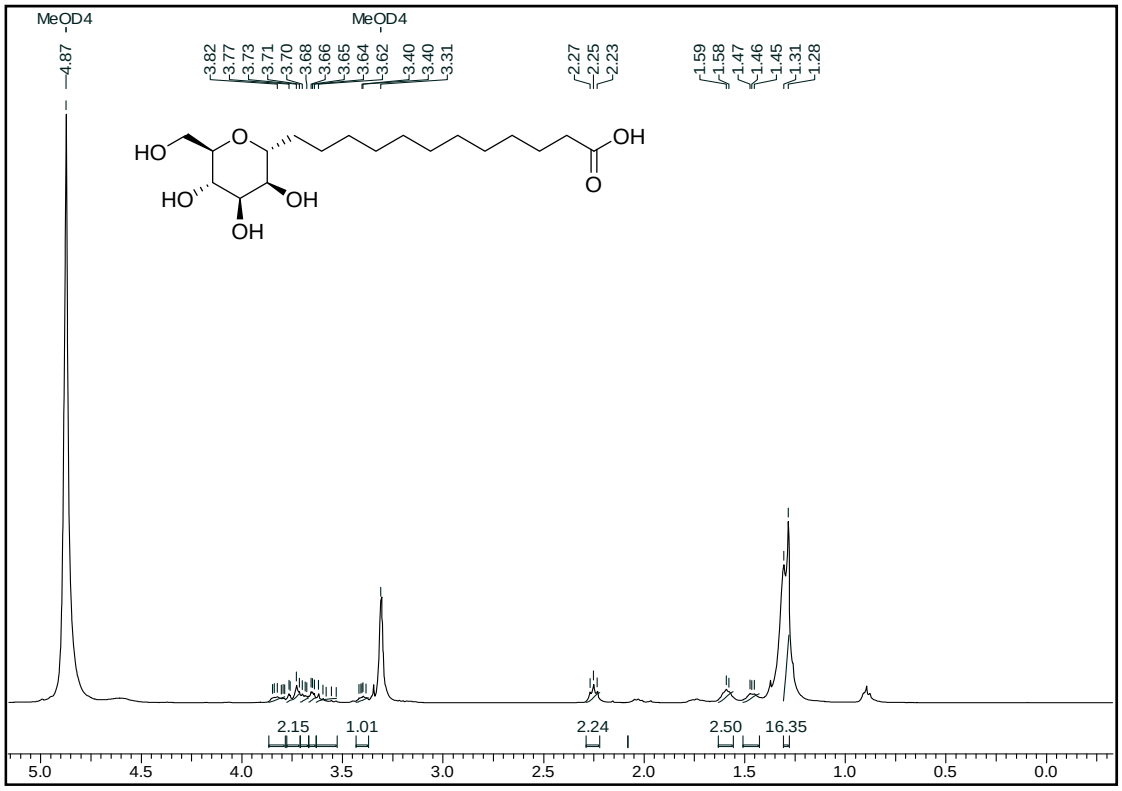

^{1}H NMR spectrum of **2.5** in MeOH-D4

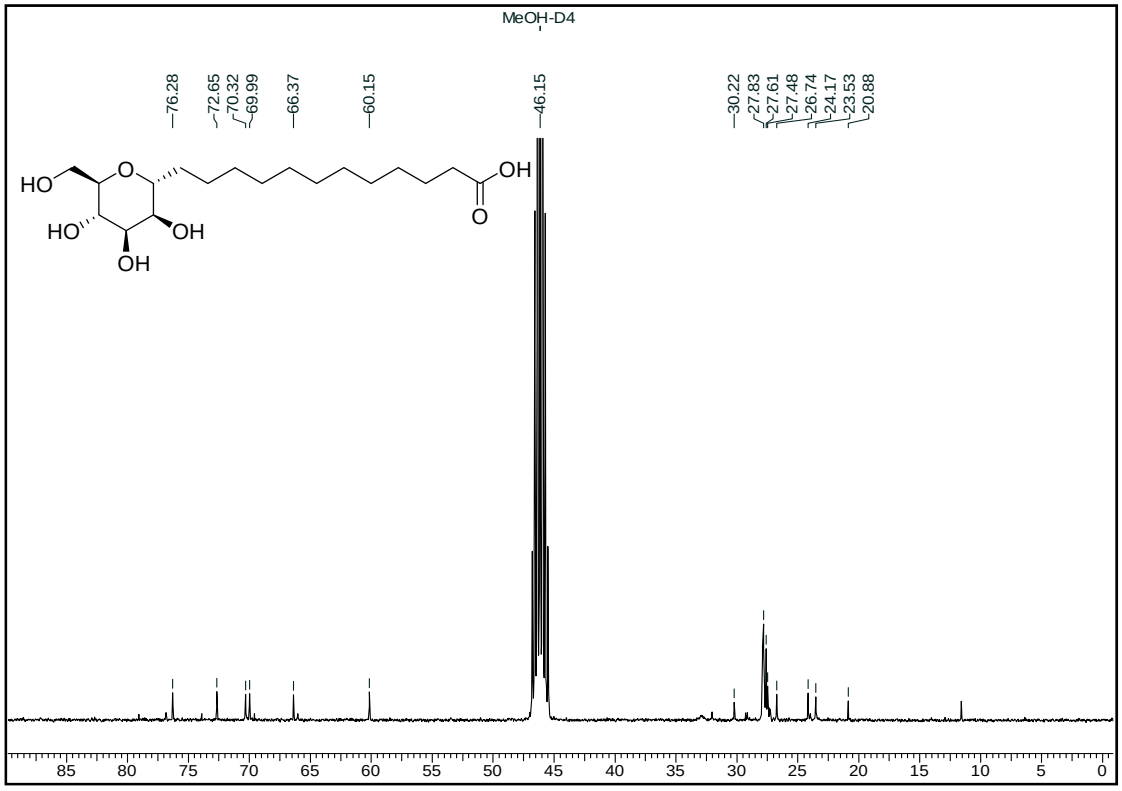

^{13}C NMR spectrum of **2.5** in MeOH-D4

2.7 References

1. C. W. M. Grant and M. W. Peters, *Biochim. Biophys. Acta*, 1984, **779**, 403-422.
2. H. Lis and N. Sharon, *Annu. Rev. Biochem.*, 1986, **55**, 35-67.
3. M. Spiess, *Biochemistry*, 1990, **29**, 10009-10018.
4. A. Frey, K. T. Giannasca, R. Weltzin, P. J. Giannasca, H. Reggio, W. I. Lencer and M. R. Neutra, *J. Exp. Med.*, 1996, **184**, 1045-1059.
5. R. A. Dwek, *Chemical Reviews*, 1996, **96**, 683-720.
6. T. Feizi and R. A. Childs, *Biochem. J.*, 1987, **245**, 1-11.
7. K. Drickamer and M. E. Taylor, *Annu. Rev. Cell Biol.*, 1993, **9**, 237-264.
8. R. Jelinek and S. Kolusheva, *Chemical Reviews*, 2004, **104**, 5987-6015.
9. E. E. Simanek, G. J. McGarvey, J. A. Jablonowski and C. H. Wong, *Chemical Reviews*, 1998, **98**, 833-862.
10. Y. Chen, T. Ji and Z. Rosenzweig, *Nano Lett.*, 2003, **3**, 581-584.
11. X.-L. Sun, W. Cui, C. Haller and E. L. Chaikof, *ChemBioChem*, 2004, **5**, 1593-1596.
12. P. Babu, S. Sinha and A. Surolia, *Bioconjugate Chem.*, 2007, **18**, 146-151.
13. J. M. de la Fuente and S. Penades, *Glycoconjugate Journal*, 2004, **21**, 149-163.
14. Y. C. Lee and R. T. Lee, *Accounts of Chemical Research*, 1995, **28**, 321-327.
15. H. Lis and N. Sharon, *Chemical Reviews*, 1998, **98**, 637-674.
16. K. M. Koeller and C.-H. Wong, *Nat. Biotechnol.*, 2000, **18**, 835-841.
17. C. R. Bertozzi and L. L. Kiessling, *Science* 2001, **291**, 2357-2364.
18. D. H. Dube and C. R. Bertozzi, *Nat. Rev. Drug Discovery*, 2005, **4**, 477-488.
19. J. M. de la Fuente, A. G. Barrientos, T. C. Rojas, J. Rojo, J. Canada, A. Fernandez and S. Penades, *Angew. Chem., Int. Ed.*, 2001, **40**, 2257-2261.
20. B. Mukhopadhyay, M. B. Martins, R. Karamanska, D. A. Russell and R. A. Field, *Tetrahedron Lett.*, 2009, **50**, 886-889.
21. J. Zhao, Y. Liu, H.-J. Park, J. M. Boggs and A. Basu, *Bioconjugate Chem.*, **23**, 1166-1173.
22. B. K. Gorityala, Z. Lu, M. L. Leow, J. Ma and X.-W. Liu, *J. Am. Chem. Soc.*, **134**, 15229-15232.

23. S. G. Spain, L. Albertin and N. R. Cameron, *Chem. Commun.*, 2006, 4198-4200.
24. M. Veerapandian, S. K. Lim, H. M. Nam, G. Kuppannan and K. S. Yun, *Anal. Bioanal. Chem.*, **398**, 867-876.
25. K. S. I. van, S. J. Campbell, S. Serres, D. C. Anthony, N. R. Sibson and B. G. Davis, *Proc. Natl. Acad. Sci. U. S. A.*, 2009, **106**, 18-23.
26. K. El-Boubbou, D. C. Zhu, C. Vasileiou, B. Borhan, D. Prosperi, W. Li and X. Huang, *J. Am. Chem. Soc.*, **132**, 4490-4499.
27. X. Wang, E. Matei, L. Deng, O. Ramstroem, A. M. Gronenborn and M. Yan, *Chem. Commun.*, **47**, 8620-8622.
28. K. A. Karlsson, *Annu. Rev. Biochem.*, 1989, **58**, 309-350.
29. M. S. Manocha and Y. Chen, *Can. J. Microbiol.*, 1990, **36**, 69-76.
30. T. Muramatsu, *Glycobiology*, 1993, **3**, 291-296.
31. M.-C. Daniel and D. Astruc, *Chem. Rev. (Washington, DC, U. S.)*, 2004, **104**, 293-346.
32. M. Brust, M. Walker, D. Bethell, D. J. Schiffrin and R. Whyman, *J. Chem. Soc., Chem. Commun.*, 1994, 801-802.
33. C. R. K. Rao and D. C. Trivedi, *Mater. Chem. Phys.*, 2006, **99**, 354-360.
34. J. Han, Y. Liu, L. Li and R. Guo, *Langmuir*, 2009, **25**, 11054-11060.
35. F. Dumur, A. Guerlin, E. Dumas, D. Bertin, D. Gigmes and C. R. Mayer, *Gold Bull*, 2011, **44**, 119-137.
36. A. Rai, A. Prabhune and C. C. Perry, *J. Mater. Chem.*, 2010, **20**, 6789-6798.
37. S. Dhar, E. M. Reddy, A. Shiras, V. Pokharkar and B. L. V. Prasad, *Chem. - Eur. J.*, 2008, **14**, 10244-10250.
38. G. Nasr, A. Guerlin, F. Dumur, S. A. Baudron, E. Dumas, F. Miomandre, G. Clavier, M. Sliwa and C. R. Mayer, *J. Am. Chem. Soc.*, 2011, **133**, 6501-6504.
39. M. Aslam, L. Fu, M. Su, K. Vijayamohanan and V. P. Dravid, *J. Mater. Chem.*, 2004, **14**, 1795-1797.
40. L. Polavarapu and Q.-H. Xu, *Nanotechnology*, 2008, **19**, 075601/075601-075601/075606.
41. S. Singh, V. D'Britto, A. A. Prabhune, C. V. Ramana, A. Dhawan and B. L. V. Prasad, *New J. Chem.*, **34**, 294-301.
42. L. Longenberger and G. Mills, *J. Phys. Chem.*, 1995, **99**, 475-478.

43. C. E. Hoppe, M. Lazzari, I. Pardinas-Blanco and M. A. Lopez-Quintela, *Langmuir*, 2006, **22**, 7027-7034.
44. S. Dhar, P. Murawala, A. Shiras, V. Pokharkar and B. L. V. Prasad, *Nanoscale*, 2012, **4**, 563-567.
45. S. Singh, P. Patel, S. Jaiswal, A. A. Prabhune, C. V. Ramana and B. L. V. Prasad, *New J. Chem.*, 2009, **33**, 646-652.
46. S. Singh, V. D'Britto, A. A. Prabhune, C. V. Ramana, A. Dhawan and B. L. V. Prasad, *New J. Chem.*, 2010, **34**, 294-301.
47. J. M. de la Fuente and S. Penades, *Glycoconjugate J.*, 2004, **21**, 149-163.
48. A. C. de Souza, K. M. Halkes, J. D. Meeldijk, A. J. Verkleij, J. F. G. Vliegenthart and J. P. Kamerling, *European Journal of Organic Chemistry*, 2004, 4323-4339.
49. J. M. De la Fuente and S. Penades, *Biochim. Biophys. Acta*, 2006, **1760**, 636-651.
50. L. Sihelnikova and I. Tvaroska, *Chem. Pap.*, 2007, **61**, 237-255.
51. J. M. de la Fuente, D. Alcantara and S. Penades, *IEEE Trans. Nanobiosci.*, 2007, **6**, 275-281.
52. Y. G. Du, R. J. Linhardt and I. R. Vlahov, *Tetrahedron*, 1998, **54**, 9913-9959.
53. R. V. Weatherman and L. L. Kiessling, *J. Org. Chem.*, 1996, **61**, 534-538.
54. R. V. Weatherman, K. H. Mortell, M. Chervenak, L. L. Kiessling and E. J. Toone, *Biochemistry*, 1996, **35**, 3619-3624.
55. D. P. Sutherlin, T. M. Stark, R. Hughes and R. W. Armstrong, *J. Org. Chem.*, 1996, **61**, 8350-8354.
56. D. Schwabisch, S. Wille, M. Hein and R. Miethchen, *Liquid Crystals*, 2004, **31**, 1143-1150.
57. C. V. Ramana, K. A. Durugkar, V. G. Puranik, S. B. Narute and B. L. V. Prasad, *Tetrahedron Letters*, 2008, **49**, 6227-6230.
58. M. S. M. Timmer, M. V. Chumillas, W. E. Donker-Koopman, J. Alerts, G. A. van der Marel, H. S. Overkleeft and J. H. van Boom, *Journal of Carbohydrate Chemistry*, 2005, **24**, 335-351.
59. S. J. Angyal, J. D. Stevens and L. Odier, *Carbohydr. Res.*, 1986, **157**, 83-94.
60. W. J. Hennen, H. M. Sweers, Y. F. Wang and C. H. Wong, *Journal of Organic Chemistry*, 1988, **53**, 4939-4945.

61. H. O. Martinez, H. Reinke, D. Michalik and C. Vogel, *Synthesis-Stuttgart*, 2009, 1834-1840.

62. A. Giannis and K. Sandhoff, *Tetrahedron Letters*, 1985, **26**, 1479-1482.

63. D. Horton and T. Miyake, *Carbohydrate Research*, 1988, **184**, 221-229.

64. G. J. McGarvey, C. A. LeClair and B. A. Schmidtmann, *Organic Letters*, 2008, **10**, 4727-4730.

65. Y. Yin, Z.-Y. Li, Z. Zhong, B. Gates, Y. Xia and S. Venkateswaran, *J. Mater. Chem.*, 2002, **12**, 522-527.

Chapter 3

Synthesis of mannose and glucose decorated Ag-glyconanoparticles, their lectin binding studies and anti bacterial activity

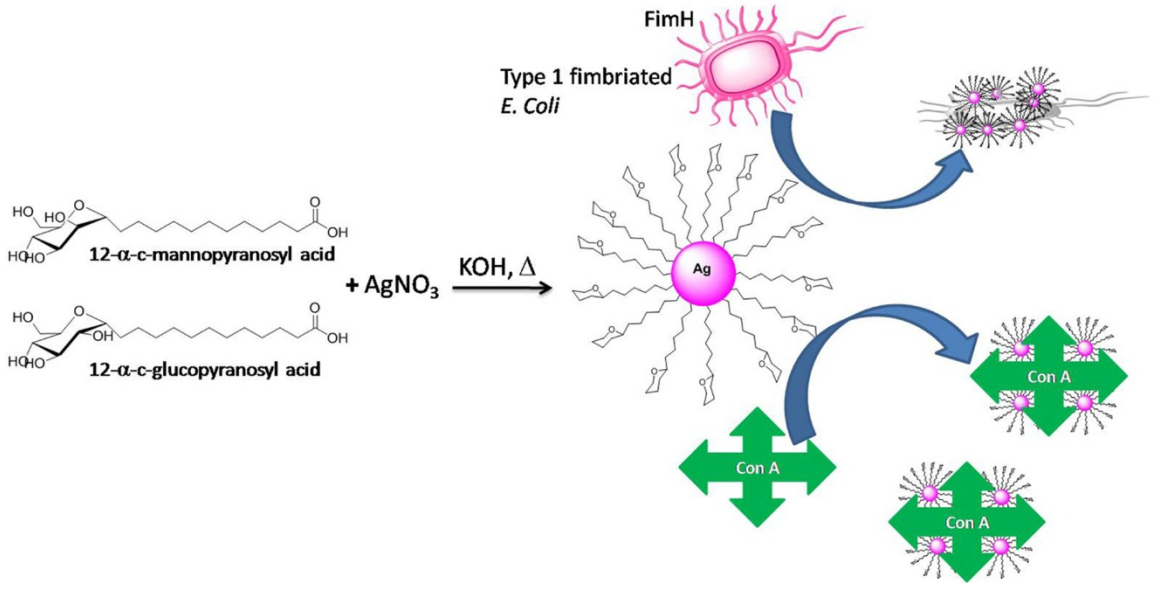

3.1 Introduction

As mentioned in the previous two chapters, the extracellular glycoprotein material present on some mammalian cells is known as ‘‘glycocalyx’’.[1] Glycocalyx has been linked to many important cellular functions, including protein folding, trafficking, stability, organ development, cellular adhesion, cell signaling, immune response, and pathological processes.[2, 3] In many of the above functions the carbohydrate-carbohydrate, carbohydrate-protein interactions that are characterized with high specificity and low affinities are known to play an important role.[4-6] Natural systems overcome the issue of low affinity by polyvalency through the presence of many ligands on the cell surface.

Lectins are proteins that binds to carbohydrates specifically and reversibly.[7] Lectins are very well known for their agglutinating nature on a variety of cells.[8, 9] Among all the commercially available lectins, Concanavalin A (Con A) is the most widely used lectin to characterize glycoproteins and glycolipids present on the various cell surfaces.[10] Con A binds specifically to α-D-mannosyl and α-D-glucosyl residues.[11]

In literature, GNPs derived from the surface modification of metal nanoparticles by molecules which are connected with sugar residues through *O*-glycoside linkages have been proposed/used for investigating carbohydrate recognition processes.[12-15] However, as for as the *in vivo* application of the GNPs are considered, the enzymatic degradation of the *O*-glycoside linkage in these GNPs becomes a great concern. For this reason, *C*-glycosides have been developed and were found to be potential carbohydrate analogs resistant to metabolic processes. *C*-glycosides where the anomeric oxygen is substituted by a methylene unit are isosteric mimics of their *O*-glycoside counterparts. The methylene substitution imparts a great deal of stability to *C*-gycosides without substantial conformational amendment.[16-19] Though the application of *C*-glycosylated long chain alkanes has been explored as liquid crystals and as surfactants,[20, 21] their use in GNPs synthesis has been very sparse and has only been unveiled very recently.[22] However, these works highlighted only synthesis and no efforts to study carbohydrate-carbohydrate or carbohydrate-protein interactions were made. Furthermore, harmful bacteria that cause millions of disease and disability every year,[23, 24] are known to establish infection after adhering to host tissues through multivalent carbohydrate–lectin interactions. Therefore, an effective antibacterial strategy is needed to inhibit these bacterial interactions with

target cells.[25] In this premise, in this chapter, we have discussed the synthesis of mannose and glucose containing 12-*C*-glycosyl long chain acids. These 12-*C*-glycosyl long chain acids were then used as capping/reducing agents for the Ag GNPs synthesis. These Ag GNPs were later utilized to investigate the carbohydrate-lectin interactions and their utility for anti bacterial activity against *E. coli* are also demonstrated.

3.2 Synthesis of mannose and glucose *C*-glycosyl acids

Detailed synthesis and characterization of 12-α-*C*-gluco-pyranosyl-dodecanoic acid (compound **2.3**) and 12-α-*C*-manno-pyranosyl-dodecanoic acid (compound **2.5**) were given in chapter 2 section 2.5.

3.3 Synthesis of Ag-glyconanoparticles

After synthesizing the desired *C*-glycosyl acids **2.3** and **2.5**, the next objective was to use them as capping/reducing agents for the synthesis of silver nanoparticles (Ag NPs). It has already been established that 12-α-*C*-glycosyl acid can be used as capping and reducing agents for Ag NPs.[22] Utilizing similar strategies the synthesis of Ag NPs using 12-*C*-glycosyl acids **2.3** and **2.5** was accomplished in the following manner. Equimolar quantities of silver nitrate (10^{-4} M) and 12-*C*-glycosyl acid **2.3** and **2.5** (10^{-4} M) were heated (~70-80 ºC) in dilute alkaline solution.[26] The reduction of Ag^{+1} to Ag^{0} was instantaneous and the Ag NPs were purified by centrifugation (12000 rpm for 3x25 mL washings with milliQ water) to remove excess ligand. The concentrated Ag NP thick dispersions were stored in sample vials covered with aluminium foils for further studies. The Ag GNPs synthesized by using 12-*C*-glycosyl acids (**2.3** and **2.5**) as capping and reducing agents, are designated as Ag-**2.3** GNPs (Ag-glucose) and Ag-**2.5** GNPs (Ag-mannose) further in the text.

A yellow- yellow/brownish coloured solution indicating the formation of Ag NPs was observed immediately on heating a mixture of Ag NO_3 and 12-*C*-glycosyl acids. The reduction of Ag^{+1} to Ag^{0} with both the glyco acids was instantaneous and within 5 min a well defined peak at λ_{max} ~415 nm developed (Fig. 3.1A). This peak is attributed to the surface plasmon resonance of Ag NPs.[27] The formation of Ag-**2.3** and Ag-**2.5** GNPs was

again conformed by powder XRD. In both cases we could observe four signature peaks (Fig. 3.1B) assigned to the (1 1 1), (2 0 0), (2 2 0) and (3 1 1) planes of fcc lattice of metallic Ag. The TEM image in Fig. 3.1C and 3.1D, correspond to the samples Ag-**2.3** (~25±3 nm) and Ag-**2.5** (19±2 nm) GNPs respectively. In both cases, GNPs formed are polydispersed and the inserts in Fig. 3.1C and 3.1D show the particle size distributions in each case respectively.

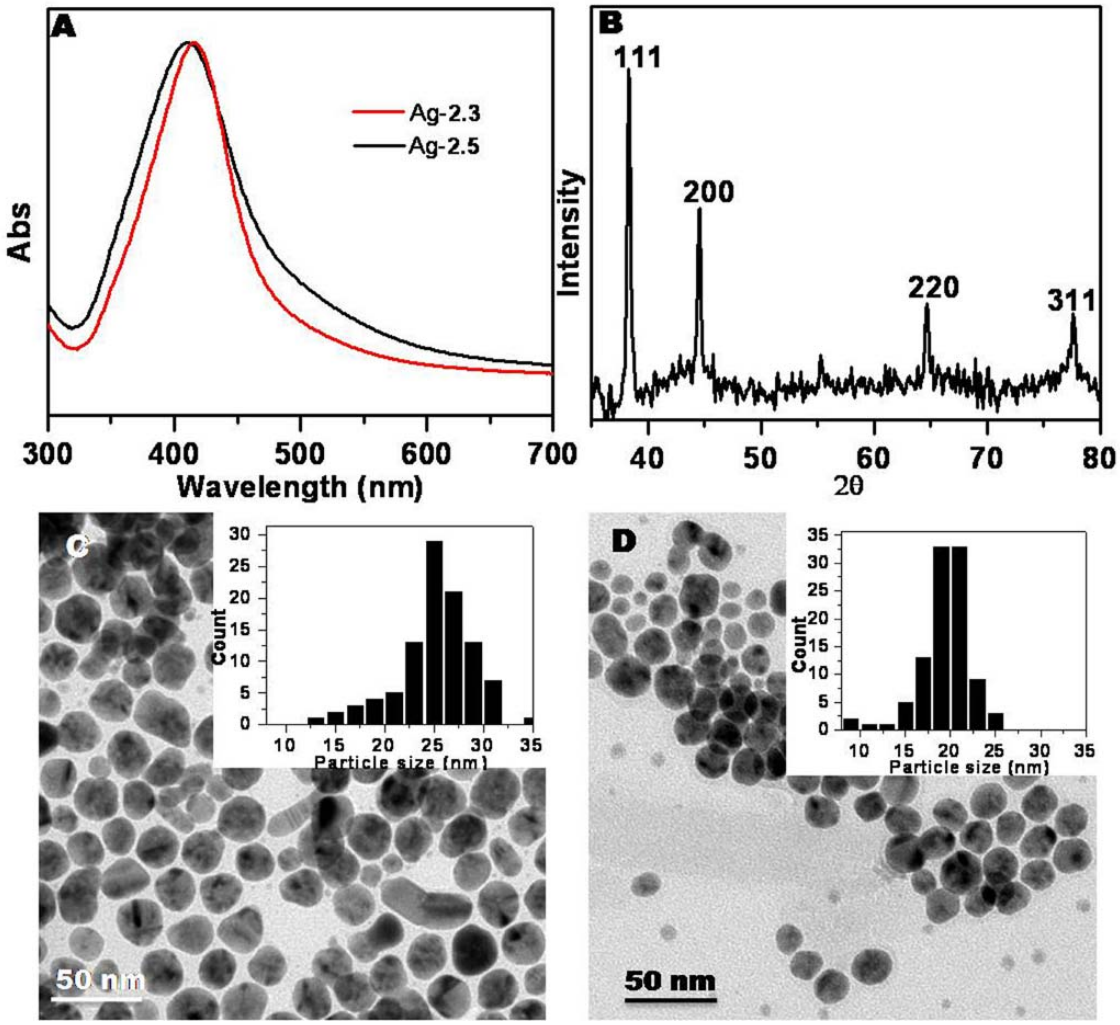

Figure 3.1. *(A) UV-visible spectrum of Ag-**2.3** GNPs (red curve) and Ag-**2.5** GNPs (block curve), (B) Powder XRD of* Ag-**2.3** and Ag-**2.5** *GNPs, TEM images of as-prepared (C) Ag-**2.3** GNPs (insert shows the particle size distribution of Ag-**2.3** GNPs) and (D) Ag-**2.5** GNPs (insert shows the particle size distribution of Ag-**2.5** GNPs).*

3.3.1 Determination of amount of Carbohydrates present in the Nanoparticle solution

The amount of carbohydrates present on Ag-**2.3** and Ag-**2.5** GNPs was determined by anthrone-sulfuric acid assay.[28, 29] Briefly, carbohydrates (1 to 15 μg) were dissolved in 0.5 mL of milli Q water. After that, 1 mL of a freshly prepared 0.5% anthrone (w/w) in 95% sulfuric acid solution was added to 0.5 mL of ice-cold sugar solution. These two solutions were gently mixed and heated to 100° for 10 min and then allowed to cool at RT. The absorbance was recorded at 620 nm, and the plot of absorbance versus concentration of carbohydrate resulted in a standard curve (Fig. 3.2). Next, different concentrations of the GNPs solution (10-50 μL) were subjected to the same method. From this concentration, the amount of sugar present on the GNP surface was estimated to be 0.2 mg/mL of glucose on Ag-**2.3** GNPs dispersion and 0.3 mg/mL of mannose on Ag-**2.5** GNPs dispersion.

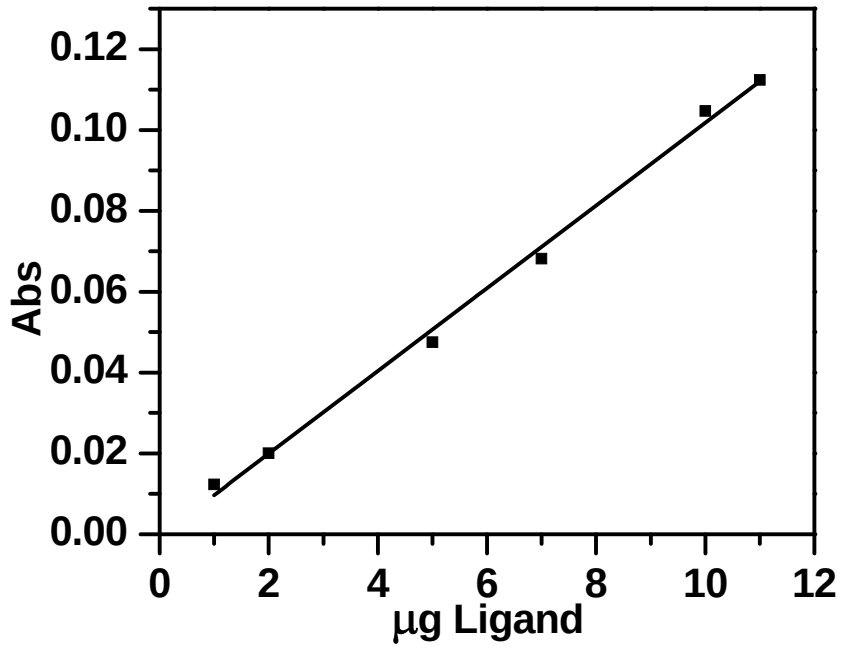

Figure 3.2. *The plot of concentration of free ligand versus absorbance @ 620 nm*

3.3.2 Binding experiment of Ag GNPs to FITC-Con A

The binding of Ag-**2.3** and Ag-**2.5** GNPs to FITC-Con A was examined by fluorescence spectroscopy. In this experiment 10 µg/mL (0.98 µM, 3 mL) of FITC-Con A in PB buffer containing 0.1 mM $CaCl_2$ and 0.1 mM $MnCl_2$ at 7.0 pH, was incubated with Ag-**2.3** and Ag-**2.5** GNPs solutions. Four different samples of Ag-**2.3** and Ag-**2.5** GNPs were prepared such that the amount of sugar present on the GNPs corresponds to 2.5, 5, 10 and 30 µg.

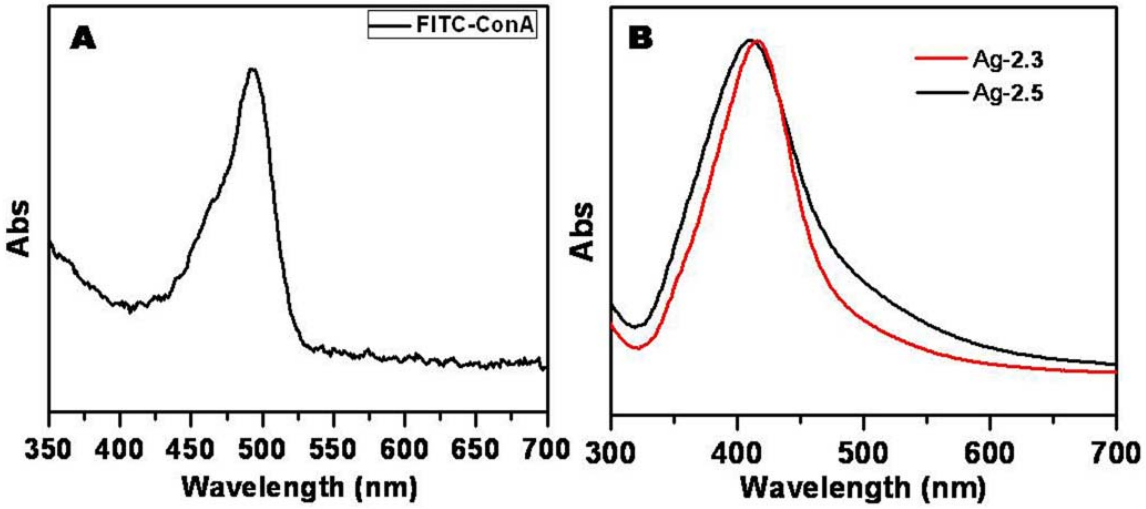

Figure 3.3. *UV-Vis spectrum of (A) FITC-Con A and (B) Ag-**2.3** GNPs (red curve) and Ag-**2.5** GNPs (black curve).*

The UV-vis spectrum of FITC-Con A shows an absorbance peak at 490 nm (Fig. 3.3A), while the pure Ag-**2.3** or Ag-**2.5** GNPs show a peak around 420 nm (Fig. 3.3B). When FITC-Con A was incubated with Ag-**2.3** (Fig. 3.4A) and Ag-**2.5** GNPs (Fig. 3.4B) samples, a red shift in λ_{max} was observed with concomitant broadening of the absorption peak of Ag GNPs. The color of Ag GNPs changed yellow to orange. This clearly indicates the binding of Con A to the sugars in both Ag-**2.3** GNPs and Ag-**2.5** GNPs. The small feature around 490 nm in the spectra obtained after incubating FITC-Con A with Ag-GNPs also evidence its presence in the composite. Fig. 3.4 C and D depict the TEM images of Ag-**2.3** and Ag-**2.5** GNPs respectively after incubation with FITC-Con A. It can be noted that both the samples formed large aggregates because of binding of FITC-Con A with glucose and mannose which are present on Ag NPs surface.

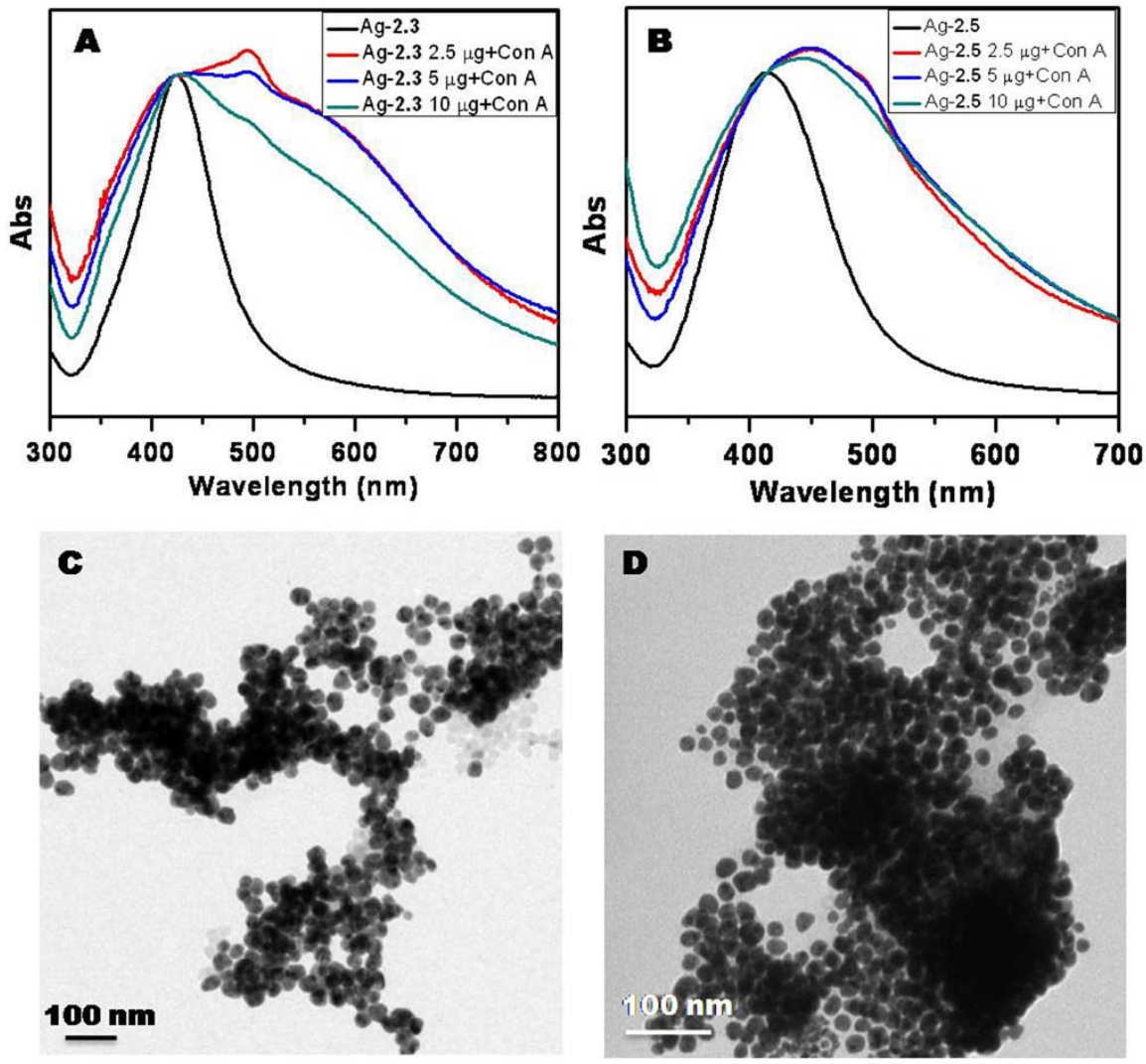

Figure 3.4. *Changes in the UV-visible spectrum of (A) Ag-**2.3** GNPs and (B) Ag-**2.5** GNPs, before and after addition of FITC-Con A, TEM images of (C) Ag-**2.3** GNPs + Con A and (D) Ag-**2.5** GNPs + Con A.*

Furthermore, the binding of Ag-**2.3** and Ag-**2.5** GNPs to FITC-Con A was also examined by fluorescence spectroscopy. The optical emission signal was recorded by exciting the sample at 490 nm. The fluorescence spectra of FITC-Con A, has been recorded at different time intervals to show that its fluorescence intensity does not decrease with time (Fig.3.5 A). However, shows that in the presence of Ag-**2.3** and Ag-**2.5** GNPs, the fluorescence intensity of FITC–Con A keeps on reducing with the addition of increasing concentration of Ag-**2.3** and Ag-**2.5** GNPs respectively (Fig. 3.5 B and C).

While the above tests with FITC-Con A prove the efficacy of glucose/mannose to bind to the lectin, no significant differences in terms of efficiencies of Ag-**2.3** and Ag-**2.5** GNPs respect to their binding to lectins could be displayed by this study.

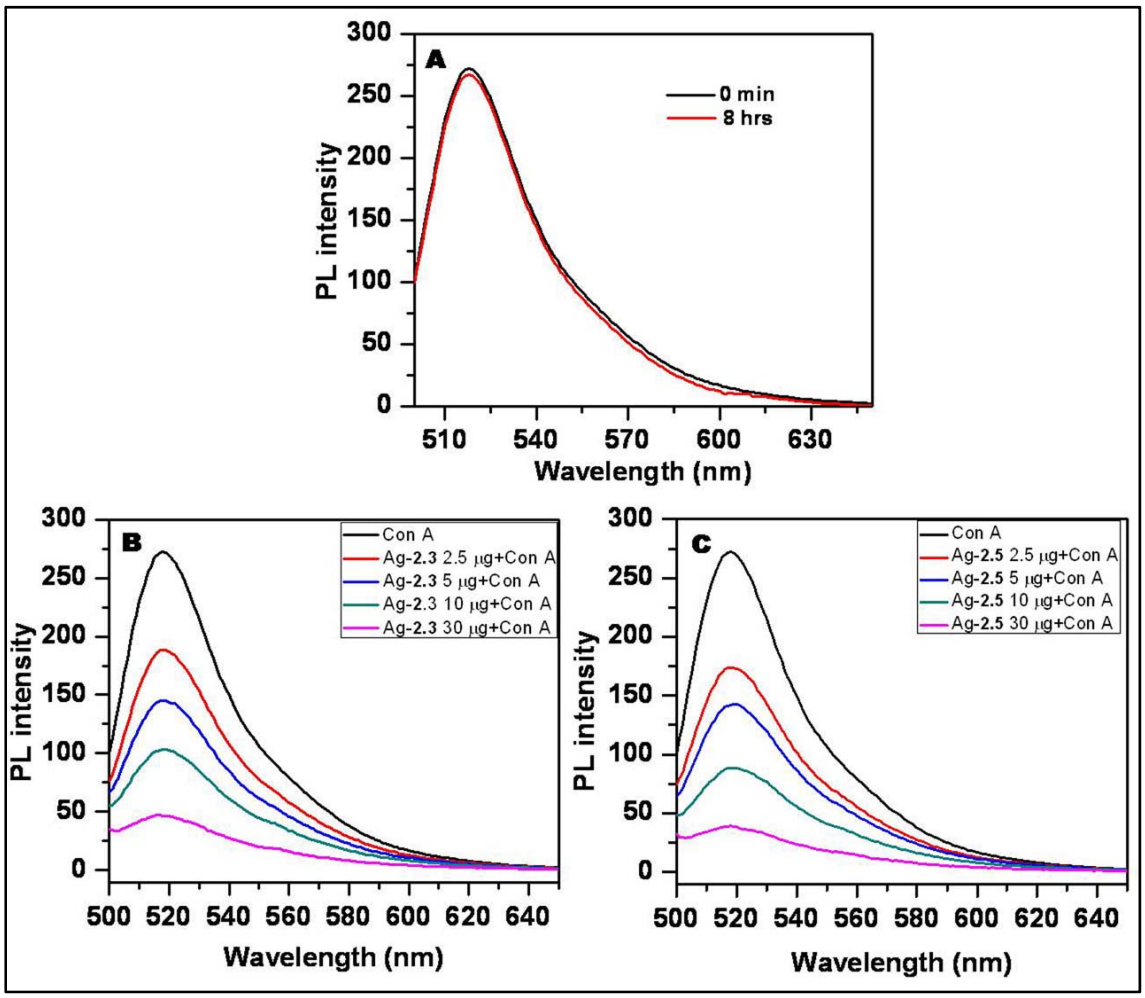

Figure 3.5. *Fluorescence intensity of FITC-Con A (10 mg/mL) (A) as prepared (black curve) and after 8 hrs (red curve), excited @ 490 nm. Change in the emission spectrum of FITC-Con A with the addition of (B) Ag-**2.3** GNPs and (C) Ag-**2.5** GNPs. All spectra measured in phosphate buffer (with 0.1 mM $CaCl_2$ and 0.1 mM $MnCl_2$) at pH 7.0 and an excitation wavelength of 490 nm.*

Thus, inorder to show the utility of mannoside capped nanoparticles in specific applications, we carried out the antibacterial assay of these Ag-**2.3** GNPs and Ag-**2.5** GNPs against *E. coli*. It has been reported that the surface of type-1 pili of *E. coli* known

to bind with mannosides[30, 31] (Fig. 3.6) and therefore an enhanced interaction of Ag-**2.5** GNPs with *E. coli* leading to their higher mortality could be expected.

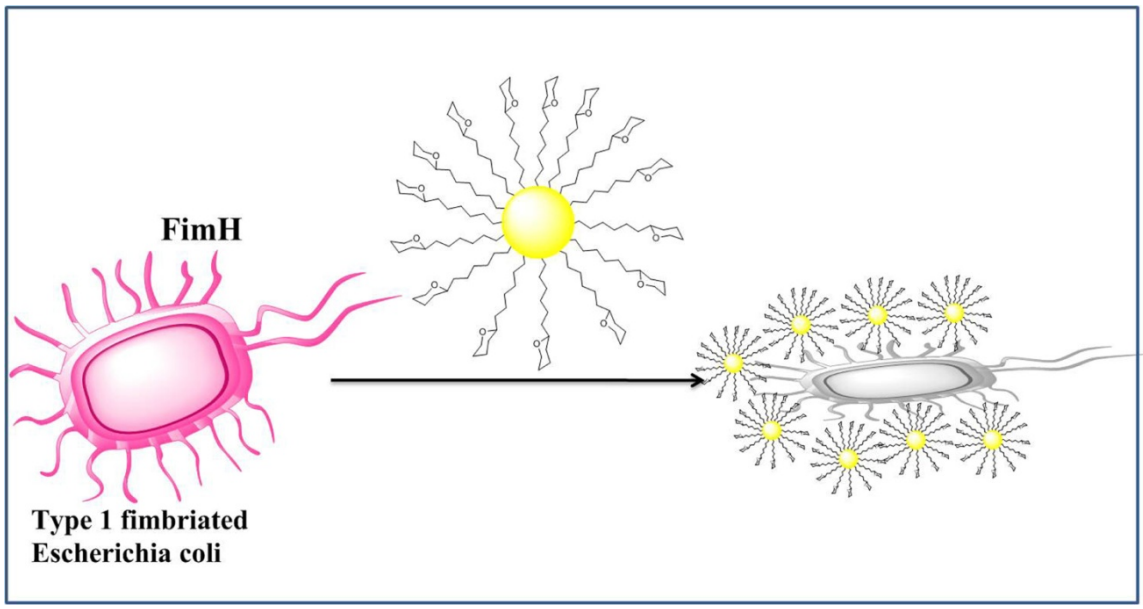

Figure 3.6*. Schematic representation of interaction of Ag GNPs with E. coli bacteria*

3.4 Organism preparation and antibacterial activity of Ag GNPs

E. coli cells (DH5α cells) was grown overnight in Luria Bertani (LB) medium at 37 °C. The washed cells were then re suspended in LB medium and optical density (OD) was adjusted to 0.1, corresponding to 10^8 CFU/ml at 600 nm. A 100 µL sample of bacterial suspension cultured in LB medium with a concentration of 10^{-8} CFU/mL of *E. coli* was placed on a nutrient agar plate by spread plate technique. To study the anti bacterial effect of Ag-**2.3** and Ag-**2.5** GNPs, approximately 10^8 colony forming units (CFU) of *E. coli* cells (DH5α cells) were platted on a Luria Bertani (LB) with 1.5% agar plate. The disks of approximately 1 cm x 1 cm were prepared and sterilized by autoclaving. The disks were placed on the bacterial platted medium with control (only sterile disk) and different concentrations (5, 10 and 15 µg) of Ag-**2.3** (Fig. 3.7A) and Ag-**2.5** GNPs (Fig. 3.7B). These plates with Ag GNPs were prepared by drop casting the nanoparticle dispersion on the disk and the plates were incubated at 37 °C for 24 hrs. After 24 hrs the zone of inhibition was measured by scale.

From the antibacterial experiment, it can be clearly seen that compared to Ag-**2.3** GNPs (Fig. 3.7A), Ag-**2.5** GNPs (Fig. 3.7B) incubated with *E. coli* show larger zone of inhibition (transparent area around the disk). This could be attributed to the FimH lectin units in the pili which are present on surface of *E. coli*. These are known to have greater affinity to mannose as compare to other sugars. This could lead to increased bindings of the Ag-**2.5** GNPs due to increased mannoside-binding activities of the bacteria (table 1). This increased local concentration of Ag/Ag^{+} ions on the bacteria surface explains the increased mortality of the bacteria in presence of Ag-**2.5** GNPs.

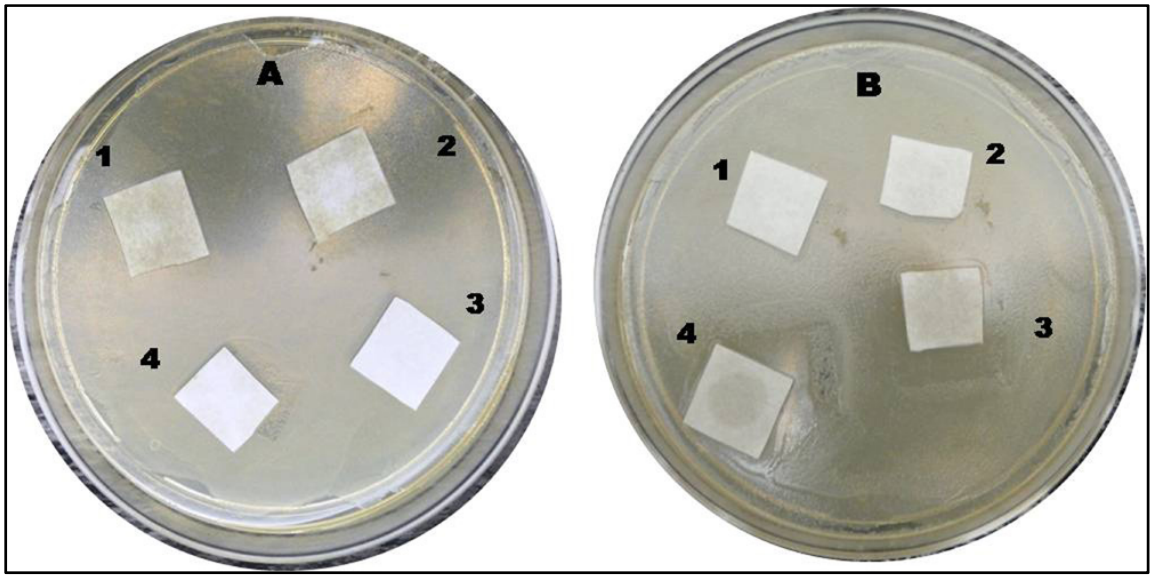

Figure 3.7. *Effect of Ag-**2.3** and Ag-**2.5** GNPs on the growth of E. coli (1.0×10^{8} CFU/mL), (A) Ag-**2.3** GNPs, (B) Ag-**2.5** GNPs were incubated on sterile disk 1 (0 µg), 2 (5 µg), 3 (10 µg) and 4 (15 µg).*

Table 1: Details of the zone of inhibitions observed with different concentrations of Ag-**1** and Ag-**2** GNPs

Sr. No.	Mannose and glucose present on Ag-**2.3** and Ag-**2.5** GNPs respectively (µg)	Ag-**2.3** GNPs zone of inhibition (mm)	Ag-**2.5** GNPs zone of inhibition (mm)
1	0	0	0
2	5	0.6±0.5	2±1
3	10	1.6±0.5	8.3±1
4	15	6±0.5	13±1

3.5 Conclusions

We described the synthesis of two 12-*C*-glycosyl long chain acids synthesis, which are used in the synthesis of biofunctional Ag NPs. Furthermore, these biofuctional Ag NPs were used for the selective detection of Con A and *E. coli*. *C*-glycosides could import greater stability to the GNPs when we use them in *in-vivo* applications.

3.6 References

1. R. A. Dwek, *Chem. Rev.*, 1996, **96**, 683-720.
2. J. D. Marth and P. K. Grewal, *Nat. Rev. Immunol.*, 2008, **8**, 874-887.
3. K. Ohtsubo and J. D. Marth, *Cell*, 2006, **126**, 855-867.
4. O. Martinez-Avila, L. M. Bedoya, M. Marradi, C. Clavel, J. Alcami and S. Penades, *Chembiochem*, 2009, **10**, 1806-1809.
5. D. C. Hone, A. H. Haines and D. A. Russell, *Langmuir*, 2003, **19**, 7141-7144.
6. A. G. Barrientos, J. M. de la Fuente, T. C. Rojas, A. Fernandez and S. Penades, *Chem. Eur. J.*, 2003, **9**, 1909-1921.
7. C. L. Schofield, R. A. Field and D. A. Russell, *Anal. Chem.*, 2007, **79**, 1356-1361.
8. M. Martinez-Cruz, E. Zenteno and F. Cordoba, *Biochim. Biophys. Acta*, 2001, **1568**, 37-44.
9. M. Slifkin and R. Cumbie, *J. Clin. Microbiol.*, 1989, **27**, 1036-1039.
10. J. N. Wang, T. C. Duan, L. L. Sun, D. J. Liu and Z. X. Wang, *Anal. Biochem.*, 2009, **392**, 77-82.
11. Y.-J. Chuang, X. Zhou, Z. Pan and C. Turchi, *Biochem. Biophys. Res. Commun.*, 2009, **389**, 22-27.
12. J. Zhao, Y. Liu, H.-J. Park, J. M. Boggs and A. Basu, *Bioconjugate Chem.*, 2012, **23**, 1166-1173.
13. S. G. Spain, L. Albertin and N. R. Cameron, *Chem. Commun.*, 2006, 4198-4200.
14. K. Petkau, A. Kaeser, I. Fischer, L. Brunsveld and A. P. H. J. Schenning, *J. Am. Chem. Soc.*, 2011, **133**, 17063-17071.
15. K. El-Boubbou, D. C. Zhu, C. Vasileiou, B. Borhan, D. Prosperi, W. Li and X. Huang, *J. Am. Chem. Soc.*, 2010, **132**, 4490-4499.
16. R. V. Weatherman and L. L. Kiessling, *J. Org. Chem.*, 1996, **61**, 534-538.
17. Y. G. Du, R. J. Linhardt and I. R. Vlahov, *Tetrahedron*, 1998, **54**, 9913-9959.
18. R. V. Weatherman, K. I. Mortell, M. Chervenak, L. L. Kiessling and E. J. Toone, *Biochemistry*, 1996, **35**, 3619-3624.
19. D. P. Sutherlin, T. M. Stark, R. Hughes and R. W. Armstrong, *J. Org. Chem.*, 1996, **61**, 8350-8354.

20. D. Schwabisch, S. Wille, M. Hein and R. Miethchen, *Liq. Cryst.*, 2004, **31**, 1143-1150.
21. M. Harenbrock, A. Matzeit and H. J. Schafer, *Liebigs Annalen*, 1996, 55-62.
22. C. V. Ramana, K. A. Durugkar, V. G. Puranik, S. B. Narute and B. L. V. Prasad, *Tetrahedron Lett.*, 2008, **49**, 6227-6230.
23. S. E. Hrudey and E. J. Hrudey, *Water Environ. Res.*, 2007, **79**, 233-245.
24. T. M. Straub and D. P. Chandler, *J Microbiol Methods*, 2003, **53**, 185-197.
25. I. Ofek, D. L. Hasty and N. Sharon, *FEMS Immunol. Med. Microbiol.*, 2003, **38**, 181-191.
26. Y. D. Yin, Z. Y. Li, Z. Y. Zhong, B. Gates, Y. N. Xia and S. Venkateswaran, *J. Mater. Chem.*, 2002, **12**, 522-527.
27. P. Mulvaney, *Langmuir*, 1996, **12**, 788-800.
28. Y.-Y. Chien, M.-D. Jan, A. K. Adak, H.-C. Tzeng, Y.-P. Lin, Y.-J. Chen, K.-T. Wang, C.-T. Chen, C.-C. Chen and C.-C. Lin, *Chembiochem*, 2008, **9**, 1100-1109.
29. A. A. Kulkarni, C. Fuller, H. Korman, A. A. Weiss and S. S. Iyer, *Bioconjugate Chem.*, 2010, **21**, 1486-1493.
30. N. Firon, S. Ashkenazi, D. Mirelman, I. Ofek and N. Sharon, *Infect. Immun.*, 1987, **55**, 472-476.
31. J. Goldhar, A. Zilberberg and I. Ofek, *Infect. Immun.*, 1986, **52**, 205-208.

Chapter 4

Synthesis of SiO_2-glyconanoparticles and their lectin binding studies

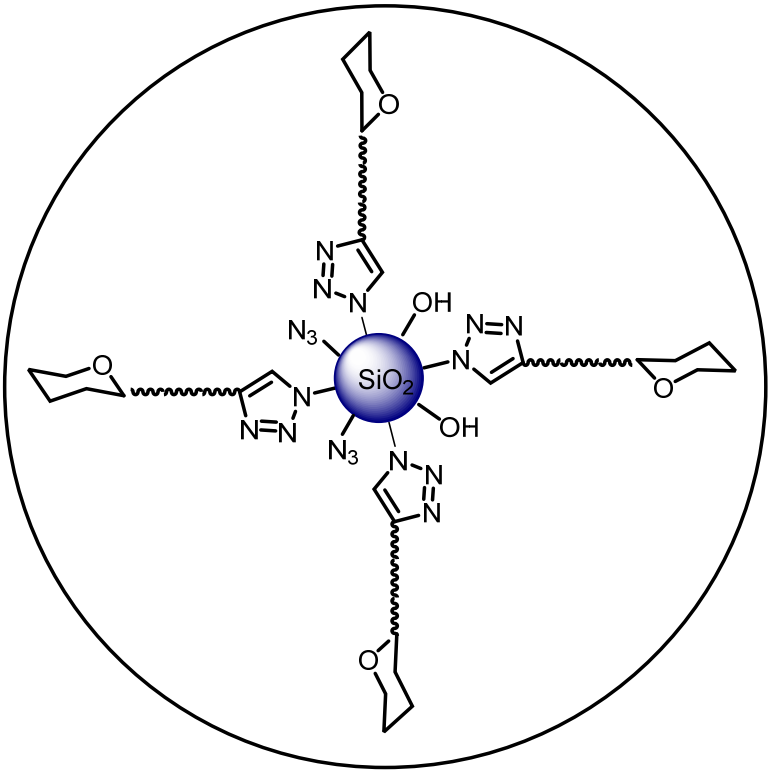

4.1 Introduction

Carbohydrates are important class of biomolecules playing crucial roles not only as energy sources and structural materials but also as signaling molecules involved in intramolecular and intercellular communication in almost all biological/physiological processes. Consequently there is now a great deal of interest to prepare carbohydrate decorated inorganic nanoparticles (GNPs) that could mimic the glycocalyx of the cell surface. The synthesis of inorganic nanoparticles in presence of glycans (chapter 1 section 1.3.1.) with appropriate nanoparticle surface anchoring groups is one way to accomplish the GNPs. However, methods based on post-synthetic surface modification steps have been evoking greater interest these days. Since the rediscovery of the Huisgen 1,3-dipolar cycloaddition of alkynes and azides, this reaction has attracted tremendous attention in the area of glycobiology where it has proved its value for the preparation of a wide range of carbohydrate containing molecular constructs.[1-5]

The introduction of the ‘‘click-chemistry’’ concept[6] has made a great impact on the chemical philosophy driving the design of synthetic biomaterials. The copper(I)-catalyzed azide–alkyne cycloaddition (CuAAC) reaction has provided a unique tool for easy access to functionalized surfaces of reliable and reproducible surface densities.[7-11] The CuAAC has transformed a purely thermal 1,3-dipolar cycloaddition process to an efficient and selective (regio- and chemo-) catalytic 1,3-dipolar cycloaddition process. The main advantage of CuAAC reaction is, it can be carried out at ambient temperature, is nearly solvent insensitive, and shows an extremely high tolerance to other functional groups. These characteristics have credited the CuAAC as a valuable ligation tool that has been rapidly adopted in fields of research as diverse as organic synthesis, polymer and materials science,[7-17] medicinal chemistry,[18-21] molecular biology and biotechnology,[1, 22-24] and supramolecular chemistry.[25, 26] CuAAC has been used in the functionalization of planar as well as curved surfaces. A large variety of systems ranging from self-assembled monolayers (SAMs), polymeric surfaces, layer-by-layer assemblies, block copolymers (BCPs), micelles, polymersomes and liposomes have been surface functionalized by using the CuAAC reaction.[15]

The versatility, reliability, robustness and especially the intrinsic chemoselectivity and bioorthogonality of the CuAAC reaction together with the mild

reaction conditions on both protected and unprotected sugar derivatives are all attractive features that have made click-chemistry particularly suitable for glycochemistry.[27, 28] In addition, the triazole groups that emerge in a click reaction act as robust linkers for the connection of different substructures in frameworks with varied complexity and have favourable physicochemical properties to mimic the sugar ring and the peptide bond. Silica-based hybrid materials possess very attractive physical and chemical properties: such as physical rigidity of their frameworks, high resistivity, negligible swelling in aqueous and organic solutions, chemical purity, high density of functional groups, chemical inertness, high biodegradation, photochemical, thermal, and microbiological stability and non-toxicity. They also have limited drawbacks such as hydrolysis at low and high pH and leaching of the functional groups from the support surface into the solution upon treatment with acidic solutions.[29, 30]

The introduction of the alkyne or azide group in to a saccharide is a routine process. This process allows easy access to mono as well as polyfunctionalized derivatives that can be rationally used for conjugation with other complementary functionalized synthetic and biological molecules or scaffolds by means of their intermolecular alkyne–azide 1,3-dipolar cycloaddition reaction. The anomeric position is usually the preferred position to place the linking azide or alkyne functionality but also the rest of the sugar ring positions have been used through adequate protection–deprotection strategies.[8, 22, 31-33]

The demand for reliable techniques for the immobilization of carbohydrates in the preparation of glyco materials has been a strong driving-force that has led to the development of a variety of glyco-functionalized solid supports (microarrays, microbeads, biosensor chips and SAMs) as valuable tools with important applications in the ‘‘omic’’ sciences.[2] The majority of these advanced materials have been constructed using non-silica matrices in spite of the positive properties mentioned above for silica-based hybrid materials. Until the recent advent of the click-chemistry methodology, silica-based hybrid glyco materials containing covalently bound sugars have been scarce in the literature, having found limited applications in boron removal,[5] and the isolation and purification of lectins.[34-37]

4.2 Present work

While scanning through the literature, we found that no-one has reported the synthesis of *C*-glycosyl decorated SiO_2 glyconanoparticles (SiO_2-GNPs) and their biological applications like lectin binding studies. However, the applications of *O*-glycosyl functionalized SiO_2-GNPs can be found in the literature as *in vitro* study of lectin binding, decontamination of *E. coli* bacteria and detection of cancer cells.[38-43] As the C-glycosides are more tolerant to enzymatic degradation, we embarked our journey to synthesize mannose and glucose containing 12-*C*-glycosyl dodecyl alkynes (Fig 4.1). These long chain glycosyl alkynes were then clicked with silica azide to get *C*-glycosyl functionalized silica nanoparticle called as SiO_2-GNPs. The *in vitro* experiment of binding of mannose and glucose decorated SiO_2-GNPs with Concanavalin A (is a lectin specific to mannose and glucose) was demonstrated by fluorescence studies and TEM analysis. Furthermore, we have demonstrated that the lectin Con A binds and aggregates NPs which are decorated with mannose and glucose sugar moieties irrespective of their core metal.

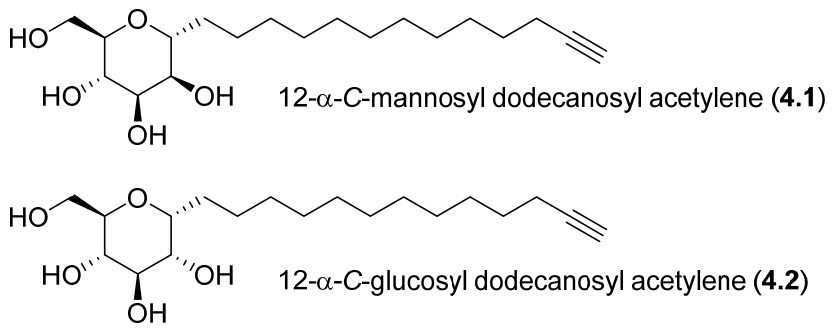

Figure 4.1. *C-glycosides of dodecanosyl acetylenes: new clicking agents for SiO_2-glyconanoparticle synthesis.*

4.2.1 Retrosynthesis

The retrosynthetic strategy for designed *C*-glycosyl alkynes is shown in Figure **4.1**. As monosaccharides can exist either in furanose or in pyranose forms in biological systems, the two compounds **4.1** and **4.2** were selected as representatives of α-hexoaldopyranoses (D-mannose, D-glucose) to carry out the synthesis. The designed retrosynthetic strategy for the *C*-glycosyl alkynes **4.1** and **4.2** is based upon the cross-metathesis of the corresponding pentaacetylated *C*-allyl glycosides **2.24** and **2.26** with 10-undecene-1-ol (**2.21**) followed by hydrogenation, oxidation and

homologation along with penta-acetate deprotection. The synthesis of different α-*C*-allylmannopyranosides **2.26**, and α-*C*-allylglucopyranosides **2.24**, were accomplished following established procedures.

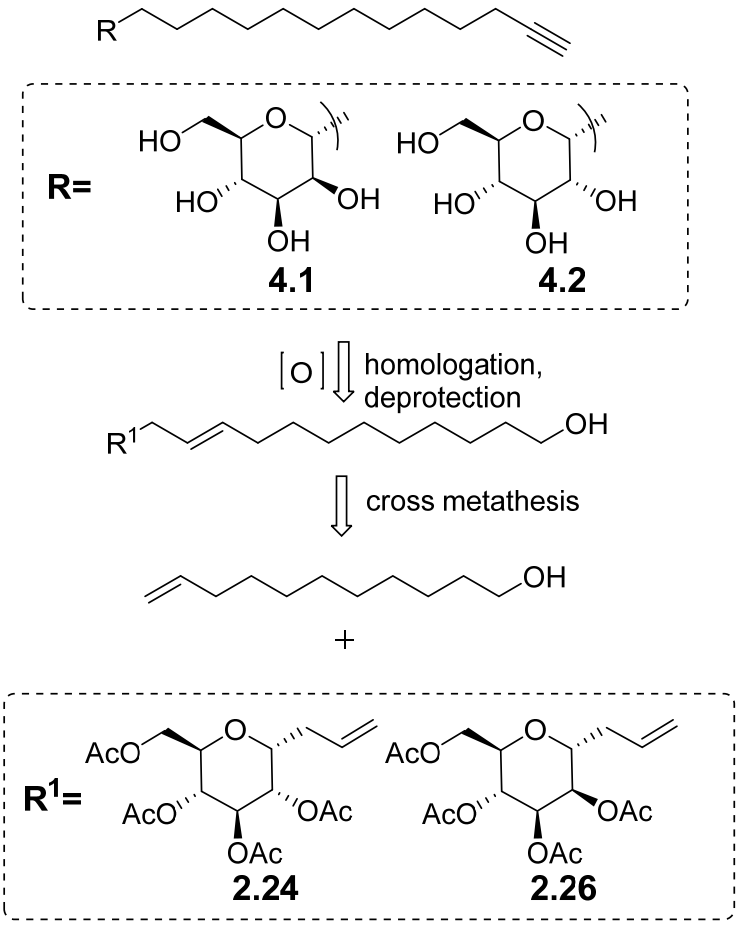

Figure 4.2**. Retrosynthetic strategy for the 12-C-glycosylated dodecanosyl acetylenes **4.1** and **4.2.

4.2.2 Synthesis

Scheme 4.1, depicts the general strategy that was followed for the synthesis of 12-*C*-glycosyl alkynes **4.1** and **4.2**, employing cross-metathesis of *C*-allyl derivatives **2.26** and **2.24** with 10-undecene-1-ol (**2.21**). The *C*-allyl sugar derivative underwent cross-metathesis with 10-undecene-1-ol using Grubbs' 1st generation catalyst (5 mol %) to afford inseparable mixture of trans/cis olefins **2.10** and **2.8**, along with the 10-undecene-1-ol dimer. The olefin mixture was hydrogenated with 5% Pd/C in methanol:ethyl acetate (1:2) to yield saturated alcohols **2.15** and **2.13**. The compounds **2.15** and **2.13** were then subjected to oxidation with IBX (2-Iodoxybenzoic acid) separately to get respective aldehydes. As the formed aldehyde is unstable, it was

immediately converted to alkyne by using Bestmann reagent and simultaneous deacetylation, which completes the synthesis of 12-*C*-glycosyldodecanosyl alkynes **4.1** and **4.2** in overall yields of 54% and 57%, respectively. The full synthetic and spectroscopic details of these compounds are given in section 4.7 and 4.8 in this chapter.

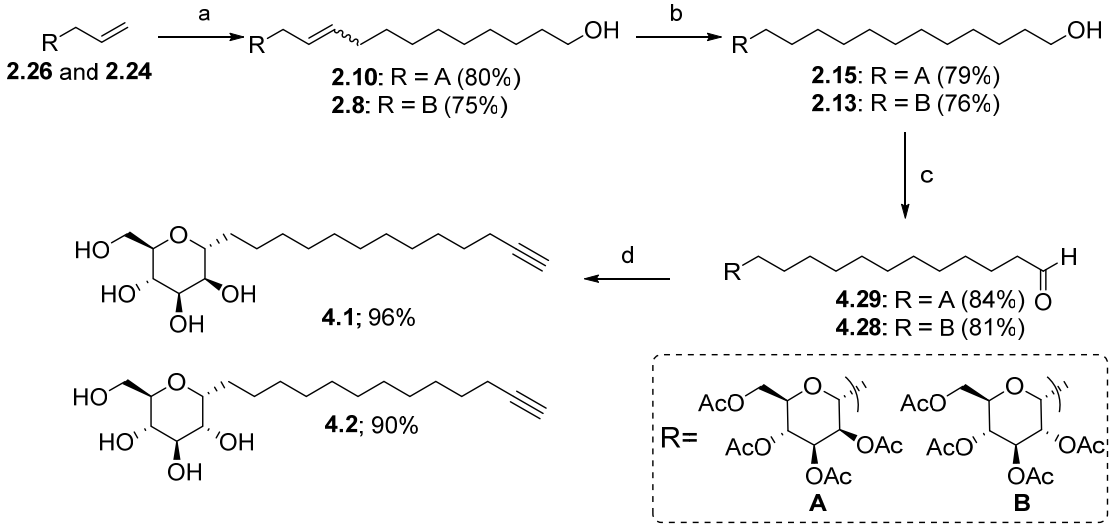

Scheme 4.1. *Reagents and conditions: (a) $C_{11}H_{23}O$ (**2.21**), 1st gen.Grubbs` catalyst (**2.27**), CH_2Cl_2, rt, 6 h; (b) H_2 5% Pd/C, MeOH/EtOAc (2:1), 1 atm, rt, 2 h; (c) IBX, DMSO, rt, 1 h, (d) Bestmann reagent, K_2CO_3, methanol, 0 ^oC , 2 h.*

4. 3 Functionalization of silica nanoparticles with Azide

To a suspension of 1 g of Ludox Silica NPs in 50 mL of ethanol, 2 mL AzPTES (azidopropyltriethoxysilane) were added, and the mixture was stirred for 16 h at 80 °C under nitrogen atmosphere. After the completion of reaction, the contents were cooled, filtered and washed with ethanol until it became free from AzPTES. The sample was then dried at 80 °C for 8h in a vacuum oven and preserved under argon atmosphere for further use. Yield: ~1.2 g. This material will be referred as SiO_2-N_3 (Fig 4.3) later in the chapter.

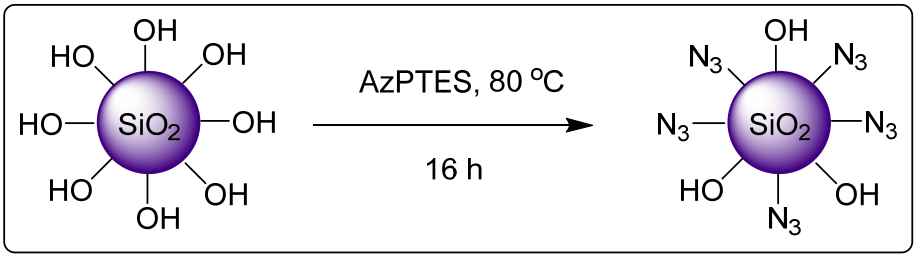

Figure 4.3. *Schematic representation azide functionalization of SiO_2-NPs.*

4.4 Synthesis of silica glyconanoparticles by click chemistry

The SiO_2-N_3 NPs and 12-*C*-glycosyl alkynes (**4.1** and **4.2**) with mannose and glucose sugar moities were subjected to CuAAC reaction (Fig. 4.4). The CuAAC reaction was attempted using $CuSO_4$/ascorbate in an equimolar mixture of t-BuOH and water. For example, treatment of SiO_2-N_3 NPs (25 mg) with **4.1** (0.1 mmol, 3-fold molar excess with respect to azide groups on azidopropyl grafted silica NPs) using $CuSO_4$/ascorbate in 1:1 H_2O/t-BuOH for 24 h converted 85% of the available azide groups into the corresponding triazole product. After the reaction, an extensive washing protocol was followed to remove the Cu(I), ascorbate and any unreacted compound **4.1**. One of the key steps in the washing was the use of dithiocarbamate to remove the Cu(I), as reported earlier.[44] The extent of the reaction was estimated using IR spectroscopy, by monitoring the decrease in the integrated intensity of $\nu_{as}(N_3)$ at 2100 cm^{-1}. The same procedure has been followed to click the compound **4.2** with SiO_2-N_3 NPs (Fig 4.4).

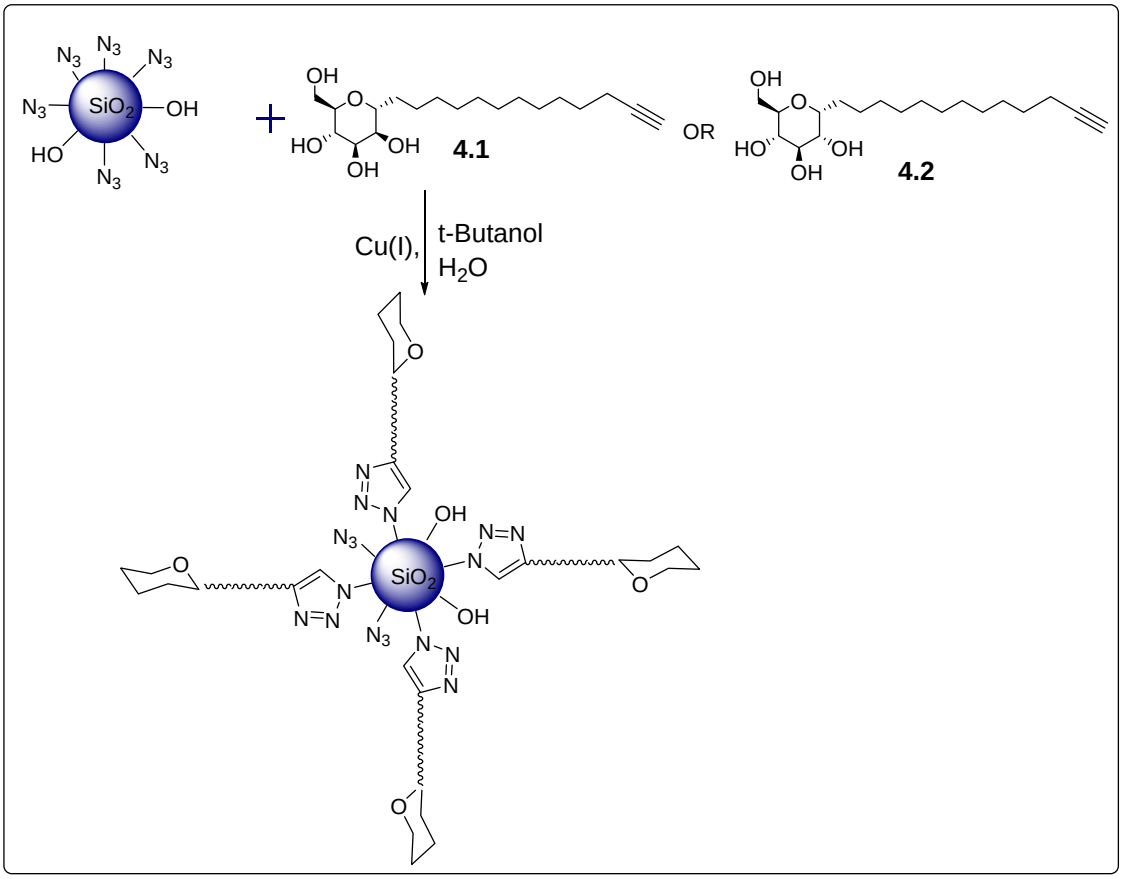

Figure 4.4. *Schematic representation of synthesis of SiO_2-GNPs with 12-C-glycosyl alkynes* ***4.1*** *and* ***4.2***.

4.5 Characterization

The as synthesized SiO_2-GNPs decorated with mannose (SiO_2-**4.1** GNPs) and glucose (SiO_2-**4.2** GNPs) were first characterized by FT-IR. To know whether the click reaction has taken place between SiO_2-N_3 NPs and 12-*C*-glycosyl alkynes **4.1** and **4.2,** the azide peek intensity at 2100 cm^{-1} was monitored by taking same amount of samples for the FT-IR measurements (Fig 4.5). We can see that in Figure 4.5, the IR intensity of azide peek in the case of SiO_2-N_3 NPs is more compared to SiO_2-**4.1** GNPs and SiO_2-**4.2** GNPs. In the FTIR spectra all the curves are normalized at 2450 cm^{-1}. We have calculated the amount of sugar present of the SiO_2 GNP surface by anthrone-sulphuric acid assay which has been discussed in chapter 3.3.1. The estimated sugar quantities are, 0.26 mg/mL of mannose on SiO_2-**4.1** GNPs dispersion and 0.32 gm/mL of glucose on SiO_2-**4.2** GNPs dispersion.

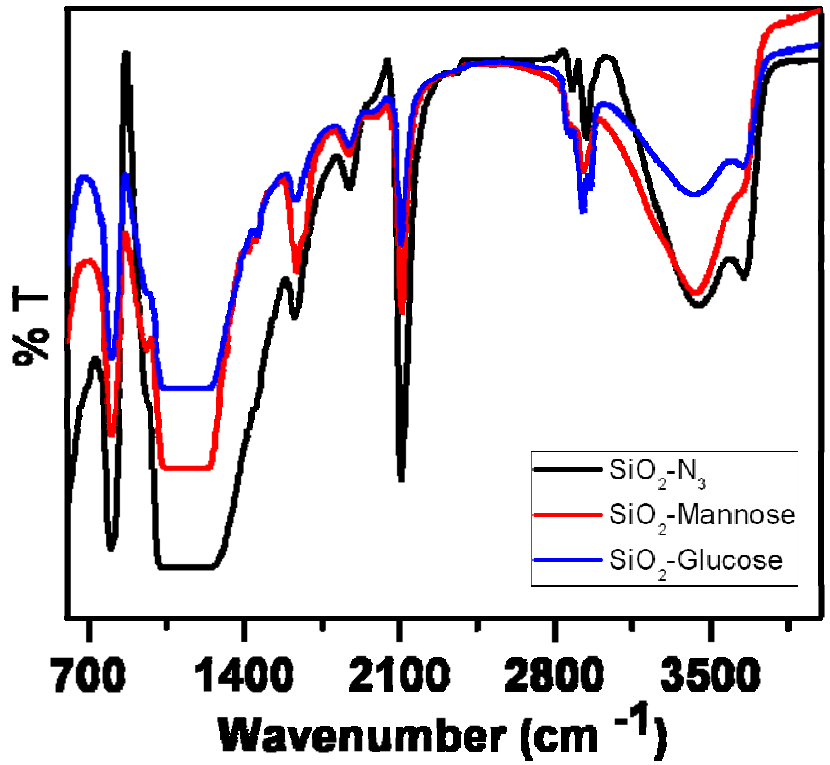

Figure 4.5. *FT-IR spectrum of SiO_2-N_3 NPs (black curve), SiO_2-**4.1** GNPs (red curve) and SiO_2-**4.2** GNPs (blue curve).*

4.5.1 Binding experiments with lectin

Although GNPs have been previously utilized to probe carbohydrate-receptor interactions,[39, 45-55] it is important to validate whether the carbohydrates immobilized

on SiO_2-GNPs retain their biological recognition specificity. This was probed using lectin, i.e., *Concanavalin A* (Con A, a mannose and glucose selective lectin). Upon incubation of a fluorescently labeled Con A lectin with SiO_2 GNPs, if the SiO_2 GNPs bind with the lectin, we should observe the formation SiO_2-GNP aggregates, in the TEM microscope. Before incubation with FITC-Con A we have taken the TEM images of SiO_2-**4.1** GNPs and SiO_2-**4.2** GNPs, which show well separated spherical particles in both SiO_2-**4.1** GNPs (Fig 4.6 A) and SiO_2-**4.2** GNPs (Fig 4.6 B) cases. Subsequently, both these GNPs were incubated with FITC-Con A for 4 h. After the completion of incubation, SiO_2-GNPs were drop casted on the TEM grid and examined under the TEM microscope. As we expected both, SiO_2-**4.1** (Fig 4.6 C) and SiO_2-**4.2** GNPs (Fig 4.6 D) got aggregated when they were incubated with FITC-Con A as both mannose and glucose are selective to Con A lectin.

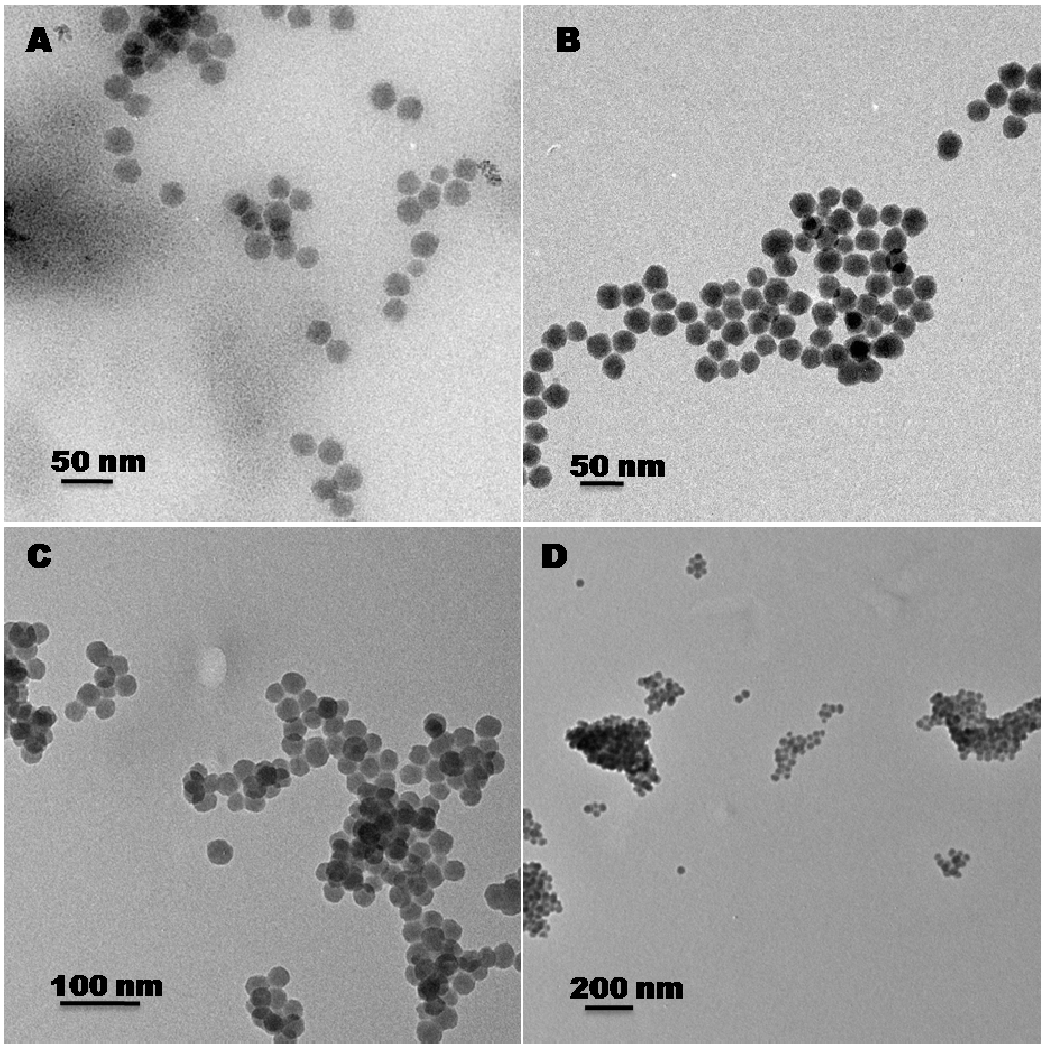

***Figure 4.6**. TEM images of (A) SiO_2-**4.1** GNPs, (B) SiO_2-**4.2** GNPs, (C) SiO_2-**4.1** GNPs + Con A and (D) SiO_2-**4.2** GNPs + Con A*

Furthermore, to conform the Con A binding with SiO_2-**4.1** GNPs and SiO_2-**4.2** GNPs, we have measured the fluorescent intensity of FITC-Con A by adding increasing amount sugar which is present on the surface of SiO_2-**4.1** GNPs and SiO_2-**4.2** GNPs. As expected increasing amount of sugar added lead to a reduction of fluorescent intensity of the FITC-Con A in the supernatant. In this experiment 10 µg/mL (0.98 µM, 3 mL) of FITC-Con A in PB buffer containing 0.1 mM $CaCl_2$ and 0.1 mM $MnCl_2$ at 7.0 pH, was incubated with SiO_2-**4.1** for 4 h**.** The fluorescent intensity of FITC-Con A remaining in the supernatant was recorded after incubating separately with three different amounts of SiO_2-**4.1** GNPs (5, 10 and 20 µg of mannose present on SiO_2-**4.1** GNPs) (Fig. 4.7 A). The FITC-Con A amount was kept constant. The same procedure has been followed for the SiO_2-**4.2** GNPs (Fig. 4.7 B). As we increase the amount of SiO_2 GNPs (sugar) the fluorescent intensity of FITC-Con A decreases, which indicated that the SiO_2-**4.1** and SiO_2-**4.2** GNPs are interacting with FITC-Con A and aggregates are being formed. This leads to the removal of FITC-Con A from the supernatant and hence the reduction in the intensity.

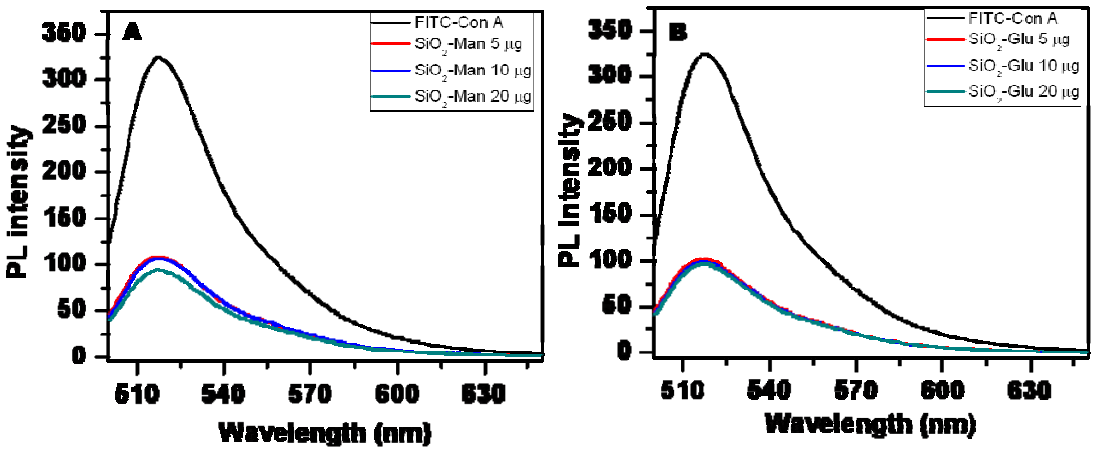

Figure 4.7*. Change in the emission spectrum of FITC-Con A with the addition of (A) SiO_2-**4.1** GNPs and (B) SiO_2-**4.2** GNPs. All spectra measured in phosphate buffer (with 0.1 mM $CaCl_2$ and 0.1 mM $MnCl_2$) at pH 7.0 and an excitation wavelength of 490 nm.*

4.5.2 GNPs bind with lectin irrespective of their core material

To validate the specificity of mannose and glucose with Con A lectin, which contains four mannose or glucose binding sites,[56] GNPs of silver and silica decorated with mannose and glucose (Ag and SiO_2 GNPs) were incubated with Con A. If the

Con A recognizes only the surface of nanoparticles a random aggregation between Ag and SiO_2 GNPs should result in (Fig 4.8).

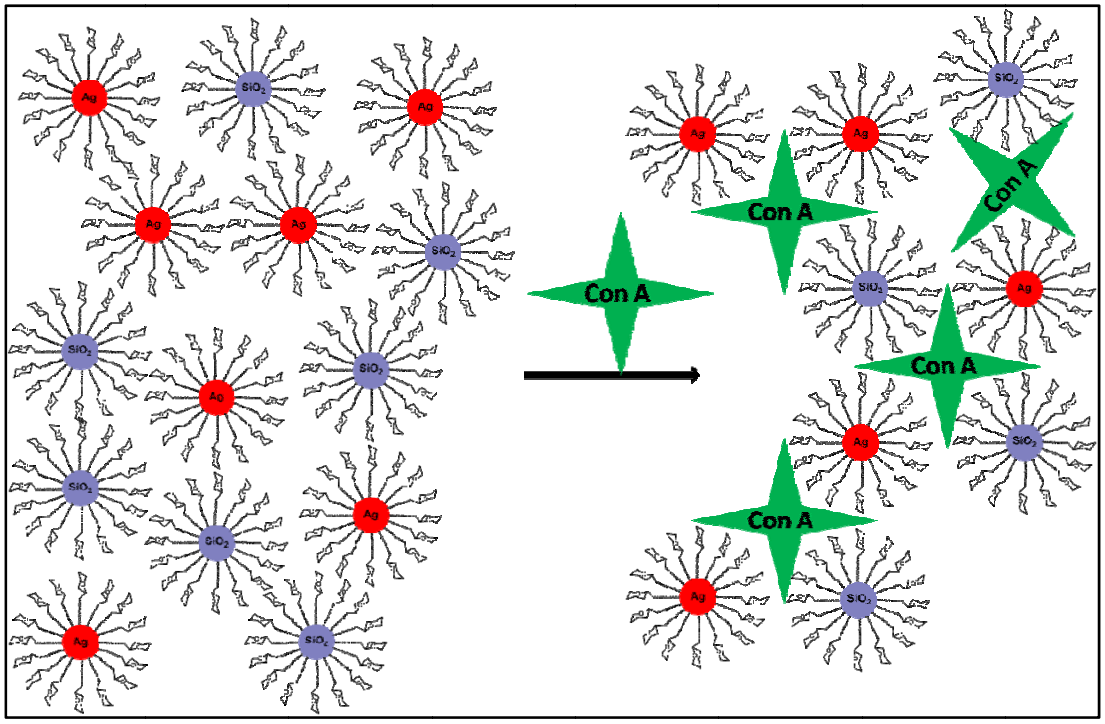

***Figure 4.8**. Schematic representation of GNPs binding with Con A irrespective of their inorganic core.*

Accordingly, we have investigated the interactions of FITC-Con A with mixture of Ag-**2.5** and SiO_2-**4.1** GNPs (mannose decorated Ag and SiO_2 GNPs) and mixture of Ag-**2.3** and SiO_2-**4.2** GNPs (glucose decorated Ag and SiO_2 GNPs). The detailed synthetic procedure and characterization for Ag-**2.5** and Ag-**2.3** GNPs has been discussed in the chapter 2.5. The binding of these GNPs mixture with FITC-Con A was ascertained from TEM images. In brief, the Ag-**2.5**, SiO_2-**4.1** GNPs and Ag-**2.3,** SiO_2-**4.2** GNPs were mixed separately in two sample vials. To these separately mixed sample vials FITC-Con A was added and incubated for 3 hrs. Subsequently, both GNPs mixtures were centrifuged and dispersed in Phosphate buffer solution. This GNPs dispersion was drop casted on the TEM grid and examined under the TEM. Figure 4.9 A shows the TEM image of Ag-**2.5** and SiO_2-**4.1** GNPs mixture before incubation with FITC-Con A, from which we can clearly observe that both Ag-**2.5** and SiO_2-**4.1** GNPs are present separately all over the grid. Same thing has been observed with the Ag-**2.3,** SiO_2-**4.2** GNPs (Fig 4.9B). Upon incubating with Con A

the TEM image is characterized with aggregates of Ag-**2.5** and SiO_2-**4.1** GNPs together. This can be attributed to the cross linking between mannose and Con A irrespective of their inorganic core and one can observe that most of the Ag GNPs are present only on SiO_2 GNPs (Fig 4.9C). The same thing has been observed in the case of Ag-**2.3,** SiO_2-**4.2** GNPs mixture when we incubated them with FITC-Con A (Fig 4.9D)

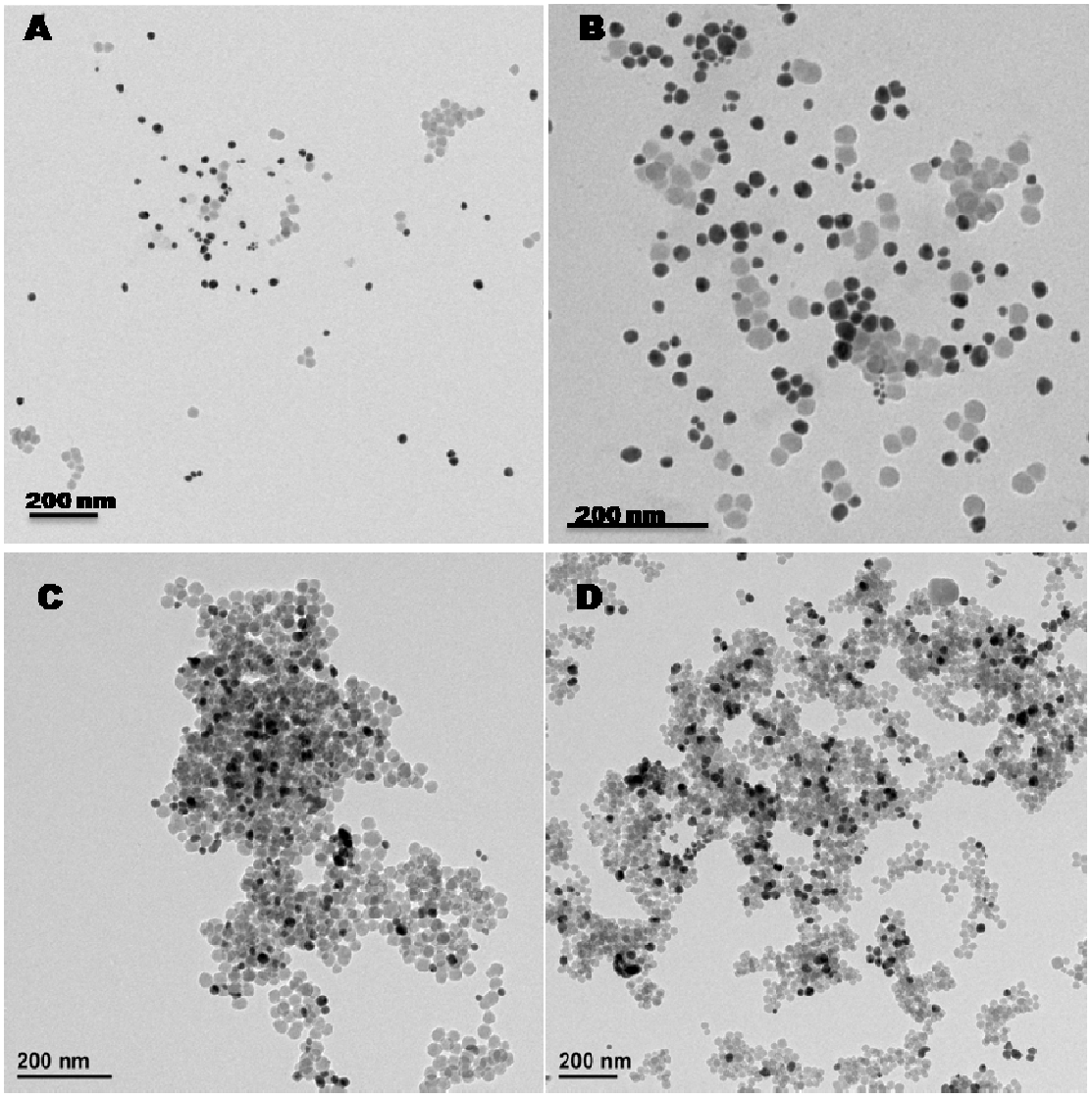

***Figure 4.9**. TEM images of (A) SiO_2-**4.1** GNPs + Ag-**2.5** GNPs, (B) SiO_2-**4.2** GNPs + Ag-**2.3** GNPs , (C) SiO_2-**4.1** GNPs + Ag-**2.5** GNPs + FITC-Con A, and (D) SiO_2-**4.2** GNPs +Ag-**2.3** GNPs + FITC-Con A.*

4.6 Conclusions

In this chapter, we described the synthesis of 12-*C*-glycosyl dodecyl alkynes containing mannose and glucose moieties. These mannose and glucose glycosyl alkynes were clicked with silica azide NPs by employing CuAAC reaction to get mannose and glucose decorated SiO_2 GNPs. The binding affinity of SiO_2 GNPs with lectin (Con A) was performed by using fluorescence spectroscopy and TEM analysis. The interaction of glycosyl moieties (which are present on the GNPs surface) with lectin (Con A) was demonstrated by talking two GNPs dispersions with same glycosyl moiety on the GNPs surface and different inorganic core (Ag and SiO_2). We could conclude that the interaction depends only on the presence of glycosyl moiety that the particles are decorated with and not on their core material.

4.7 Experimental work

The detailed synthesis, characterization and NMR data of compounds **2.8, 2.10, 2.13 and 2.15** has been given in the chapter 2. Please see the experimental section 2.5 in the chapter 2.

1-(α-D-mannopyranosyl)-12-yne-tridecane (4.1)

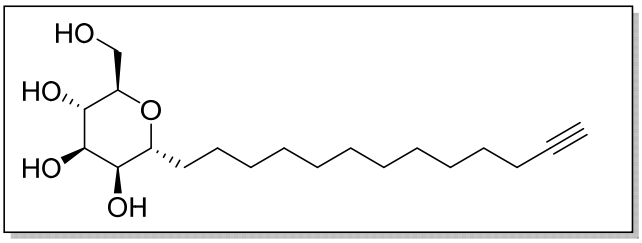

IBX **(**250 mg, 0.9 mmol) was added to a solution of **2.15 (**135 mg, 0.6 mmol) in **4** mL of THF. The reaction mixture was refluxed for 2 h, and then it was diluted with THF **(**15 mL) and filtered. The solvent was evaporated to dryness. The crude was dissolved in EtOAc **(**15 mL), washed with water **(**3 x 5 mL), dried (Na_2SO_4) and evaporated to dryness gave yellow liquid **4.28 (**123 mg, 0.5 mmol, 84%). The procedure has been followed to synthesize the compound **4.29** from the **2.13.** These aldehyde compounds **4.28** and **4.29** are unstable, so these compounds were immediately subject for the bestmann reaction to get alkynes **4.1** and **4.2**.

$[\alpha]_D^{25}$ = +12.42 (*c* 4.0, MeOH). IR ($CHCl_3$): ϑ 3365, 2853, 1709, 1569, 1455, 1377, 1032, 721 cm^{-1}. ^1H NMR (400 MHz, CD_3OD): δ 1.31 (br s, 14H), 1.44–1.50 (m, 4H), 2.13 (t, *J* = 2.5 Hz, 1H), 2.16–2.19 (m, 2H), 3.38–3.46 (m, 1H), 3.55–3.64 (m,

2H), 3.68–3.71 (m, 1H), 3.75 (dd, J = 2.7, 7.3 Hz, 2H), 3.80–3.86 (m, 1H). ^{13}C NMR (100 MHz, MeOH-d_4): δ 23.8 (t), 30.2 (t), 30.3 (t), 30.6 (t), 30.9 (t, 3C), 30.9 (t, 2C), 31.9 (t), 33.2 (t), 63.2 (t), 69.4 (d), 73.0 (d), 73.3 (d), 75.7 (d), 79.2 (d), 114.8 (d), 120.4 (q) ppm. ESI-MS: *m/z* 342.4 (100%, $[M+Na]^+$). Anal. Calcd for $C_{19}H_{34}O_5$: C, 59.65; H, 9.45. Found: C, 59.69; H, 9.49.

1-(α-D-Glucopyranosyl)-12-yne-tridecane (4.2)

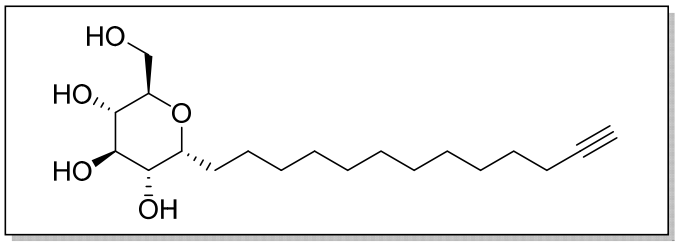

Dimethyl-1-diazo-2-oxopropylphosphonate (1.2 mmol) was added to a solution of aldehyde **4.28** (1.0 mmol) and K_2CO_3 (2.0 mmol) in MeOH (15 mL) and stirring was continued for 8 h. The reaction mixture was diluted with Et_2O (25 mL), washed with an aq solution (5%) of $NaHCO_3$ (10 mL) and dried over Na_2SO_4. After filtration and evaporation of the solvent in vacuum the alkyne **4.1** remained in analytically pure form. The same procedure has been followed for the synthesis of alkyne **4.2** from aldehyde **4.29**.

$[\alpha]_D^{25}$ = +15.46 (*c* 4.0, MeOH). IR ($CHCl_3$): υ 3365, 2853, 1709, 1569, 1455, 1377, 1032, 721 cm^{-1}. ^{1}H NMR (400 MHz, MeOH-d_4): δ 1.31 (br s, 14H), 1.56–1.58 (m, 2H), 1.63–1.69 (m, 2H), 2.66–2.67 (m, 2H), 3.32–3.27 (m, 1H), 3.35–3.41 (m, 2H), 3.50–3.58 (m, 2H), 3.62–3.66 (m, 1H), 3.76–3.80 (m, 1H), 3.85–3.90 (m, 1H). ^{13}C NMR (100 MHz, MeOH-d_4): δ 25.5 (t), 25.7 (t), 26.8 (t), 30.7 (t), 30.7 (t), 30.8 (t), 30.8 (t), 30.9 (t, 3C), 33.8 (t), 53.4 (t), 63.2 (d), 72.5 (d), 73.3 (d), 74.4 (d), 75.4 (d), 77.4 (d), 106.3 (q) ppm. ESI-MS: *m/z* 342.4 (100%, $[M+Na]^+$). Anal. Calcd for $C_{19}H_{34}O_5$: C, 59.65; H, 9.45. Found: C, 59.69; H, 9.49.

4.8 NMR Spectra

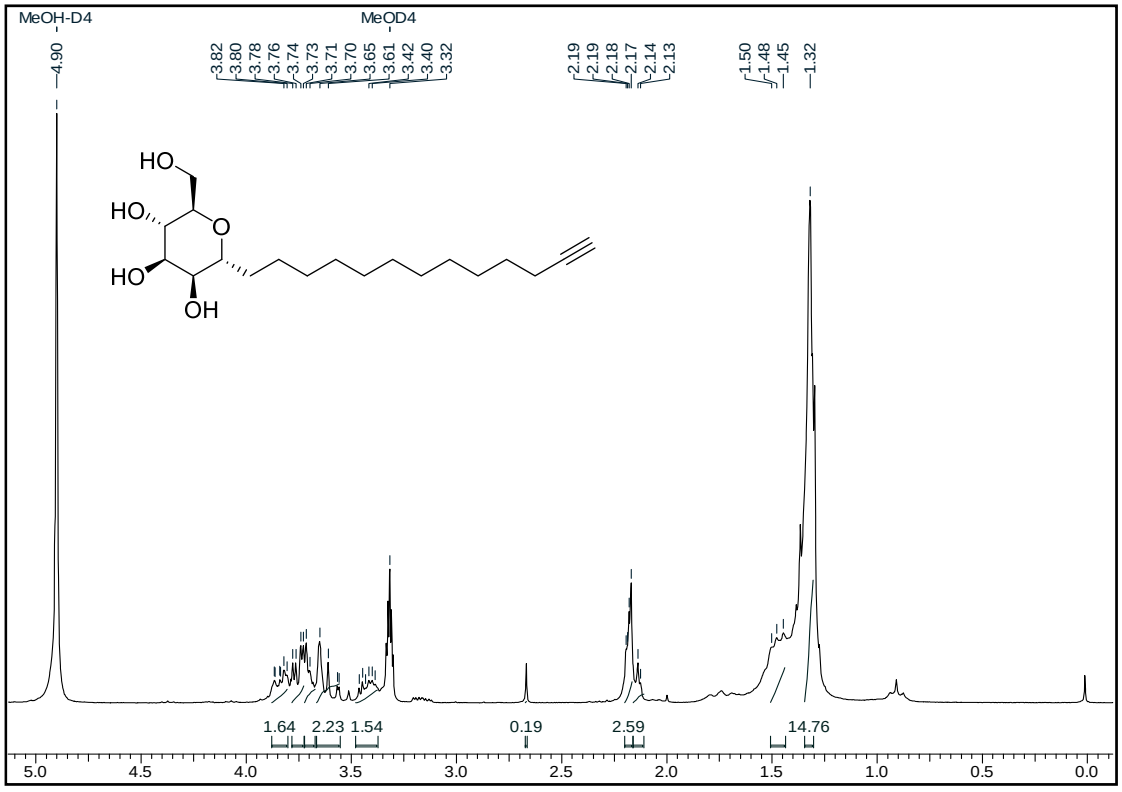

^{1}H NMR of spectrum of compound 4.1 in MeOH-D4

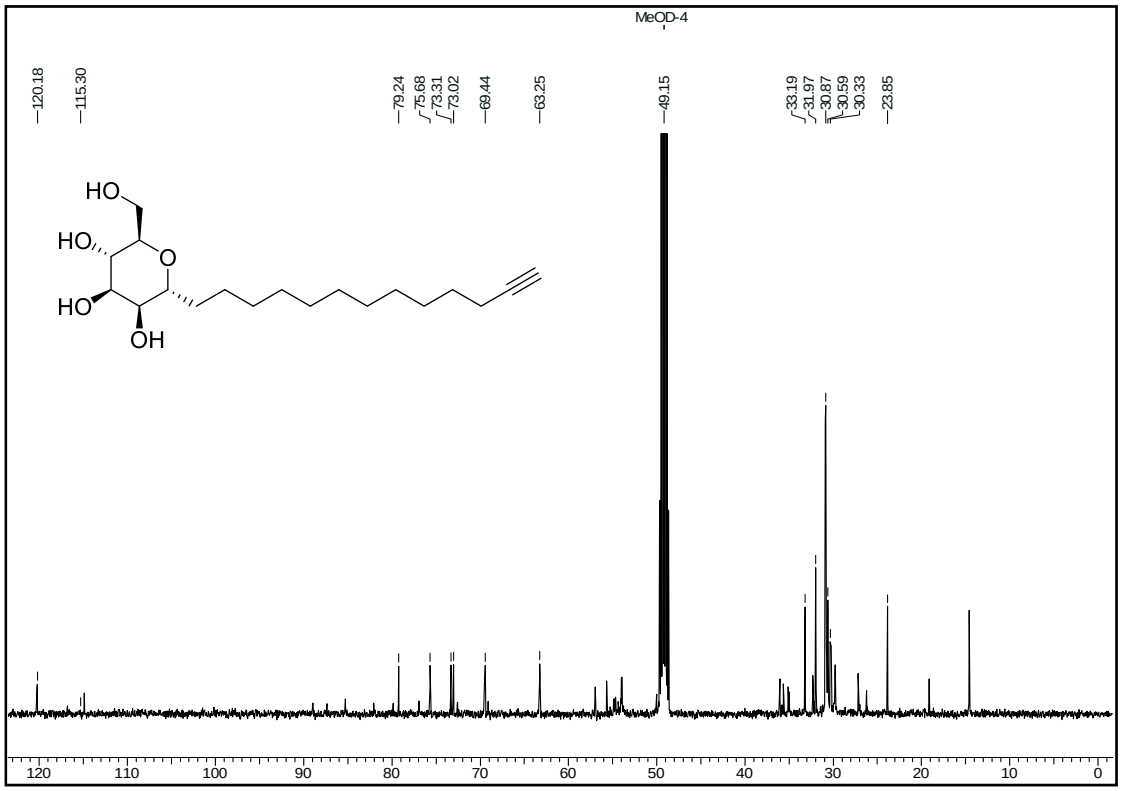

^{13}C NMR of spectrum of compound 4.1 in MeOH-D4

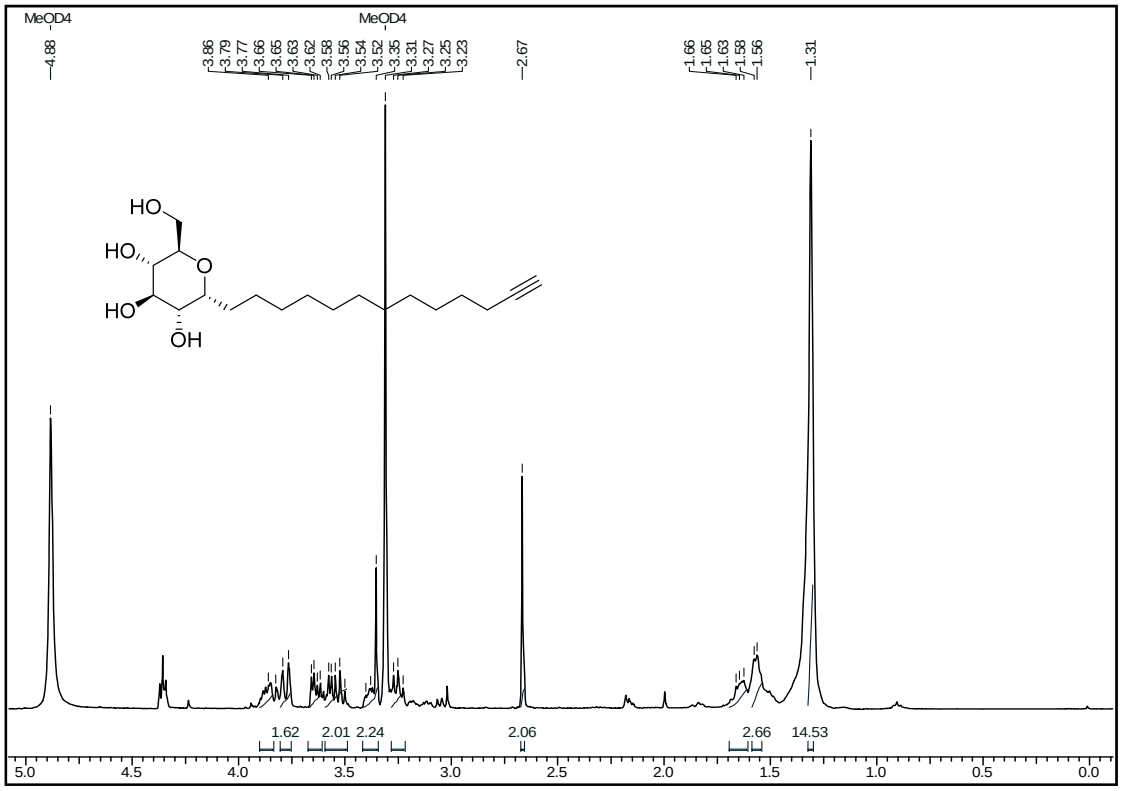

^{1}H NMR spectrum of compound 4.2 in MeOH-D4

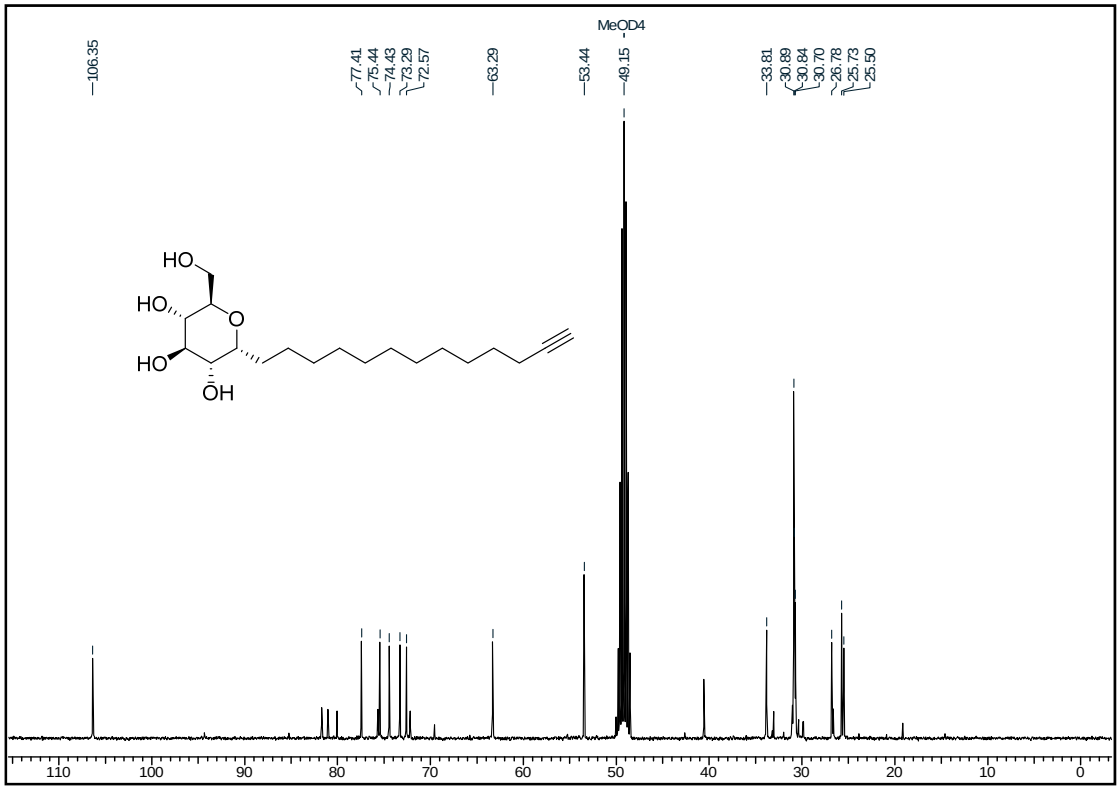

^{13}C NMR of spectrum of compound 4.2 in MeOH-D4

4.9 References

1. R. J. Pieters, D. T. S. Rijkers and R. M. J. Liskamp, *QSAR Comb. Sci.*, 2007, **26**, 1181-1190.
2. F. Santoyo-Gonzalez and F. Hernandez-Mateo, *Top. Heterocycl. Chem.*, 2007, **7**, 133-177.
3. S. Dedola, S. A. Nepogodiev and R. A. Field, *Org. Biomol. Chem.*, 2007, **5**, 1006-1017.
4. A. Dondoni, *Chem. - Asian J.*, 2007, **2**, 700-708.
5. S. R. Hanson, W. A. Greenberg and C.-H. Wong, *QSAR Comb. Sci.*, 2007, **26**, 1243-1252.
6. H. C. Kolb, M. G. Finn and K. B. Sharpless, *Angew. Chem., Int. Ed.*, 2001, **40**, 2004-2021.
7. H. Nandivada, X. Jiang and J. Lahann, *Adv. Mater.* , 2007, **19**, 2197-2208.
8. J.-F. Lutz, *Angew. Chem., Int. Ed.*, 2007, **46**, 1018-1025.
9. N. K. Devaraj and J. P. Collman, *QSAR Comb. Sci.*, 2007, **26**, 1253-1260.
10. W. H. Binder and R. Sachsenhofer, *Macromol. Rapid Commun.*, 2008, **29**, 952-981.
11. M. Meldal, *Macromol. Rapid Commun.*, 2008, **29**, 1016-1051.
12. W. H. Binder and C. Kluger, *Curr. Org. Chem.*, 2006, **10**, 1791-1815.
13. D. Fournier, R. Hoogenboom and U. S. Schubert, *Chem. Soc. Rev.*, 2007, **36**, 1369-1380.
14. P. L. Golas and K. Matyjaszewski, *QSAR Comb. Sci.*, 2007, **26**, 1116-1134.
15. W. H. Binder and R. Sachsenhofer, *Macromol. Rapid Commun.*, 2007, **28**, 15-54.
16. J.-F. Lutz and H. G. Boerner, *Prog. Polym. Sci.*, 2008, **33**, 1-39.
17. P. Lundberg, C. J. Hawker, A. Hult and M. Malkoch, *Macromol. Rapid Commun.*, 2008, **29**, 998-1015.
18. H. C. Kolb and K. B. Sharpless, *Drug Discovery Today*, 2003, **8**, 1128-1137.
19. S. Roper and H. C. Kolb, *Methods Princ. Med. Chem.*, 2006, **34**, 313-339.
20. K. B. Sharpless and R. Manetsch, *Expert Opin. Drug Discovery*, 2006, **1**, 525-538.
21. A. D. Moorhouse and J. E. Moses, *ChemMedChem*, 2008, **3**, 715-723.
22. J. M. Baskin and C. R. Bertozzi, *QSAR Comb. Sci.*, 2007, **26**, 1211-1219.

23. A. J. Dirks, J. J. L. M. Cornelissen, D. F. L. van, H. J. C. M. van, R. J. M. Nolte, A. E. Rowan and F. P. J. T. Rutjes, *QSAR Comb. Sci.*, 2007, **26**, 1200-1210.
24. C. M. Salisbury and B. F. Cravatt, *QSAR Comb. Sci.*, 2007, **26**, 1229-1238.
25. I. Aprahamian, O. S. Miljanic, W. R. Dichtel, K. Isoda, T. Yasuda, T. Kato and J. F. Stoddart, *Bull. Chem. Soc. Jpn.*, 2007, **80**, 1856-1869.
26. O. S. Miljanic, W. R. Dichtel, I. Aprahamian, R. D. Rohde, H. D. Agnew, J. R. Heath and J. F. Stoddart, *QSAR Comb. Sci.*, 2007, **26**, 1165-1174.
27. M. Ortega-Munoz, J. Lopez-Jaramillo, F. Hernandez-Mateo and F. Santoyo-Gonzalez, *Adv. Synth. Catal.*, 2006, **348**, 2410-2420.
28. Y. Zhang, Z. Guo, J. Ye, Q. Xu, X. Liang and A. Lei, *J. Chromatogr. A*, 2008, **1191**, 188-192.
29. F. Hoffmann, M. Cornelius, J. Morell and M. Froeba, *Angew. Chem., Int. Ed.*, 2006, **45**, 3216-3251.
30. Z. Yang, Y. Lu and Z. Yang, *Chem. Commun.* , 2009, 2270-2277.
31. J.-F. Lutz and Z. Zarafshani, *Adv. Drug Delivery Rev.*, 2008, **60**, 958-970.
32. C. D. Hein, X.-M. Liu and D. Wang, *Pharm. Res.*, 2008, **25**, 2216-2230.
33. Y. L. Angell and K. Burgess, *Chem. Soc. Rev.*, 2007, **36**, 1674-1689.
34. T.-Y. Guo, P. Liu, J.-W. Zhu, M.-D. Song and B.-H. Zhang, *Biomacromolecules*, 2006, **7**, 1196-1202.
35. M. Ejaz, K. Ohno, Y. Tsujii and T. Fukuda, *Macromolecules*, 2000, **33**, 2870-2874.
36. K. Hatano, T. Yamazaki, K. Yoshino, N. Ohyama, T. Koyama, K. Matsuoka and D. Terunuma, *Tetrahedron Lett.*, 2008, **49**, 5593-5596.
37. W.-C. Lee, C.-C. Hsiao and R.-C. Ruaan, *J. Chem. Technol. Biotechnol.*, 1995, **64**, 66-72.
38. K. El-Boubbou, D. C. Zhu, C. Vasileiou, B. Borhan, D. Prosperi, W. Li and X. Huang, *J. Am. Chem. Soc.*, **132**, 4490-4499.
39. K. El-Boubbou, C. Gruden and X. Huang, *J. Am. Chem. Soc.*, 2007, **129**, 13392-13393.
40. J. Zhao, Y. Liu, H.-J. Park, J. M. Boggs and A. Basu, *Bioconjugate Chem.*, 2012, **23**, 1166-1173.

41. Q. Tong, X. Wang, H. Wang, T. Kubo and M. Yan, *Anal. Chem.* , 2012, **84**, 3049-3052.
42. F. Santoyo-Gonzalez and F. Hernandez-Mateo, *Chem. Soc. Rev.*, 2009, **38**, 3449-3462.
43. A. Agostini, L. Mondragon, A. Bernardos, R. Martinez-Manez, M. D. Marcos, F. Sancenon, J. Soto, A. Costero, C. Manguan-Garcia, R. Perona, M. Moreno-Torres, R. Aparicio-Sanchis and J. R. Murguia, *Angew. Chem., Int. Ed.*, 2012, **51**, 10556-10560.
44. T. J. Terry and T. D. P. Stack, *J. Am. Chem. Soc.*, 2008, **130**, 4945-4953.
45. A. G. Barrientos, l. F. J. M. de, M. Jimenez, D. Solis, F. J. Canada, M. Martin-Lomas and S. Penades, *Carbohydr. Res.*, 2009, **344**, 1474-1478.
46. C.-H. Liang, C.-C. Wang, Y.-C. Lin, C.-H. Chen, C.-H. Wong and C.-Y. Wu, *Anal. Chem.* , 2009, **81**, 7750-7756.
47. M. Marradi, D. Alcantara, l. F. J. M. de, M. L. Garcia-Martin, S. Cerdan and S. Penades, *Chem. Commun.* , 2009, 3922-3924.
48. K. S. I. van, S. J. Campbell, S. Serres, D. C. Anthony, N. R. Sibson and B. G. Davis, *Proc. Natl. Acad. Sci. U. S. A.*, 2009, **106**, 18-23.
49. R. Kikkeri, B. Lepenies, A. Adibekian, P. Laurino and P. H. Seeberger, *J. Am. Chem. Soc.*, 2009, **131**, 2110-2112.
50. M. B. Thygesen, J. Sauer and K. J. Jensen, *Chem. - Eur. J.*, 2009, **15**, 1649-1660.
51. B. Mukhopadhyay, M. B. Martins, R. Karamanska, D. A. Russell and R. A. Field, *Tetrahedron Lett.*, 2009, **50**, 886-889.
52. A. Sundgren and J. J. Barchi, *Carbohydr. Res.*, 2008, **343**, 1594-1604.
53. d. S. A. Carvalho, K. M. Halkes, J. D. Meeldijk, A. J. Verkleij, J. F. G. Vliegenthart and J. P. Kamerling, *ChemBioChem*, 2005, **6**, 828-831.
54. D. C. Hone, A. H. Haines and D. A. Russell, *Langmuir*, 2003, **19**, 7141-7144.
55. C.-C. Lin, Y.-C. Yeh, C.-Y. Yang, G.-F. Chen, Y.-C. Chen, Y.-C. Wu and C.-C. Chen, *Chem. Commun.* , 2003, 2920-2921.
56. Z. Derewenda, J. Yariv, J. R. Helliwell, A. J. Kalb, E. J. Dodson, M. Z. Papiz, T. Wan and J. Campbell, *EMBO J.*, 1989, **8**, 2189-2193.

Chapter 5

Conclusions

5.1 Summary of the thesis

In this thesis our focus was mainly to synthesize new, straightforward and robust functional glycans to immobilize carbohydrates on metal and metal oxide surfaces for glycobiological studies. We have discussed detailed synthesis of five different α/β-12-*C*-glycosyl acids in chapter 2. The as synthesized 12-*C*-glycosyl acids were used as capping and as well as reducing agent in the synthesis of Ag GNPs, which removes the necessity of an extra reducing agent, thus preventing the formation of extra side products. These *C*-glycosides are more stable in physiological conditions as compared to their *O*-glycoside counterparts. *C*-glycans could enhance biological activity of GNPs to greater extend.

Ag-GNPs decorated with mannose and glucose sugar moieties were used to study the lectin (Concanavalin A) binding with carbohydrates using techniques like fluorescence spectroscopy, UV-visible spectroscopy and TEM analysis. Both the glycan-functionalized Ag-GNPs have displayed good selectivities toward lectin (Con A). Furthermore, the anti bacterial activity of Ag-GNPs decorated with mannose and glucose were tested against *E coli* (DH5α cells). This experiment has revealed the specific binding of mannose coated Ag-GNPs towards the type 1 pili of *E coli* (DH5α cells).

In chapter 4, we have discussed the detailed synthesis of mannose and glucose containing long chain terminal alkynes, which are clicked with silica azide by using CuAAC click reaction to get mannose and glucose coated silica GNPs. These silica GNPs were used to study the carbohydrate-Con A binding studies by using fluorescence spectroscopy and the TEM analysis. To show that these interaction mainly depends on carbohydrate and are independent of inorganic core, we have mixed two GNPs solutions (Ag and SiO_2) containing mannose and glucose on their surfaces and incubated with con A. Without Con A, we have observed the Ag and SiO_2 GNPs separately on the TEM grid. However, with Con A we observed Ag+SiO_2 GNPs together on the TEM grid confirming that the carbohydrate-lectin interaction is independent of the core material.

5.2 Scope of future work

Our studies show that glycosyl acids containing long aliphatic chains can be used as capping well as reducing agents in the synthesis water soluble of GNPs. Taking advantage of water solubility and surface glycan moieties, these GNPs can be effectively use in the detection of various cancer cells, imaging techniques and in the drug delivery applications. We can extend the capping and reducing property of glycosyl acids to synthesis different metal GNPs like Au which are more biocompatible.

APPENDIX I

Ultraviolet-visible (UV-vis) absorption spectrophotometry: UV-vis Spectroscopic measurements were carried out on a Cary 300 Conc UV-Visible spectrophotometer operated at a resolution of 2 nm.

X-ray Diffraction: The diffractograms were recorded on a PANalytical Xpert pro machine using a CuKα (λ=1.54 Å) source and operating conditions of 40 mA and 30 kV at different scan rates depending upon the sample.

FTIR spectrophotometer: FTIR spectra were recorded on a Perkin Elmer Spectrum One FTIR spectrophotometer in diffuse reflectance mode, operating at a resolution of 4 cm^{-1}.

Transmission Electron Microscopy: TEM measurements were performed on a TECHNAI G2 F30 S-TWIN instrument (Operated at an acceleration voltage of 300 kV with a lattice resolution of 0.14 nm and a point image resolution of 0.20 nm). TEM samples were prepared by placing drops of dispersed samples over carbon coated copper grids and allowing the solvent to evaporate.

Fluorescence spectrophotometer: Fluorescent measurements were carried out on a Varian Cary Eclipse fluorescence spectrophotometer with slit widths of 5 nm.

NMR spectrometer: ^{1}H and ^{13}C NMR spectra were recorded on AV–200 MHz, AV–400 MHz, and DRX–500 MHz spectrometer using tetramethylsilane (TMS) as an internal standard. Chemical shifts have been expressed in ppm units downfield from TMS.

Mass spectrometer: EI Mass spectra were recorded on Finngan MAT–1020 spectrometer at 70 *eV* using a direct inlet system.

Polarimeter: Optical rotations were measured with a JASCO DIP 370 digital polarimeter.

While synthesizing glycosyl ligands:

• All reactions are monitored by Thin Layer Chromatography (TLC) carried out on 0.25 mm E-Merck silica gel plates (60F–254) with UV light, I_2, and anisaldehyde in ethanol as developing agents.

• All reactions were carried out under nitrogen or argon atmosphere with dry, freshly distilled solvents under anhydrous conditions unless otherwise specified. Yields refer to chromatographically and spectroscopically homogeneous materials unless otherwise stated.

• All evaporations were carried out under reduced pressure on Buchi rotary evaporator below 45 °C unless otherwise specified.

• Silica gel (60–120), (100–200), and (230–400) mesh were used for column chromatography.

APPENDIX II

List of abbreviations:

Ac: Acetyl

AcOH: Acetic acid

Ac_2O: Acetic anhydride

Aq: Aqueous

Conc: Concentrated

DMSO: Dimethyl sulfoxide

EtOH: Ethanol

Et_2O: Diethyl ether

EtOAc: Ethyl acetate

IBX: Iodoxybenzoic acid

Na_2CO_3: Sodium carbonate

NaN_3: Sodium azide

NMR: Nuclear magnetic resonance

Pd/C: Palladium on Carbon

K^{t}OBu: Potassium tertiary butoxide

Bestmann reagent: Dimethyl (diazomethyl)phosphonate

Rpm: Rotations per minute

Rt: Room temperature

GNPs: Glyconanoparticles

Ag: Silver

SiO_2: Silica

Ag-GNPs: Silver glyconanoparticles

SiO_2-GNPs: Silica glyconanoparticles

FTIR: Fourier Transform Infrared Spectroscopy

TEM: Transmission Electron Microscopy

XRD: X-ray diffraction

APPENDIX III

List of publications

1. Synthesis of Ag-glyconanoparticles with *C*-glycosides, their lectin binding studies and anti bacterial activity

Vilas Ramtenki, D. Raju, Urmil J Mehta, C. V. Ramana and B. L. V. Prasad,

New J. Chem., 2013, DOI: 10.1039/C3NJ00496A

2. Gold nanoparticle embedded hydrogel matrices as catalysts: Better dispersibility of nanoparticles in the gel matrix upon addition of N-bromosuccinimide leading to increased catalytic efficiency

Vilas Ramtenki, V.D. Anumon, Manohar V. Badiger and B.L.V. Prasad, *Colloids and Surfaces A: Physicochem. Eng. Aspects*, **2012**, 414, 296–301.